https://doi.org/10.15388/vu.thesis.980
https://orcid.org/0000-0001-7713-4347

VILNIUS UNIVERSITY

Skomantas Serapinas

The Development of Electrochemical Genosensors Based on Nucleic Acid Affinity

DOCTORAL DISSERTATION

Natural Sciences,
Biochemistry (N 004)

VILNIUS 2026

The dissertation was prepared between 2020 and 2026 at the Institute of Biochemistry, Life Sciences Center, Vilnius University. The research was supported by the Research Council of Lithuania via doctoral students support program.

Academic Supervisor – Dr. Marius Dagys (Vilnius University, Natural Sciences, Biochemistry – N 004).

Academic Consultant – Dr. Dalius Ratautas (Vilnius University, Natural Sciences, Biochemistry – N 004).

This doctoral dissertation will be defended in a public meeting of the Dissertation Defence Panel:

Chairman – Dr. Rima Budvytytė (Vilnius University, Natural Sciences, Biochemistry – N 004).
Members:
Dr. Edita Kriukienė (Vilnius University, Natural Sciences, Biochemistry – N 004),
Dr. Edita Voitechovič (Center for Physical Sciences and Technology, Natural Sciences, Biochemistry – N 004),
Dr. Rasa Petraitytė-Burneikienė (Vilnius University, Natural Sciences, Biochemistry – N 004),
Prof. Dr. Sergey Shleev (Malmö University, Natural Sciences, Biochemistry – N 004).

The dissertation shall be defended at a public meeting of the Dissertation Defence Panel at 13:00 on the 17th of September 2026 in Room R401 of the Vilnius University Life Sciences Centre.
Address: R401, Life Sciences Centre, Saulėtekio al. 7., Vilnius, Lithuania
Tel. +370 5 223 4419; e-mail: info@gmc.vu.lt.

https://doi.org/10.15388/vu.thesis.980
https://orcid.org/0000-0001-7713-4347

VILNIAUS UNIVERSITETAS

Skomantas Serapinas

Elektrocheminių genojutiklių paremtų nukleorūgščių afiniškumu kūrimas

DAKTARO DISERTACIJA

Gamtos mokslai,
Biochemija (N 004)

VILNIUS 2026

Disertacija rengta 2020–2026 metais Vilniaus Universitete, Gyvybės mokslų centre, Biochemijos Institute.
Mokslinius tyrimus rėmė Lietuvos mokslo taryba.

Mokslinis vadovas – dr. Marius Dagys (Vilniaus universitetas, gamtos mokslai, biochemija – N 004).

Mokslinis konsultantas – Dr. Dalius Ratautas (Vilniaus universitetas, gamtos mokslai, biochemija – N 004).

Gynimo taryba:
Pirmininkė – dr. Rima Budvytytė (Vilniaus universitetas, gamtos mokslai, biochemija – N 004).
Nariai:
Dr. Edita Kriukienė (Vilniaus universitetas, gamtos mokslai, biochemija – N 004)
Dr. Edita Voitechovič (Fizinių ir technologijos mokslų centras, gamtos mokslai, biochemija – N 004)
Dr. Rasa Petraitytė-Burneikienė (Vilniaus universitetas, gamtos mokslai, biochemija – N 004)
Prof. dr. Sergey Shleev (Malmö universitetas, gamtos mokslai, biochemija – N 004)

Disertacija ginama viešame Gynimo tarybos posėdyje 2026 m. rugsėjo mėn. 17 d. 13 val. Vilniaus universiteto Gyvybės mokslų centro R401 auditorijoje. Adresas: Gyvybės mokslų centras, Saulėtekio al. 7., Vilnius, Lietuva, tel. +370 5 223 4419; el. paštas: info@gmc.vu.lt

Medicinal chemists would rather have a method that proceeds in 10% yield on 90% of the substrates, than one that proceeds in 90% yield but on only 10% of the substrates.

Phil Baran, 2023 (paraphrased)

INDEX

LIST OF PUBLICATIONS 8
LIST OF ABBREVIATIONS 10
THESIS LAYOUT 12
INTRODUCTION AND SCIENTIFIC NOVELTY 13
1. Objectives 14
2. Defense statements 15
3. Publications 15
LITERATURE REVIEW 22
1. Genotyping methods and pharmacogenetic assays 22
2. Nucleic acid preparation 23
3. Nucleic acid capture and detection 25
DISCUSSION 40
CONCLUSIONS 55
SANTRAUKA/SUMMARY 56
CONFERENCES 62
CURRICULUM VITAE 63
SOFTWARE USED 64
REFERENCES 65
APPENDICES 89
1. Appendix I 90
2. Appendix II 93
3. Appendix III 97
4. Appendix IV 103
5. Appendix V 111
COPIES OF PUBLICATIONS 120
1. Publication I 120
2. Publication II 128
3. Publication III 137

4. Publication IV 149
ACKNOWLEDGEMENTS 159

LIST OF PUBLICATIONS

Publication 1:

Serapinas, S.; Gineitytė, J.; Butkevičius, M.; Danilevičius, R.; Dagys, M.; Ratautas, D.

Biosensor Prototype for Rapid Detection and Quantification of DNase Activity. *Biosensors and Bioelectronics* **2022**, *213*, 114475. https://doi.org/10.1016/j.bios.2022.114475.

Author contributions: Conceptualization: **S.S.**, J.G., M.B., R.D., M.D. and D.R.; Software: **S.S.**, J.G., M.B., M.D. and D.R. Investigation: **S.S.**, J.G., M.B.; Methodology: **S.S.**, J.G., M.B., M.D. and D.R.; Data curation: **S.S.**, J.G.; Formal analysis: **S.S.**, M.B., J.G., and D.R.; Validation: **S.S.**, J.G.; Writing (original draft): D.R.; Resources: R.D., M.D., and D.R.; Writing – review & editing: **S.S.**, M.B., J.G., R.D., M.D. and D.R.; Visualization: D.R.; Supervision: D.R.

Publication 2:

Gineitytė, J.; **Serapinas, S**.; Ratautas, D.

Electrochemical DNA Hybridization Signal Amplification System Using Methylene Blue and Ascorbic Acid. *Electrochimica Acta* **2024**, *507*, 145146. https://doi.org/10.1016/j.electacta.2024.145146.

Author contributions: Conceptualization: **S.S.**, J.G. and D.R.; Data curation and investigation: **S.S.**, J.G., and D.R.; Formal analysis: **S.S.**, J.G. and D.R.; Writing (original draft): J.G. and D.R.; Funding acquisition and supervision: D.R.; Writing (review, editing and graphics): **S.S.**, J.G., and D.R.

Publication 3:

Žalnėravičius, R.; Talaikis, M.; Klimas, V.; **Serapinas, S.**; Butkevičius, M.; Vaičiūnienė, J.; Morkvėnas, A.; Karabanovas, V.; Niaura, G.; Jagminas, A.; Dagys, M.

Fabrication of Porous Black Gold Films by One-Step Anodic Treatment: Towards the Development of SERS-Active Nanosensors. *Materials Today Chemistry* **2025**, *47*, 102849.

https://doi.org/10.1016/j.mtchem.2025.102849.

Author contributions: Writing – original draft: R.Z., Validation: R.Z., Methodology: R.Z., Writing – review & editing: R.Z., M.T., V.K., **S.S.**, M.B., J.V., V.K., G.N., A.J. and M.D.; Visualization: R.Z., **S.S.** and M.B., Supervision: R.Z. and M.T., Conceptualization: R.Z., V.K., V.K., G.N., A.J. and M.D.; Investigation: M.T., Data curation: M.T., Formal analysis: M.T., **S.S.**, M.B., J.V. and A.M., Resources: A.J. and M.D.; Funding acquisition: M.D.

Publication 4:

Serapinas, S.; Stakelytė, D.; Tučinskytė, K.; Tomkuvienė, M.; Dagys, M.; Ratautas, D.

Constant Temperature Electrochemical Biosensor for SNP Detection in Human Genomic DNA Based on DNA Melting Analysis. *ACS Sens.* **2025**, *10* (9), 6819–6827. https://doi.org/10.1021/acssensors.5c01577.

Author contributions: Conceptualization: **S.S.** and D.R.; Data curation and investigation: **S.S.** and D.R.; Formal analysis: **S.S.**, D.S. and K.T.; Writing (original draft): **S.S.** and D.R.; Funding acquisition and supervision: D.R.; Writing (review, editing and graphics): **S.S.**, D.S., M.T., M.D. and D.R.

LIST OF ABBREVIATIONS

AFM	Atomic force microscopy
ALP	Alkaline Phosphatase
AuNP	Gold nanoparticles
cfDNA	Cell free DNA
CV	Cyclic voltammetry
DMAP	4-Dimethylaminopyridine
DPV	Differential pulse voltammetry
ECD	Electrochemical detection
FET	Field-effect transistor
FRET	Förster resonance energy transfer
FTIR	Fourier transform infrared spectroscopy
HPLC	High performance liquid chromatography
LSV	Linear sweep voltammetry
MOSFET	Metal-Oxide Semiconductor Field-Effect Transistor
PCR	Polymerase chain reaction
PEDOT	Poly-(ethylenedioxythiophene)
PM-IRRAS	Polarization-modulation infrared reflection absorption spectroscopy
RCA	Rolling circle amplification
RNA-pol	RNA polymerase
RPA	Recombinase polymerase amplification
SAM	Self-assembled monolayer
SCE	Standard calomel electrode
SERS	Surface-enhanced Raman spectroscopy
SPE	Screen printed electrode
SPR	Surface plasmon resonance
SWV	Square wave voltammetry
TMA	Transcription-mediated amplification
TMB	3,3′,5,5′-Tetramethylbenzidine
WGA	Whole genome amplification
XPS/ESCA	X-ray photoelectron spectroscopy / Electron spectroscopy for chemical analysis

Abbv.	Reference electrode	V vs. NHE/SHE[1,2]
SCE	Standard calomel electrode	0.242 V (4.7 V*)
$Ag/AgNO_3$	Silver-Silver nitrate (10 mM $AgNO_3$ in acetonitrile)	0.54 V
Ag/AgCl	Silver-silver chloride (3M KCl)	0.197 V
SHE	Standard hydrogen electrode	0 V

** Estimated potential in absolute terms (vs. vacuum). In electroanalytical chemistry the convention is using relative potentials.*

Note: Substrate – this term (depending on context) is used to describe both an enzymatic/biomolecular target (a chemical species) and a solid material on which a process is occurring (a solid phase).

Note: Amplification – this term (depending on context) is used to describe both sample amplification (e.g., DNA synthesis) and signal amplification (e.g., a catalytic reaction, an accumulation reaction or an electronic approach).

Note: A probe generally means a chemical species.

Note: Label-free terminology is used to mean the absence of a labeling step, and not purely the absence of a label.

THESIS LAYOUT

This thesis is composed of four publications and a discussion of their interplay in the field of biochemical assay and sensor design.

The four publications are included at the end. The related supplementary material was not included but is available at the publisher website.

This Thesis also includes appendices with additional unpublished experimental data to further expand on the practicality and the relevance of the publications provided.

DNA detection has very broad importance in screening for various pathogens as well as identifying and monitoring other (micro- and macro-) organisms. Some of the most important cases of DNA detection can be found in various healthcare applications for instance, diagnosing a specific tumor type or patient pharmacogenetic marker before prescribing a medical intervention.

Nucleic acid biosensors are devices capable of recognizing and detecting a target nucleic acid and can be referred to as genosensors. These devices are promising in their highly accessible nature with the potential benefits of sensor and data ownership, privacy and the convenience of low-power, miniaturized sensors, thus enabling distributed use of diagnostic tools.

The first intended users of these sensors would be analysts (professionals) with the vision of a broader acceptance by the public.

The opening quote from Dr. Baran offers wonderful insights into the critical aspect of medicinal (electro)chemistry end-user preferences. I feel this sentiment is directly translatable to the analysis field, where an assay with excellent cross-compatibility is generally more desirable and reliable than one with narrow application scope even if such an assay were to have greater sensitivity.

One exciting target for a genosensor would be pharmacogenes. It is only through extraordinarily good design or luck that pharmaceuticals are broadly safe and effective despite a massive quantity of variants of receptors, hydrolases, oxidases, ligases and transport proteins in the human population. While some medicines have pharmacogenomics–based guidelines[3–5], screening is yet to become commonplace. Some of the challenges in broader adoption include the cost and other difficulties in testing, a lack of clinical expertise or guidance, ethical concerns and the lack of clear cost–benefit evidence. [6,7] Looking ahead, broad integration of pharmacogenetic screening may improve outcomes and additionally facilitate the highly important processes of drug design and clinical trials and introduce a larger variety of precision pharmaceuticals.[8]

Microbial contamination of food, water and other samples is also a highly relevant target for a genosensor, as often a portable solution may be preferable. Notable environmental examples include *Legionella pneumophila*,[9] *Escherichia coli*[10] and *Enterococcus* spp.[11] **in water**, various mould species[12] **in air**, with *Campylobacter jejuni*[13] and *Cyclospora cayetanensis*[14] being some of the **food–borne** cases.

Diagnosis of infection in humans and animals is also an excellent application for genetic detection. Identification of infectious agents and of resistance genes like SARS-CoV-2, Ebola, HIV, Hepatitis C as well as *C. difficile* strains, MRSA *Staphylococci*, *Mycobacterium tuberculosis,* VanA *Enterococci* and others is used in practice in the form of dedicated clinical devices and highly valuable.[15,16]

The development of electrochemical DNA detection offers certain unique advantages, such as miniaturization, low power modules and thus portability and modularity. Electrochemical biosensors are also quite amenable to motion and positioning.

The goal of this dissertation is the advancement of genetic assays towards highly approachable and accessible genosensor devices. This is to be approached through the development of biosensors for specific DNA sequence recognition. Some small progress has been made in DNA sample preparation and DNA modified electrode array synthesis, however these areas are outside the scope of the thesis. The core focus of the dissertation is to assess the analytical performance and workflow design of genosensors and gain insight into their advantages and limitations, before committing to a specific design or application.

1. Objectives

To achieve this goal 3 objectives were set:

1. The detection of the presence of a specific DNA sequence with biosensors.

2. The differentiation between single-point mutations and between the two homozygous alleles of a DNA target and the heterozygous variant based on nucleic acid affinity.

3. An overarching theme of this work is achieving these tasks in a manner that is easily translatable into a portable and inexpensive device – a sensor.

The workflow of achieving these goals can be broadly described as nucleic acid target selection and recognition system design; the formation of DNA monolayers and solid-phase hybridization research; electrochemical measurements and signal analysis; supporting characterization, manufacturing and design tasks.

2. Defense statements

1. Specific detection of oligonucleotides, including the quantitation of the target nucleic acid (detectable at 3.5 nM) and its digestion by nucleases in complex biological samples can be achieved via simple electrochemical methods.
2. A novel single-surface isothermal melting approach has been developed and precalibrated genotyping of important pharmacogenes from non-invasive saliva samples was performed at 5/5 concordance with sequencing.
3. One or multiple base mutations were electrochemically measured in the target DNA sequence via their dissociation rate constants and expressed as shifts in binding affinity (with propagated standard deviations of 0.2 kcal mol^{-1}), correlating well with computed values.

3. Publications

The results of this work were published as four articles. Some further supporting data was added as thesis appendices.

The first publication "**Biosensor prototype for rapid detection and quantification of DNase activity**" and its supplement Appendix I cover the development of a sensor for the detection and quantification of nucleases.

The biosensor was able to detect DNase I – an important target in biotechnology at 0.34 mU ml^{-1} via dsDNA probe lysis – providing a convenient method for quantifying the nuclease activity of a sample. The target was first digested with a sample by mixing it into a liquid sample or an extract from a solid and allowing the reaction to occur at an elevated temperature. Afterwards the hybridization rate was monitored *in situ*, i.e., the read-off was being performed in a diluted digestion solution. Notably the digestion sample was diluted with a very high salinity electrochemical solution intended to stop the hydrolysis reaction.

Interestingly, when the system was tested with an ssRNA probe for RNase A, the sensitivity was quite good – 1×10^{-6} Kunitz U ml^{-1}, due to high intrinsic RNase stability and activity.

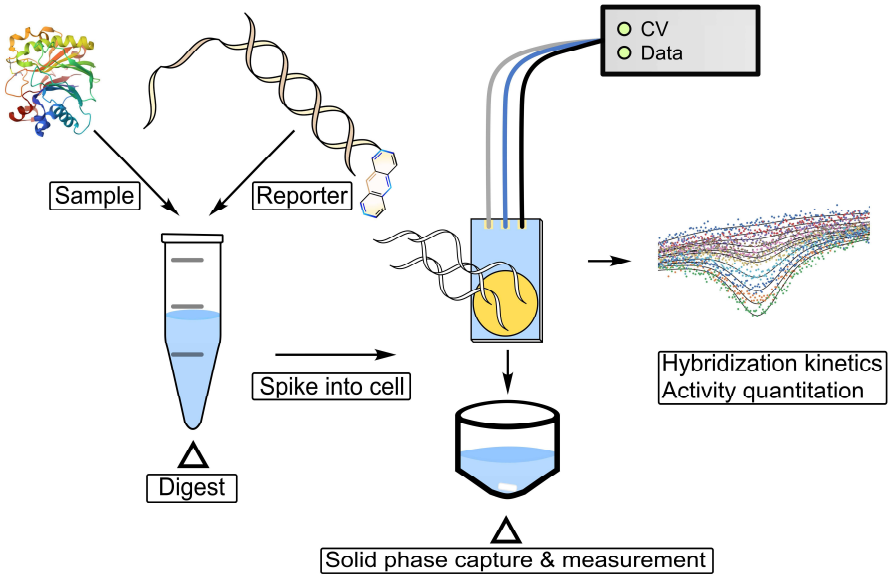


Figure 1. A representation of the workflow of the nuclease quantitation assay. CV - cyclic voltammetry.[17]

The device prototype design includes a measurement container with a Peltier thermostated cell, magnetic stirring and an electrode holder. In this case a fluidic system was not developed as the sample preparation may vary significantly. An Arduino Due based potentiostat which had been developed in–house was applied to the prototype with a custom python program to collect and fit and output the data.

Based on these results, it was concluded that MB-labeled oligo capture on gold to be suitable for further genosensor development, with hybridization rate as a viable parameter for nucleic acid quantitation.

The second publication "**Electrochemical DNA Hybridization Signal Amplification System Using Methylene Blue and Ascorbic Acid**" and its supplement Appendix II cover the development of a method for amplifying DNA hybridization signal and observing the hybridization to solid phase at temporal resolution on the order of seconds.

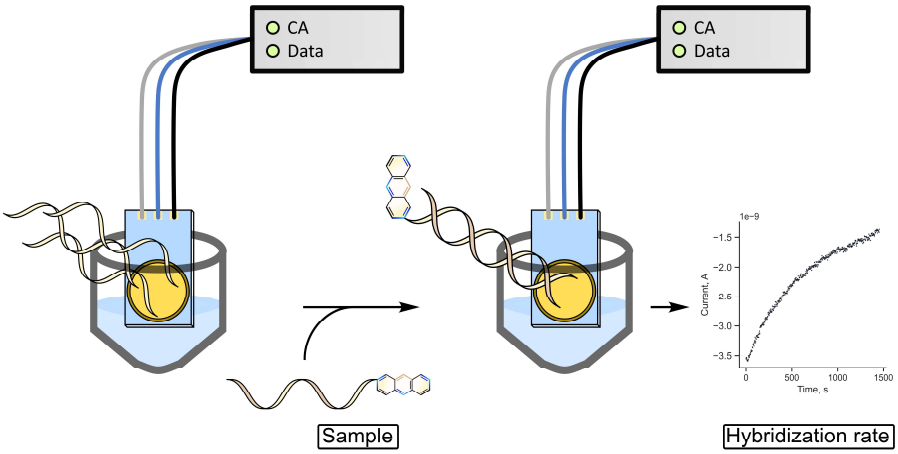


Figure 2. A representation of the workflow of the ascorbate mediated real-time hybridization monitoring assay. CA – chronoamperometry.

This was achieved via labeling the target strand with an oxidizer (MB^+) and introduction of a reducer into the solution (ascorbic acid) thus allowing for amperometric signal monitoring. The assay showed response in the 5-100 nM range producing signal on the order of 0.5-2.5 nA. The oligo association rate constants were measurable at different conditions and were in the range of 1000-8000 M^{-1} s^{-1} for varying [NaCl].

Based on these results I would expect a genosensor workflow to be in the range of 1-2 hours and predict the need to employ nucleic acid amplification for the measurement of real samples.

The third publication "**Fabrication of porous black gold films by one-step anodic treatment: towards the development of SERS-active nanosensors**" and its supplement Appendix III cover the development of a method for manufacturing SERS active electrode surfaces.

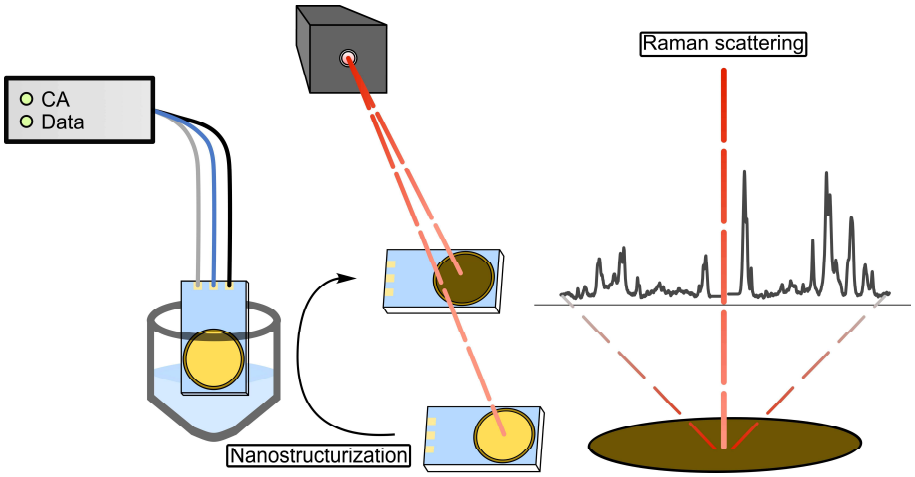


Figure 3. A representation of the workflow for generating SERS-active gold electrode surfaces. CA – chronoamperometry.

The electrodes prepared by our team show the promise of facile manufacturing and powerful Raman enhancement of 1.4×10^7. An enhancement factor of 10^5-10^6 is generally considered reasonable.[18] Clear SERS spectra of (Au-bound) 4-mercaptobenzoic acid and (SAM-adsorbed) doxorubicin were observed. Interestingly, the electrodes could be used to verify covalent surface modification and distinguish between adsorbed and bonded species.

While novel synthesis of solid phase DNA surfaces was not completed in this thesis, I am in the process of developing novel coupling reactions with varying degrees of success. Highly sensitive structural characterization is a key step towards developing such chemistries.

The fourth publication "**Constant Temperature Electrochemical Biosensor for SNP Detection in Human Genomic DNA Based on DNA Melting Analysis**" and its supplements Appendix IV and V cover the development of an assay for detecting the CYP2C19*17 (NG_008384.3:g.4220C>T) allele. 4220C>T is an interesting pharmacogene in that it is located in the non-coding region of the genome. The CYP2C19 enzyme contributes to the oxidative metabolism of many pharmaceuticals. We have successfully detected the *1 (normal), *1/*17 (rapid) and *17/*17 (ultrarapid) diplotypes in synthetic and PCR amplified biological samples. The sensor was melting kinetics-based, showing a >2σ signal difference between the diplotypes. The signal measured was the dissociation rate constant ratio or in other words, relative affinity for two reporter sequences.

The two reporter sequences were read over a 20-minute interval each at 0.05 Hz providing two 60 datapoint decay curves. Significant improvements over previous publications were achieved by performing *ex situ* hybridization by adding a small amount of buffer directly to the PCR amplicon and immersing the electrode in a small volume of concentrated sample for target capture. Additionally, polycationic ZNA probes were used on the electrode to allow the DNA duplex to collapse and transduce the signal even with longer DNA targets. Of the 6 tested saliva samples 5 were identified correctly with 1 QC fail. Additional sequence data can be obtained from the melting kinetics.

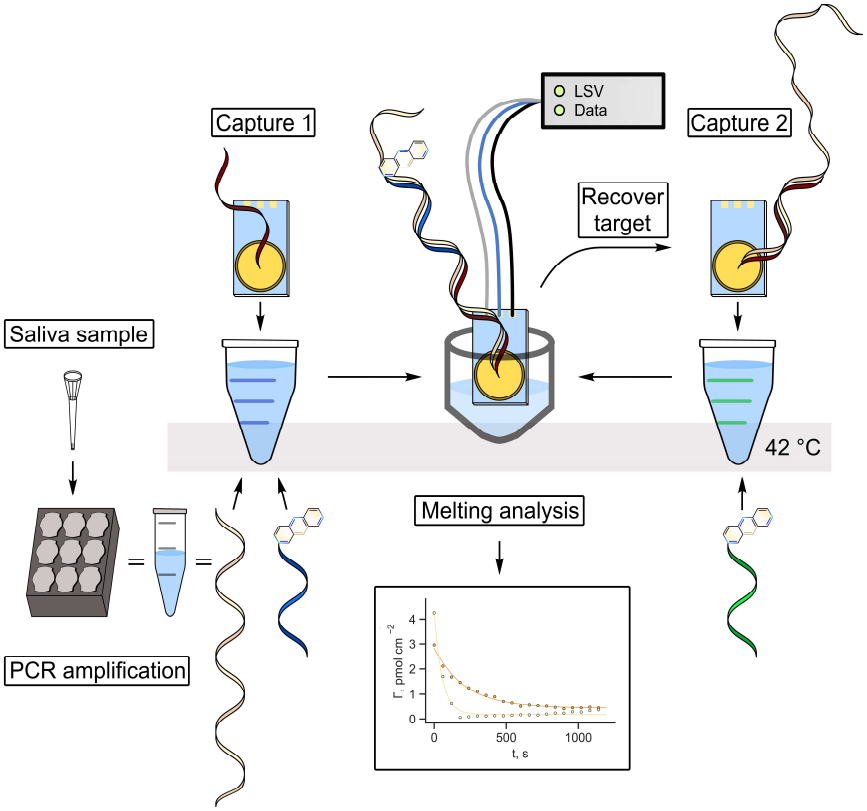


Figure 4. A representation of the workflow of the isothermal genotyping assay. LSV – linear sweep voltammetry.

While a device prototype was not constructed the design does not require many additional parts relative to our nuclease detection prototype device, where the measurement comprises potential sweeps under stirring and constant temperature. In fact, if the hybridization and the isothermal DNA amplification were to be conducted at the 42 °C measurement temperature, the devices would almost be cross-compatible.

Scientific novelty

A novel device for nuclease detection was produced. The device was able to measure DNase I concentration using screen-printed electrodes.

A novel biosensor for cytochrome P450 2C19 promoter region variants was designed. The biosensor utilizes a novel approach to detection via isothermal electrochemical dissociation rate monitoring. I believe I have developed the first isothermal dissociation kinetics-based DNA biosensor. A somewhat similar single molecule, polarization-based approach has been previously described. [19] While not completely novel, the design also grants a rare capability of differentiating between the homozygous and heterozygous samples on a single electrode. I believe this research was also the first to describe an electrochemical measurement of a single stranded nucleic acid base stacking energy.

A novel approach to gain additional sequence information from electrochemically measured melting rates via lookup of computed sequence–based properties was developed.

A novel method for manufacturing SERS–active electrodes was also developed.

Relevance

Publication I – DNase detection was mainly intended as an environmental test, but it may have various applications in diagnostics. Nucleolytic activity in saliva was measured. For further example application in RNase detection, see Appendix I.

Publication II – DNA hybridization signal amplification and real time hybridization monitoring are mostly relevant to research. For additional data on the applicability of the system to a sandwich configuration and one-pot multiplexing, see Appendix II. Amperometric multipotentiostat measurements at steady temperature may be feasible as a DNA quantitation platform.

Publication III – SERS-electrochemistry cross-compatible electrodes are mainly relevant in research at the moment. The flexibility of two detection methods may prove very powerful either in analyzing captured molecules or for electrode quality control (QC). In terms of QC, this method does allow for a facile surface chemistry standardization. For additional data on the application of SERS in characterizing surface conjugation see Appendix III.

Publication IV – Highly specific DNA detection with SNP discrimination has broad relevance, however the target is a pharmacogene, therefore, it is mainly relevant in diagnostics, however the system could be adapted to any short desired sequence.

For further data on signal transduction, see Appendix IV.

For further sequencing calculations, see Appendix V.

LITERATURE REVIEW

1. Genotyping methods and pharmacogenetic assays

For genetic diagnostics and research, sequencing methods are generally considered the best option due to the amount of information they provide and how powerful these methods are in terms of indels and short tandem repeats. There are special cases like OGM (optical genome mapping) for aneuploidies[20], imaging methods like ChIPSEQ for DNA-protein interaction[21] and MassARRAY for methylation.[22]

DNA microarrays have improved considerably since they began seeing widespread use and have continued to improve even recently.[23] They typically range from 200 000 to 4 000 000 features (e.g., SNPs) and can accommodate on the order of 1-24 samples. Typically, these assays require relatively clean, fragmented whole genome amplicon which is usually prepared in large amounts due to the number of targets. The whole assay may take on the order of 3-4 days (Thermo Fisher Scientific Axiom, Illumina Infinium)[24,25] and usually has a large footprint (e.g., a dedicated laboratory) due to the number of steps and equipment involved in amplifying, extraction, hybridization and scanning. However, the end result provides a large amount of highly valuable data and this approach is still generally cheaper than sequencing. Multiplex ligation-dependent probe amplification (MLPA) is a powerful approach with a feature number closer to 60.[26,27] Another electrophoretic method named Shifted termination assay (STA) while lower in feature number (~20) is much more rapid than MLPA (~3 h vs. ~18 h) and has reasonable mutant allele fraction sensitivity of ~ 1-2%.[28,29]

For detecting a smaller number of features (e.g., 6), ddPCR and qPCR methods dominate. These methods are generally quite fast and require very little sample. TaqMan StepOnePlus and SpartanRX have been used as on-site assay and point of care approaches for pharmacogenetic testing in a clinical trial with reported measurement time of 2-3 h.[30] ddPCR solutions currently are bulkier than what would be considered point of care, however they are used for high sensitivity applications such as cfDNA and have high throughput.[31,32]

In terms of point of care or "point of use" devices for so-called "molecular diagnostics" bacterial and mycobacterial tests are of note. For instance, in water system applications, relatively recently LuminUltra launched a GeneCount® Cube qPCR device for *Legionella* spp.[33] Genomadix's PCR-based pharmacogenetic Cube CYP2C19 System has been approved in 2023, for genotyping buccal swab samples in ~1 hour.[34] For

application in food, a *cyclospora* targeting device/assay was recently developed by Rheonix.[14]

For infectious disease, Cepheid provides a GeneXpert POC device dedicated for mostly infectious disease such as Influenza, Streptococcus, Chlamydia, SARS-CoV-2 and a number of others.[15]

2. Nucleic acid preparation

Nucleic acid extraction

As a common step prior to DNA analysis, DNA isolation can be extremely important. As a more universal approach, DNA is traditionally extracted by homogenizing the cells via proteinase K and surfactants with or without a chaotropic agent such as urea or guanidine.[35] The sample is usually further treated with ~5 M NaCl, optionally washed with a non-polar solvent and precipitated with EtOH or i-PrOH followed by centrifugation.

For small samples, guanidinium SCN-phenol-chloroform extraction is a highly practical approach, considering that the method is amenable to DNA or RNA extraction.[36,37]

Another popular approach is affinity chromatography, sometimes referred to as "spin column chromatography" where lysed samples are passed through a stationary phase in a centrifuge tube.[38] This approach conveniently allows for DNase pretreatment on solid phase before elution.

Pipette-tip affinity chromatography has emerged as an appealing next step for oligonucleotide isolation. TruTip offers an approach where a lysed sample is bound, washed and eluted inside a pipette tip for RNA or DNA extraction.[39] It has incorporated a monolithic stationary phase – a great approach for minimizing pressure difference and allowing for high flow, while the affinity methodology negates any monolithic column drawbacks – such as manufacturing repeatability or inferior resolution. Chromatography-based approaches are amenable to automation. An alternative automatable approach entails nucleic acid binding on magnetic beads – following a very similar protocol, except with the solid phase dispersed in the sample and magnetically retained.[40]

Another proposed approach is the ePrep system wherein a disposable electrophoresis chamber is used to isolate nucleic acids rapidly and with high throughput. [41] Currently, magnetic bead-electrowetting combined systems are considered state of the art.[42]

Nucleic acid amplification – targeted

Regular PCR amplification is very commonly used for amplifying a specific sequence. With regards to solid-phase capture, an advantage of PCR lies in performing an asymmetric amplification – adding an overabundance of the desired primer. This removes the need for denaturing the product – which has a tendency to renature – leaving only a limited amount of ssDNA available for binding. Isothermal sample amplifications are especially attractive – recombinase polymerase amplification (RPA) has been applied successfully in point of care applications.[43] What's even more exciting is that asymmetric RPA has been performed in a point of care prototype electrochemical platform and combined with the phosphorylated primer exonuclease digest, where it was found that asymmetric amplicon was not further improved by exonuclease treatment.[44]

Nucleic acid amplification – WGA

WGA (whole genome amplification) methods are currently exclusively or almost exclusively intended for DNA production. MSD (multiple strand displacement) is a highly appealing method as it is isothermal and provides reasonable yields of DNA.[45] Another method for unbiased single–cell amplification is MALBAC[46] (multiple annealing and looping–based amplification cycles), additionally providing "labeled" amplification products – which may be important for designing assays. This method, however is not isothermal.

Notably, RNA polymerase-mediated nucleic acid amplification methods like TMA[47] (Transcription-mediated amplification) and Self–sustained sequence replication[48] exist since the 1990s. There, a RNA-pol promoter is introduced into a DNA amplicon and then transcribed into many RNA copies (to be reverse-transcribed by RT or detected otherwise). This would seem like an appealing technology for WGA – rapidly and isothermally generating a single stranded, easily fragmentable RNA amplicon. Yet to the best of my knowledge, no such product or suitable (i.e., promoter–free) novel RNA polymerase has come to market since the inception of this idea. In spite of all that could have been, TMA–like *targeted* amplification has been incorporated into genosensors.[49]

Nucleic acid fragmentation

If WGA is performed – often the fragments are far too long to hybridize to a sensor or difficult maintain in a denatured state. Commonly used fragmentation methods include uracil glycosylase (if the amplification was performed with uracil), restriction endonuclease digestion and ultrasound.[50]

Covaris ultrasound based fragmentation has been used with genome sequencing.[51]

A unique non-enzymatic, approach involves guanine alkylation and opening of the ribose by piperidine, to the best of my knowledge, it appears this chemistry has been completely abandoned.[52] Non-specific exo/endonucleases have been used.[53,54]

Statistically, we can calculate, that when fragmenting (assuming completely random cuts) to ~100 bp fragments, a hydrolytic approach is expected to produce reasonable amounts of ~ 35 % guaranteed intact 100 bp "target" fragments (1 cut/100 bp ~ 35 % yield; 2 cuts/100 bp ~ 12 % yield) regardless of starting fragment size: (20 Mbp - 2 kbp):

$$P(\textit{Non-sequence bonds}) = \frac{\textit{Non-sequence bonds}}{\textit{Total bonds}} * \frac{\textit{Non-sequence bonds-1}}{\textit{Total bonds - 1}} * \ldots * \frac{\textit{Non-sequence bonds - n cuts}}{\textit{Total bonds - n cuts}}$$

$$\textit{n cuts} = \textit{DNA size} / 100 - 1$$

The complete fragmentation of the complementary strand is an equally important approach to allow and to speed up hybridization. Digestion with lambda exonuclease (λ Exo) after amplification with phosphorylated primers is a common approach.[55]

3. Nucleic acid capture and detection

Hybridization

For high selectivity the probe-target duplex length must be relatively short. We can see an example of a 7 bp-mismatch target showing a high affinity at 55 °C when the probe is quite long (70 bp).[56] While high resolution melting is able to distinguish between 300 bp sequences[57], realistically, a probe above 30 bp may already be less-suitable for detecting SNPs.[58] For recognition at "low" temperature toehold hybridization has been developed.[59] Toehold probes allow for excellent tuning of affinity[60] and have been used for high sensitivity genotyping.[61] We must however acknowledge that they may suffer from the fact that a liable blocking strand is required – therefore hybridization cannot be carried out at elevated or cycling temperatures. On the other hand, in sandwich hybridization at elevated temperature it is quite viable for two shorter *synthetic* strands (in stoichiometric excess) to displace one longer *native* complementary strand thus securing the target strand. This however only applies if a simultaneous sandwich hybridization is performed.

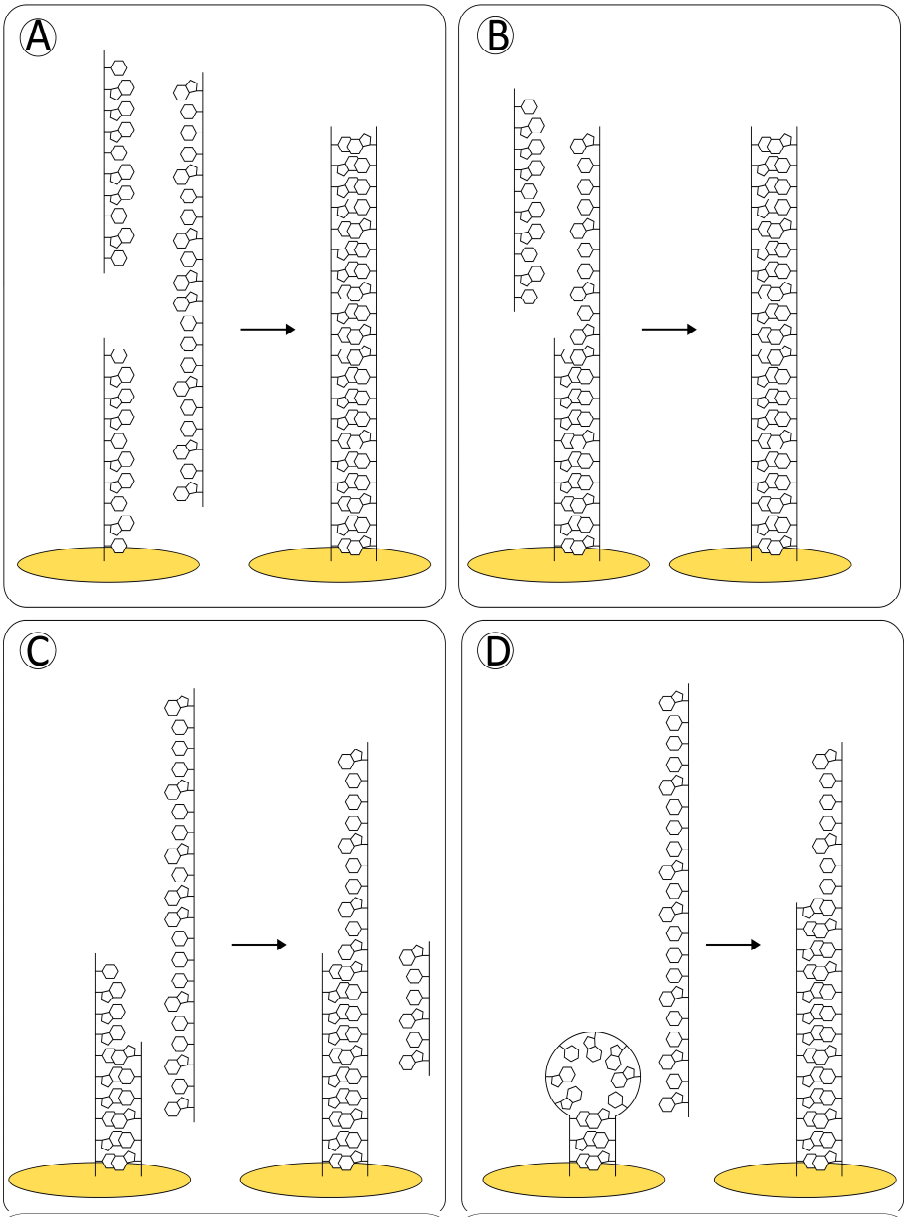


Figure 5. Possible solid phase hybridization approaches. A – simultaneous sandwich, B – stepwise sandwich, C – distal toehold probe, D – hairpin probe

When it comes to hybridizing to a solid substrate, the probe density plays an important part in the possibility and the density of hybridization. It is generally thought that ~4×10^{12} molecules cm^{-2} is a viable density with ~1×10^{13}

being excessive.[62–64] Conceptually reminiscent of molecular beacon FRET quencher systems, liquid phase hybridization detection (i.e., without DNA on solid phase) via electrochemical and HPLC has been proposed.[65,66]

Electroanalytical methods

Generally, potentiostatic (and potentiodynamic) methods (i.e., electrolytic mechanisms driven by the potentiostat as opposed to galvanic mechanisms) will be used in this work in order to induce the desired electrochemical reactions by applying a voltage, leading to a measurement of an analytical signal as an amperage.

Linear sweep voltammetry (LSV), where a linear increase in potential at the working electrode (Volts) up to a desired point produces a current response (Amperes) and cyclic voltammetry (CV), where the potential scan is additionally reversed are classic electroanalytical techniques. In a voltammogram we typically look for current-potential peaks. They provide the potential at which a species reacts, the number of electrons involved in the reaction and offer insight into the species' diffusion behavior and electron transfer rate. In regards to the methods used herein, the direct quantitation of a surface-adsorbed species can be achieved, via the quantity of electrons transferred (over a surface area) by fitting an electrochemical peak using the following equation:

$$i(E) = -\frac{n^2F^2v\,[Olig]\,exp\left[\frac{nF}{RT}\,(E - E_0)\right]}{RT\left(1 + exp\left[\frac{nF}{RT}\,(E - E_0)\right]\right)^2} + a_0 + a_1(E - E_0) + a_2(E - E_0)^2$$

Equation 1. The monolayer voltammetric current–potential curve fitting equation with background compensation for the quantitation of a redox-active species.[1,67] The left side of the equation is in the shape of a peak and the right side is a polynomial background:

i – current (A, the y-axis),

n – the number of electrons participating in the reaction (for methylene blue (MB) – 2 electrons),

F – Faraday constant (96 485 C mol^{-1}),

ν – the chosen potential scan rate (e.g., 0.05 V s^{-1}, while for surface adsorbed species high scan rates – in V s^{-1} are often desirable, labeled DNA performed poorly under high scan rates),

R – the gas constant (8.3145 J K^{-1} mol^{-1}),

T – the chosen temperature (in K),

E – electrode electrochemical potential (the x-axis),

E_0 – standard redox potential of the electroactive species (i.e., MB) (~0.255 V vs. Ag/AgCl; this value is fitted within a narrow range as it depends on the DNA-MB layer behavior; although not extensively applied in this work, the obtained E_0 is a useful metric for bound DNA construct characterization),

a_0:a_2 – the background current coefficients (although not extensively applied in this work, the obtained coefficients may be useful for the detection of abnormal/faulty electrodes in an automated device),

[Olig] – the amount of the surface adsorbed species (i.e., MB modified DNA (mol),

Note: in this case the electrode area is not considered; in my experience it is more convenient to calculate the absolute moles and to normalize the surface area afterwards if needed. It is assumed that the MB reduction reaction does not change the labeled DNA reporter strand hybridization affinity in any impactful way.

For sharp, well background–subtracted peaks, the maximal current at the voltammetric peak could be used to extract the surface–bound reporter quantity (*symbols as previously defined; A – area in cm^2; [Olig] in mol cm^{-2}*). [68]

$$i_p = [n^2 F^2/4RT]\,[Olig]\,A\,v$$

Equation 2. Peak current – surface coverage and scan rate relationship.

This approach may be beneficial for a more rapid, facile computation avoiding the need for non-linear least squares, especially if an assay is intrinsically ratiometric.

Figure A5 3.1 is presented as an LSV example sweeping from 0 mV (relative to Ag/AgCl 3M KCl) towards -450 mV. The downward–facing peak is caused by electron transfer from the electrode to a DNA–tethered redox species (MB) – inducing a reduction reaction. LSV does not reverse the scan, providing less information, but for quantitation purposes, it enables a faster scan and minimizes the time the electrode is passing current. Kinetics can be monitored by running voltammograms sequentially on the order of every few seconds to minutes depending on the scan rate (mV s^{-1} – V s^{-1}).

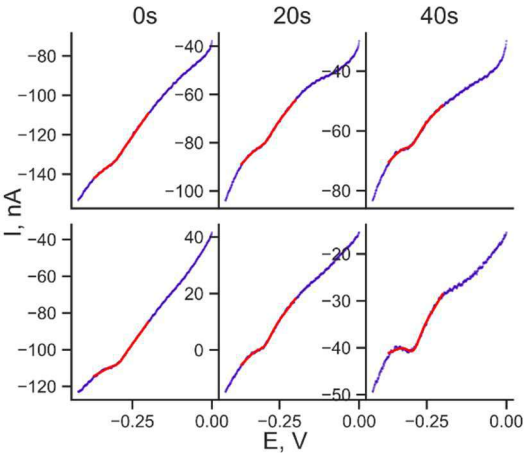


Figure A5 3.1. LSV peaks of surface-adsorbed MB label with fitting (red trace, Equation 1), under non-melting conditions (these LSVs are averaged to produce the 20 nM target DNA datapoints in **Figure A5 3 (A)**). Top: 0.5 mm, bottom: 1.6 mm electrodes.

Amperometry is a simple electrochemical technique where a static potential is applied and not varied and the current is monitored over time, producing a current vs. time curve. With fast current sampling this technique is effectively a real-time measurement.

For context, while (electrosynthetic) electrolysis may be performed at multiple (tens) of volts (albeit this is usually relative voltage), in sensors amperometry is often performed at hundreds of milivolts. This method practically eliminates all capacitive current and the measured faradaic current is proportional to the concentration of the electroactive species. The measured faradaic current is typically continuously decaying as the electroactive species is consumed, however this effect can be quite small at small electrodes. [69,70]

$$i(t) = i_{(t=0)}\, exp\, -\frac{D\,A}{\delta\,V}\, t$$

Equation 3. The function of the current decay over time under stirred conditions in constant potential amperometry.

i – current (A, the y-axis),
D – the diffusion coefficient ($\mu m^2\ s^{-1}$)
A – the electrode area (μm^2)
δ – the diffusion layer thickness (μm)
V – the solution volume (μm^3)
t – time (s)

Notably, sometimes an exhaustive electrolysis method can be desirable, and a membrane or a frit may be employed to prevent the migration to and regeneration of an electroactive species at the counter electrode.

Grafting and monolayer formation

To create a heterogeneous phase suitable for DNA recognition the DNA probe (or another recognition molecule) must be affixed to the surface. Preferably, the spaces in between the DNA probes are to be backfilled in a way that does not interfere with hybridization but eliminates non-specific signal.

The coupling of gold to thiols is a classic approach where a sulfhydryl or a disulfide generates an Au-S bond on a gold surface.[71] This reaction is rapid (a few minutes for initial coverage) and forms high density, highly repeatable self-assembled monolayers (SAMs).[72] The Au-S bond has significant stability issues at reductive voltages and elevated temperatures.[73] Trithiolated layers have been used at relatively high (80° C) temperatures.[74]

Gold-alkyne bonding is a novel approach showing somewhat improved stability over thiols.[75] Gold-phosphine monolayer bonding has been described in literature[76–78] but is very uncommon in practice.

Grafting of highly stable aromatic layers can be achieved in mild reductive conditions via *in situ* formed aryldiazonium compounds – this conjugation can yield well-controlled relatively thin layers.[79] The aryldiazonium salts can be prepared *in situ* via a traditional cold acidic $NaNO_2$ solution or in organic solvents via organic nitrites.[80,81] The electrochemically generated radicals seemingly did not destroy a linked antibody during grafting.[82] It must be emphasized that it is easy to deposit a very thick polymer-like layer especially if the diazonium solution is formed *in situ* and the concentration may be unknown. Diazotization of aliphatic amines is almost never performed due to poor stability.

Non-diazotized aromatic and importantly – aliphatic amines can be grafted directly via electrochemical oxidation, providing a convenient way of highly stable *directed* aliphatic modification.[83–85]

It is important to be aware of potential driven decarboxylation[86] which occurs at similar potentials (around ~950-1000 mV vs. SCE). From personal experience in grafting Ω-amino acids, this can make later functionalization via amidation impossible, however carboxyls can be preserved by carefully controlling the potentials (I would recommend up to ~600 mV vs. $Ag/AgNO_3$ in acetonitrile). The decarboxylation is *in and of itself* an another approach to graft (oxidation-stable or protected) functional groups. Notably, an entire

research field of carbon-carbon bond formation via (electrochemical) decarboxylation has recently come to the foreground[87], despite being proposed in the 1890s.[88]

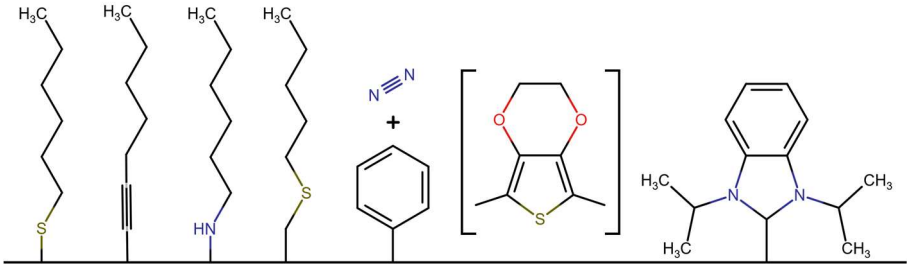


Figure 6. From left to right: Thiol SAM, Alkyne SAM, Grafted aliphatic amine, Thiol-ene grafting, Aryldiazonium grafting, PEDOT polymer, N-heterocyclic carbene SAM (see text for details).

A functionalization-ready surface can be prepared by electrochemical polymerization – such as the formation of an azido-PEDOT layer.[89]

A classic approach common in immunoassays has also been used where target DNA is adsorbed on polystyrene-polybutadiene copolymer from solution.[90] Electrochemically triggered grafted group deprotection is possible.[91,92] An elegant photocatalyzed thiol-ene approach has been put forth for both directed conjugation and patterning, but we must be aware that the generation of a sulfhydryl covered surface is not an easy task.[93] An approach with wonderful acid/base, thermal, oxidative and organic solvent stability based on N-heterocyclic carbene (NHC) films has come to the fore recently. These SAMs are created on gold via a carbene – a (shelf-stable) neutral diradical–like compound derived from a deprotonated heavily substituted imidazolium salt.[94] Unfortunately, despite otherwise superb layer stability, NHC layer degradation is observed upon electrochemical reduction. Commercial applications like CombiMatrix[95] protect their platinum surfaces with a polymer, presumably to i) allow reliable covalent bonding, ii) prevent metal-catalyzed side reactions.

A notable outlier in generating monolayers is the non-covalent pyrenebutyric acid (and derivative) stacking onto graphene and related substrates.[96]

Conjugation

The DNA probe may be introduced via grafting or chemically linked to the grafted molecular layer as a separate step.

Crosslinking may have originally become highly relevant as a method of gluing cellulose with the classical agents such as glutaraldehyde, polyepoxides and divinylsulfone now having been used for around a century.[97] Shortly after the introduction of "one carbon bridge" and "zero-length" crosslinkers[98] via formaldehyde activation and EDC crossreaction respectively, the concept of "two step zero-length crosslinking" in the form of activated esters was proposed via R-CO-NHS for amides in 1990.[99] Notably, the concept of an activated carboxylic acid in the form of R-CO-DMAP$^+$ cation for ester synthesis emerged much earlier in 1979.[100] This procedure was a massive leap forward and is still commonly used, with powerful new acylation agents still emerging.[101–106] Emphasis on longer heterobifunctionalized crosslinkers came soon after.[107]

The notable Sharpless Lab changed the landscape of conjugation chemistry with their selective aqueous azide-alkyne addition.[108,109] An amino-yne reaction with terminal or non-terminal electron withdrawing group containing alkynes has been shown.[110] Similarly, the thiol-ene click reaction is another useful approach.[111] DNA is traditionally linked via the azide-alkyne addition, maleimide coupling or via amide bonds.[112]

Unlabeled DNA signal transduction

One of the simplest ways to transduce a hybridization signal is via an intercalating agent. Intercalation can usually occur via:

- Outside edge binding – more phosphate specific (e.g., $[Ru(bpy)_3]^{+2}$)
- Intercalation – usually flat aromatic compounds (e.g., ethidium bromide)
- Groove binding – usually larger molecules than intercalation (e.g., Hoechst dyes) [113,114]

Intercalators besides fluorescence and redox signals can also produce a catalytic signal.[115] Unfortunately, this chemistry can be unreliable – for instance binding to ssDNA[116] as well as adsorbing to proteins, lipids or a solid substrate.

Intercalation of agents like methylene blue to detect DNA is still used as an alternative to covalent modifications or for binding structures like G-quadruplexes.[117]

Labeled DNA signal transduction

Covalently bound labels are available via: a complementary reporter strand via sandwich hybridization[118], distance-dependent signal via opening of a hairpin[119], modified dNTP incorporation via a polymerase[120] and (indirectly) via covalently modified Cas9.[121]

In electrochemical analysis, it can be very difficult to eliminate the signal from soluble redox-active molecules and DNA labeling is by far the more reliable approach for specificity.

Although electron transfer via the DNA duplex in a fashion similar to a highly conjugated molecular wire has been proposed[118,122,123] (usually under very strict conditions), it is difficult to account for and rule out the effects of geometry changes when solubilized dsDNA is interrogated on a surface.

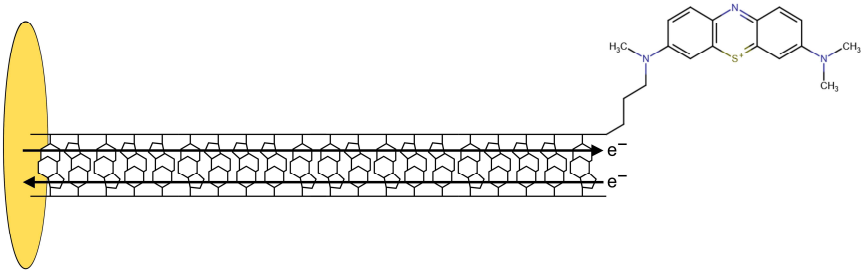


Figure 7. A representation of charge transport through a DNA molecule.

For instance, a case of reported rapid, low voltage, long-distance dsDNA charge-transfer[118] could be explained by the presence of spermidine, which is now known to collapse the DNA strands on surfaces.[124,125] If such relatively flat DNA duplexes were produced by DNA collapse, they would likely result in behavioural similarities between long and short redox-labeled oligomers (appearing as intantaneous, through-DNA conduction). Further support of contact-mediated charge transfer is expressed in literature from observations where both duplex formation and increasing monolayer densities result in lowered charge-transfer rate.[126] Since 2000s-2010s DNA seemingly has achieved limited application as a molecular wire at mild votages and highly conjugated modifications yield vast improvements in its conductivity.[127] Generally, an electroactive label proximal to the electrode produces a powerful signal and the label distal to the electrode produces a weak signal (i.e., minimal dsDNA conductivity is observed). These effects have been demonstrated via SWV to occur simultaneously as the DNA hybridization process “quenches” an existing distal label signal and introduces an increasing proximal label signal. The authors note that proximal reporter signal is still

diminished due to ion screening and should be higher.[128] In a similar fashion, many assays utilize the dsDNA signal quenching as a means to detect hybridization via a labeled hairpin probe.[129] The restraining of a dsDNA molecule has also been attempted via increasing viscosity through addition of glycerol.[128] I suspect that the changes in the screening ability of the solution by glycerol were quite marked, recognizing the difficulty to increase the matrix viscosity without affecting the matrix in other ways.

Similar behavior has been demonstrated via CV also reporting the electron transfer rate constant via SWV to be 0.7:140 s^{-1} for distal and proximal MB labels respectively.[130]

Signal amplification

Note: The categories are arbitrary. There may be large overlaps between the concepts.

Oligomerization

By forming large clusters of a signaling molecule the signal can be significantly amplified. In electrochemical assays by conjugating a large amount of MB onto gold nanoparticles detection in the 50fM range has been reported.[131] As biotin-steptavidin can form dendritic structures via anti-strepatvidin-biotin and the reagents are commercially available, this approach is common. Commercially available large beacons such as FluoSpheres (Thermo Fisher Scientific) or DiagNano™ Streptavidin Quantum Dot Beads (CD Bioparticles) are also available.

Catalytic

Catalytic signal amplification entails connecting an enzyme or another catalytic subunit as a signal transducer. Often the difference between a catalytic and a cumulative signal is arbitrary and I make these distinctions to create a theme for the reader. Conjugates such as streptavidin-HRP or ALP are a common and powerful approach. One of the mainstay methods is the HRP-H_2O_2-TMB reaction in ELISA[132]. For electrochemical genosensors sensitivity with HRP detection down to 60fM has been reported.[133]

Cumulative

Cumulative signal amplification approaches typically rely on deposition or growth of a product on the signal transducer. This category includes one of the original signal amplification approaches: silver staining in microbiological and medical imaging.[134] Biometallization approaches can be regarded as cumulative and very high sensitivities have been achieved.[135,136]

Resistive signal amplification

Resistive signal amplification is again, almost identical to cumulative approaches as some analyte or product must be deposited onto a conductive

surface. However, in this case the focus is on generating a very large signal on the "naked" sensor which subsequently is quenched by analyte recognition. For electrochemical genosensors HRP mediated precipitation of benzo-4-chlorohexadienone with reported sensitivities in the 600fM range.[137] Polymer and dendrimer[138] substrates are used for obtaining high resistive signals.

Charge accumulation

It is less common to accumulate a large potential bias or like-polarity ion concentration. Such processes are highly unfavorable and are more frequently encountered in biofuel cells. Minute charge accumulation can be detected by tuning to a specific gate voltage in a MOSFET. If a charged molecule (such as DNA with counter ions) is captured this small change in gate voltage produces a large source to drain current.[121]

Captured sample amplification

Additional sample amplification can be performed after hybridization. RCA has been applied to massively increase the size of DNA reporters.[139] Solid phase RPA utilizing modified dNTPs as ferrocene labels has been applied for simultaneous signal amplification and sequence recognition.[120]

Electrochemical genosensors

To date some excellent electrochemical genosensor designs have been proposed. A highly accurate device for measuring a genotype has been reported by Yang et al. (2014).[74] In this case a synthetic unlabeled ssDNA target is used. The sensor captures the target onto solid phase via a distally labeled trithiolated probe. These probes are remarkably thermally stable up to ~80 °C. After the hybridization the device can be filled with fresh electrolyte and a stepwise temperature ramp is performed. The melting is monitored via alternating current voltammetry. The device consists of a Peltier element with a gold electrode containing PDMS microfluidics requiring sample volumes on the order of 10 µl.

Yenice et. al. (2023) has demonstrated a wonderful melting temperature-based device. The sample is prepared from a capillary blood sample which undergoes in-solution hybridization with a ferrocenylated primer and is amplified isothermally via asymmetric RPA.[44] This yields a sample solution with proximal-side ferrocenylated ssDNA targets which bind to solid phase probes. As targets are synthesized with a preexisting label, sandwich hybridization or probe labeling methods are not needed. The electrode array is then placed into a solid phase thermal block and the temperature is scanned stepwise with a DPV recording at each temperature. This creates a thermal

melting curve, allowing to discern between alleles including heterozygous samples.

The device consists of an Arduino-based syringe pump and Peltier element with a 64 gold electrode array containing PMMA microfluidics. A really meaningful design change reported therein is the use of an Au pseudoreference, which greatly simplifies array manufacturing and makes the method highly scalable.

A highly innovative approach to accelerate the k_d of a dsDNA strand via an electrostatic bias was proposed by Vernick et al. (2017).[19] In contrast to potentiostat where a bias is measured versus the reference and an unknown bias exists versus the counter electrode, the study used FET electrodes where the bias is recorded versus the gate (V_g) which represents the surrounding solution. The DNA probe is grafted to a carbon nanotube via aryldiazonium followed by amide condensation and is hybridized to the target. The team found that melting curves can be recorded at a constant temperature by changing the V_g and these melting curves differentiate a SNP target. As the device records source-drain current, and not a voltammetric measurement, the bias can be applied constantly.

Realistically such FET devices are very powerful but extremely difficult to manufacture. As the grafting is electrically switchable there is great potential for miniaturization. While on paper nucleic acid amplification may not be needed using FET electrodes, realistically capturing unamplified neat genomic or viral DNA is not an easy task.

A different mode of recognition in a FET device has been shown by Hajian et al. (2019).[121] In this case the DNA recognition event modulates the V_g-V_s potential which causes a change in current. In this approach the DNA recognition occurs via a dCas9 which is complexed with a target-specific RNA sequence.

The most pressing issues in genosensors

Some excellent prototype devices have been proposed to date, such as MEQ-LAMP and others.[44,120,140] While some signal amplification methods are justifiable, polymerase-based amplification clearly serves as the foremost, multi-purpose tool. Generally, it would be desirable to have fewer plausible points of failure and limit the amount of enzymes, nanomaterials, master-mixes, etc.

Label-free methods are very popular but as they are intrinsically capable of producing a signal without any secondary labeling, it may be difficult to maintain full confidence under variable test conditions without a full suite of controls.

One of the biggest issues in genosensors is the sample automation. Generally, sample-to-answer platforms are the most convenient and desirable. While some simple tasks are soluble via capillary action or vacuum-chambers, the complex sample preparation for genetic measurements has typically been done by a pipetting robot. Currently, various microfluidic, electrowetting on dielectric (EWOD), magnetic beads or centrifugation options are encountered commercially for more complicated tasks.

Another very important challenge in genosensors is miniaturization. This means removal of the pumps, heat control, as well as power supply potentiostat and electrode size diminution by clever design. These two latter areas (sampling and miniaturization) are generally difficult to approach as doing so requires complete commitment to the current (electro)chemistry.

Genotyping is an important function that does not always get directly addressed in genosensors. The approaches of adding genotyping capability are often via multiplexing electrodes[120], temperature sweep melting[74,141] and using two allele-specific reporters on one surface.[61]

Generally, it is difficult to avoid readout multiplexing which poses assay and device design implications – intermittent versus constant electrochemistry, one-pot versus separate cells, shared microfluidics versus EWOD chips, analog signal conditioning and conversion and other important parameters.

In a broader context, electrochemical genosensor development to commercial products may be stifled by intrinsically low throughput. As compared to e.g., fluorescence where no direct chemical interaction is required (i.e., touching the solution), and 50-100 samples may be plausible in a minute with a single sensor. Highly intricate mechanochemical (QCM) or semiconductor (gFET) electrodes are at a further disadvantage from this perspective.

What about sequencing?

There are many applications where DNA sequencing simply cannot be replaced by genotyping or target detection, such as haplotype determination (e.g., identifying the interplay and assigning all present variations to one specific protein). Impressively, such subtle differences have been mechanistically verified *in vitro*.[142]

Electrochemical and electronic methods have been prolific in the rapidly evolving field of DNA sequencing and they will be briefly covered to contrast the technologies better.

In the early days of Sanger sequencing the only electrochemical application was gel, capillary[143] and later multi-capillary electrophoresis (Applied Biosystems 3100).[144–146]

Despite capillary analyzer improvements to 384-formats [147–149] electrophoretic methods had a general throughput limitation and the optical array-based Roche 454 analyzer brought a start to the NGS revolution in the mid-2000s.[150]

Despite the dominance of the chemiluminescence driven Roche 454 analyzer in the late 2000s and the latter overwhelmingly fluorescence-based systems (such as Illumina MiSeq, NovaSeq; PacBio RS; Thermo Fisher Scientific SOLiD; MGI DNBSEQ), electronic analysis methods have continuously brought innovations in the genetic assay field.

Sequencing by synthesis (SBS) was elegantly translated into electrical detection bringing about the Ion torrent analyzer soon after its commercial breakout via ion-sensitive field-effect transistor (ISFET) based detection.[151]

A very exciting approach to electrical sequencing readout followed with Oxford Nanopore MinION. [152–154] The device uses a transposase and sequencing adapters ligated onto a long genomic DNA strand. The readout is at 400 bases s^{-1} and over 4Mb length. The basecalling is processed via measuring current passed through the nanopore at a bias voltage. The company followed up with PromethION in 2017 massively expanding the throughput with 24 flow cells.

Prayoga Life Sciences GenapSys Sequencing Platform added to the list with their novel electrically detected SBS approach. It uses solid phase one nucleotide at a time addition which produces continuously increasing electrical impedance in steps corresponding to the added nucleotide.[155]

LiDia-SEQ, an ISFET-based device with sample-to-answer onboard processing is being developed by DNAe.[156]

Further innovation has been demonstrated by the recently announced Roche Axelios 1 sequencer. The device will measure current through a nanopore by using a chemically labelled DNA sequence. The target sequence is converted to Xpandomer sequence by coupling expandable nucleoside triphosphate bases containing polyamine, polyphosphate and polyether moieties. As the Xpandomer surrogate passes through a nanopore, the current for each base is much more identifiable than for a corresponding DNA polymer. [157]

Structural variations (such as alterations in gene copy numbers or translocations) are detected at larger scales of the genome (100s to 100 000s of base pairs) than DNA sequence mutations. OhmX, a solid-state resistance-

based electronic nanochannel commercial solution (single-molecule) has been developed by Nabsys and released in 2023. [158]

Overall, electronic or electrochemical DNA sequencing readout has seen numerous applications. While sequencing workflows are generally significantly more expensive than a genetic ("molecular diagnostics") assay, they can provide invaluable insights.

The relevance of DNase and RNase in environmental and diagnostic fields.

Both RNase and DNase monitoring are important and effective tools in biobank, calibration and testing laboratories.[159] This is especially noteworthy for laboratories where nuclease digestion takes place as a step in nuclear material isolation or fragmentation. At the same time, bacterial DNA/RNA in environmental or food samples may undergo rapid degradation in presence of nucleases, making genetic environmental tests unreliable. Therefore, detecting the nuclease activity in samples may be a viable precaution. Extraneous DNase seemingly did not impact DNA detection in intact *C. jejuni* cells (20 °C and 55 °C pretreatment), but for cells lysed at high temperatures, external DNase significantly decreased the nuclear material.[13] Extraneous RNase I has been shown to degrade environmental RNA with a strong impact on 16S rRNA, which is generally a good target for determining species.[160] Considering that environmental tests for known sequences are strong candidates for affinity based detection, the ability to screen samples for nucleases is a powerful feature for future genosensors. Our sensor (**Publication 1**, workflow: **Figure 1**, mechanism: **Figure 8**) measured DNases recovered in environmental samples (swabs) ranging between 0.05 U ml^{-1} (a breakroom table) and 0.0013 U ml^{-1} (a computer keyboard) DNase I equivalents.

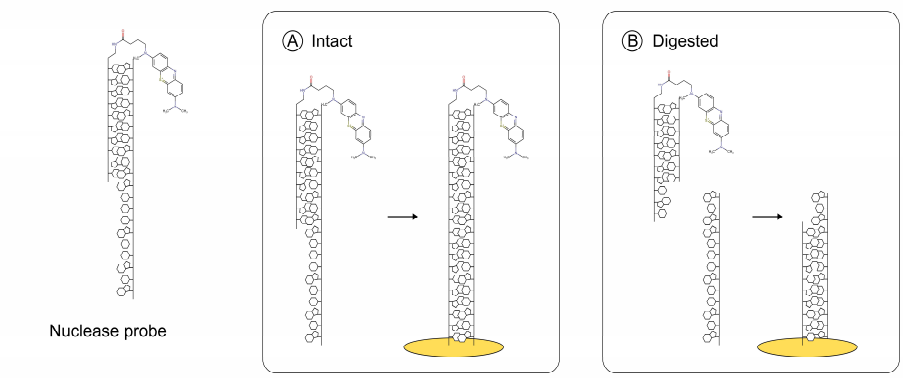


Figure 8. A representation of the nuclease detection mechanism used.

Similarly, discernible activity was detected in commercial protein preparations >0.05 U ml^{-1} (Glucose oxidase) and 0.0058 U ml^{-1} (Papain),[161] indicating a widespread and unpredictable, nuclease contamination. Overall

performance was comparable to commercial assays (**Figure A1 1**, **Appendix I**)

Both human endonucleases[162] and exonucleases[163] have been reported to have significance in cancer diagnosis.

In short, our nuclease biosensor can be used in biotechnological and diagnostic fields. Both RNase and DNase detection sensitivities were comparable to commercial kits but had lower dynamic range.

The relevance of signal amplification in genosensors.

The sensitivity in affinity based detection is twofold: there are the equilibrium association and dissociation constants and there is the signal to noise. Increasing the signal therefore entails producing a *stronger response* at, say 0.1% surface saturation and/or increasing the *target density* on the surface.

We can see that the 1–10 nM limit of detection in our genosensors could perhaps be attributed to the fact that a substantial fraction (a few %) of the target is captured and concentrated on the surface. At 0.8 nM [Target] there are more *available* probes on the surface than there is sample in the entire bulk of the solution (100-120 µl), (**Table 1**).

Target, nM	Target, nmol	Target captured, nmol 0.031 cm^{-2}	Target captured, %	Molecules, cm^{-2} (Reporter)	Probe molecules, cm^{-2} (RuHex)	Surface saturation, %
0.8	9.6×10^{-5}	$1.42\pm0.2\times10^{-6}$	1.5%	2.7×10^{10}	3.5×10^{12}	0.8%
3	3.6×10^{-4}	$1.19\pm0.4\times10^{-6}$	0.3%	2.3×10^{10}	3.5×10^{12}	0.7%
12.5	1.5×10^{-3}	$6.7\pm4.6\times10^{-5}$	4.5%	1.3×10^{12}	3.5×10^{12}	37.3%
50	6×10^{-3}	$1.5\pm0.08\times10^{-4}$	2.4%	2.8×10^{12}	3.5×10^{12}	81.1%

Table 1. 5×SSC solution hybridization (20 minutes, one-pot, 37°C) efficiency, of a flush DNA target on regular DNA probes (data from **Appendix V, Figure A5 2**). At 0.8 and 3 nM, detection is not observed (*Note: with density-controlled ZNA electrodes, 3.2 nM [Target] is readily visible*).

Indeed, an increase in target density via probe density seems unproductive. An improvement of 3–6× was achieved in our system by controlling the probe density (see **Figure A5 3B**) and this likely cannot be improved any further. Packing more DNA onto the surface will decrease the hybridization efficiency, where "high density" surfaces (>5×10^{12} molecules cm^{-2}) trend towards 10–20% efficiency.[64] In our case, the area just above the gold (12.5 nm) should have on the order of 4 mM DNA.

Target hybridization efficiency improvement at low DNA concentrations was attempted by "forcing" the hybridization through different hybridization buffers as improvements have been noted in literature.[164] The differences between the 5×SSC and the 30% EtOH HEPES buffers were minimal (See **Appendix V, Figure A5 2**). Some other buffers (such as 20% MeCN HEPES or regular PBS with a large amount of blocking oligonucleotides – to check for target depletion via adsorption onto plastics or degradation) have been briefly tested and showed no signal at low (a few nM or lower) DNA concentrations and such experiments were not further pursued. As an article by Vanderhoeven et. al. succinctly states: "… *spot intensity and the final detection limit are purely equilibrium-dominated quantities, and can hence not be improved by hybridization enhancement methods*…"[165] and arrives to the conclusion that only changing the dimensionality or reducing the feature size may improve the LOD. Notably the authors state that the LOD is improved via the sample **concentration** increase through volume contraction. Our experiments led us in a similar direction arriving at low volume *ex situ* hybridization in a dedicated low volume vessel which is not used for any measurements. Another team has found that smaller feature size improves the hybridization efficiency and that the feature edges show much improved hybridization efficiency.[166] An improvement in efficiency was also observed through glycol spacers – where a longer spacer (up to a certain point) results in higher DNA capture.[167] Others report that a 5 µm feature microarray behaves as well as a 30 µm one. The study shows that the median fluorescence intensity follows the trend 5 µm > 8 µm > 30 µm, but it is difficult to tell if the arrays are directly comparable. [168] My preliminary results (See **Appendix V**) indicate that no real improvement in sensitivity was had by lowering the feature size (K_D: 2 mm = 3.8 nM, 1.6 mm = 3.7 nM, 0.5 mm = 3.5 nM) (**Figure A5 1**). At 0.5 mm diameter, it is notable that the overall current and the signal to background become quite poor (i.e., any electrical noise or system capacitance will have a larger impact).

Ø	K_D
0.5 mm (ds-SAM)	3.5 nM
1.6 mm (ds-SAM)	3.7 nM
2.0 mm (ds-SAM)	3.8 nM
2.0 mm (ss-SAM)	28.5 nM



Figure A5 1. The hybridization sensitivities of different electrode disc sizes.

Albeit these were not true microelectrodes, a decrement of 2 mm → 0.5 mm, represents an area reduction of around 15×, therefore a change in the sensitivity on this scale would be clearly distinguishable, bringing the K_D to 0.2 nM range. This mechanistically represents the total probe molecule impact, ruling out the target depletion mechanism.

In these electrodes, the concentration gradient is maintained at around 3 nM → 4 mM solution to surface (4 mM is an arbitrarily calculated "concentration" of the DNA monolayer). These results strongly imply that the mass transport (I typically used a 20-minute solid phase capture interval for practicality) is the main limitation.

At the same time, (assuming 5 nm DNA molecule diameter), the fraction of the "outer layer" probes (circumference probes at the electrode edge, having few neighbors and thus very easily accessible) to total probes on the electrode increases around 4 times. However, the outer layer fraction is meaninglessly small, on the scale of 1 in 10^6; therefore, this size reduction does not realistically test the impact of the probe accessibility mechanism. This mechanism was not further explored as very small electrodes would mandate very low current measurement, which brings its own hardware and non-diffusing molecule LSV signal transduction problems.

The bottleneck of low currents when measuring very small electrodes with slow charge transfer via potential-sweep methods emphasizes the appeal of constant-potential methods with a diffusing molecule as a signal carrier, therefore, amperometry may be a viable choice for miniaturization.

In terms of an amperometric detection we have published a method for chemical reduction-mediated signal amplification (**Publication 2**, workflow: **Figure 2,** mechanism: **Figure 9**).[169]

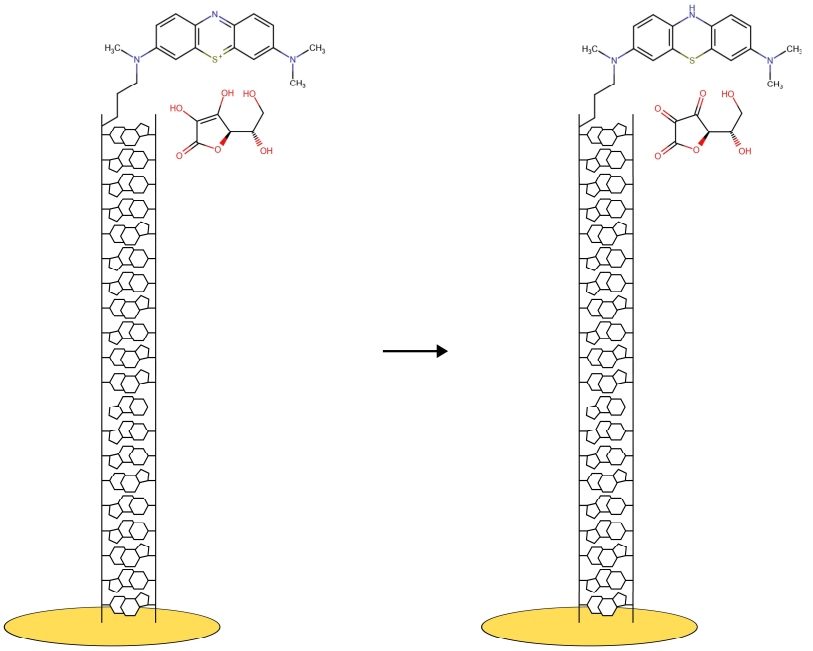


Figure 9. Chemical MB label reduction at the electrode.

While relatively small signal amplification was achieved (a few nanoamperes at saturation) this method remains intriguing for microelectrode use. It is possible that drastically lowering the surface area will allow for extremely low sample volumes. At the same time, ascorbic acid diffusion would be improved. An amperometric approach may perform better at very low currents than a potential sweep as it eliminates the capacitive component. Thus, this approach remains interesting. I have demonstrated for clarity that the reaction still works in a sandwich configuration and in multiplex readout, but was unable to improve the reaction rate via label positioning (see **Appendix II**). Reaction rate loss has been reported in a similar system upon chemically modifying nucleobases, indicating that the oligo construct clearly impacts the reaction.[170] In my experiments, positioning the MB label in the middle of the DNA chain completely destroyed the detection with DNA probes, but not with ZNA probes (see **Appendix II, Figure A2 2**).

In short, sample size contraction and DNA probe density control produce viable but limited improvements in sensitivity. Altering hybridization buffer composition or electrode size reduction down to 0.5 mm did not notably improve sensitivity. Further feature size

reduction is desirable but will likely present very low currents. A reaction monitoring approach for real-time measurement of hybridization is presented.

The relevance of conjugation in biosensors:

Broadly speaking in chemical and biochemical assay **methods** and standalone **components** (e.g., magnetic beads, affinity resin, solid phase peptide synthesis, batteries etc.) solid phase (bio)molecule grafting is a process of the highest importance. However, it is in my personal experience and observed by some others that verifying *the nature* of the coupling chemistry is difficult.[171,172] In fact even differentiating between adsorption/ agglomeration/ precipitation and grafting presents extreme difficulties. This is due to i) minute chemical differences between a ligated and an adsorbed molecule and ii) a single molecular layer represents a small quantity thus requiring a high sensitivity method. Therefore, it is common for a grafted molecule to be confirmed via i) function or ii) presence but not often via iii) chemical bonding. Often the various ligation chemistries (e.g., comparing the assay using two completely different surfaces, solvents or antibodies, etc.) are compared as "apples to oranges". This is somewhat unavoidable because the reagents, the biomolecules and the surfaces have drastically different behavior (due to size, charge, intermolecular interactions etc.), which cannot be easily compensated for. Unfortunately, "non-ligation controls" (e.g., minus carbodiimide) are not standard especially in more complex assays.[172–174]

The inability to confirm coupling with high confidence can become a serious problem when designing new grafting chemistries and manufacturing processes.

The widespread use of blocking agents (often containing naturally occurring proteins, oligosaccharides or synthetic polymers[175]) in bioassays further emphasizes the pervasive problem of unexpected adsorption events. If a low solubility compound forms a strong non-polar interaction, it can be surprisingly difficult to remove.

For nucleic acid detection, solution phase recognition is the extremely scalable in terms of price and volume, e.g., for primer-polymerase methods you could manufacture a million reactions worth of master mix. Unfortunately, it becomes impossible to manage a library of >1000s of primers, unless they are adhered onto a substrate. Currently, it is desirable to attach DNA probes via various linkers to change their behavior (e.g., flexibility, charge) and to selectively bind specific sequences to multielectrodes.

The main methods to study grafting or chemical modification of a surface at the moment are XPS/ESCA for **composition** and oblique reflection FTIR/PM-IRRAS or AFM-IR for **bonding**.[176,177] All three are highly specialized methods. Other methods like AFM,[178] SEM,[179] liquid scintillation,[180] antibody staining[95] or SPR[181] are capable of confirming the presence of a modification but are not usually able to indicate bonding.

Through this discussion I wish to bring attention to an important bottleneck in sensor array development (research and optimization) and manufacturing (quality control). When developing a novel directed ligation chemistry (*I wish to keep the methods outside of the scope of this dissertation as these processes are still in development*) I have run into a case of interfering non-directed ligation or adsorption problems which serve as a good example of SERS-active electrode application. (**Figure A3 6**).

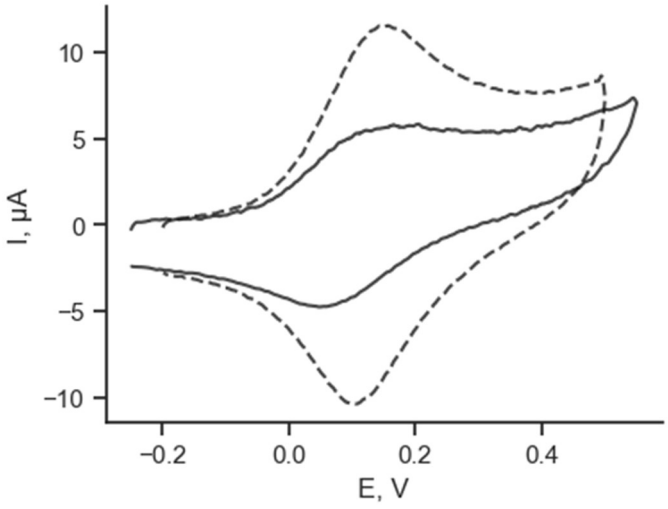


Figure A3 6. A directed ligation chemistry currently in development. **Dashed line:** directed ligation, **solid line:** simultaneous non-directed coupling side-reaction onto a nearby electrode.

In other words, a neighboring electrode in an array (intended for a subsequent modification for a separate target) may parasitically couple to a biomolecule during the first step, and perhaps, show an electrochemical signal (i.e., presence detected, without revealing the mechanism). Such non-directed cross-reaction may well occur in photo/electrochemical, fluidic, thermal, dropcasting or other means of directed array modification, underscoring the importance of a rapid, inexpensive, sensitive and spatially-addressable auxiliary surface structural analysis method.

An interesting prospect arose during our SERS-active electrode testing (**Publication 3**, workflow: **Figure 3**), where various surface modifications could be structurally detected. Turns out, the adsorption and ligation of 4-aminobenzonitrile (used as a proxy for a biomolecule) can be differentiated based on the relevant functional group bands (see **Appendix III, Figure A3 4**).

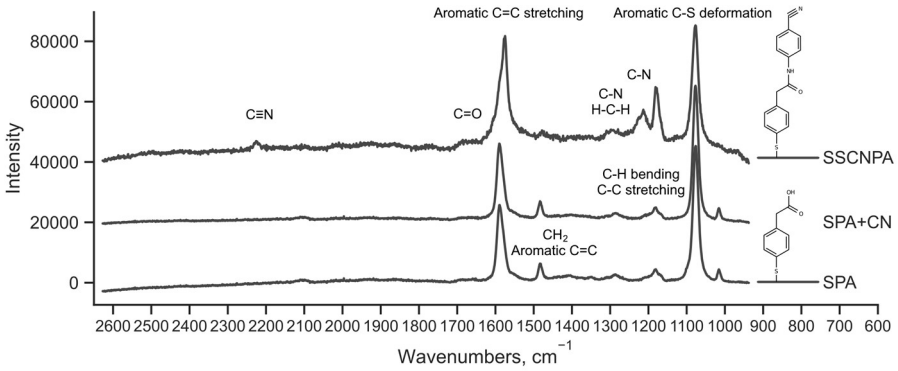


Figure A3 4. SERS spectra of SSCNPA, SPA + CN and SPA (clean) with tentative peak assignments.[182]

While limited to a gold substrate this is a facile and rapid means to measure bonding. Such an application clearly elevates the research and manufacturing relevance of these electrodes. Most interestingly, the preliminary SERS experiments indicate that nanostructured gold enhances the proximal (nearby) functional groups much better than the more distant ones. Therefore, in principle there is selectivity for nearby bonds while far-away bonds may perhaps be selectively enhanced separately afterward.

Aside from one or two-step couplings/graftings, conductive polymers and MIPs (molecularly imprinted polymers) are some of the very few commonly encountered solid phase synthesis products in electrochemical analytical methods.

On the other hand, "piece-wise" receptor construction on the electrode is almost never used (i.e., solid phase synthesis of peptides[95] and proteins to capture small molecules, oligonucleotides to capture DNA or, for instance, oligosaccharides to be used as antigens).

Fundamentally, step-wise solid phase synthesis is a perfectly viable and powerful approach, especially for highly diverse molecules. If a deprotection or a coupling reaction can be easily confirmed via a SERS measurement, these step-wise methods may become more approachable.

Another plausible application yet to be explored is confirming directed (oriented) antibody linking.

In short, if solid phase synthesis or directed conjugation methods on electrode surface do gain traction in the future, SERS will be a good option for verifying the reactions. Verifying one-step coupling is currently viable on SERS-active electrodes.

The importance of signal transduction in affinity genosensors:

A major signal transduction problem was encountered with larger DNA target molecules where the distal DNA overhang produced significant interference (**Publication 4**, workflow: **Figure 4**, signal transduction: **Figure 10**). It was suspected that the MB label was encapsulated by the overhanging strand's negative charges or lost mobility through the increased hydrodynamic radius and thus, the MB label was unable to approach the electrode.

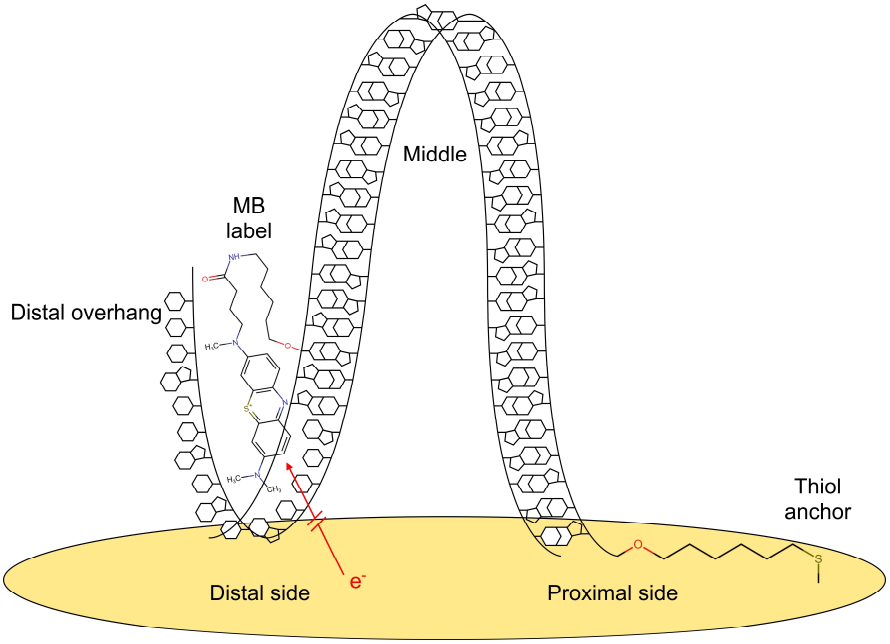


Figure 10. Sandwich representation containing the **DNA probe** and **R*1** which has a distal MB label. Only the distal **T*1** overhang is shown. The sandwich is likely in a more "upright" conformation than shown. This is an attempt to represent a macromolecular structure. The "average" conformation is not known. Elements are not to scale.

As the label is on an upper reporter strand it was impossible to get the MB labels proximal to the surface. An attempt was made to chain the electron transfer through:

ReporterMB → ProbeMB → Probe|Target → Electrode

This approach would dramatically increase the remaining MB background post melting but I expected to account for it via data fitting. Unfortunately, this approach was also unsuccessful (see **Appendix IV, Figure A4 2.2.**).

Our results were comparable to other sources. Silva et. al.[183] show findings where if we assume perfect hybridization, as the probe density is quite low, we can extrapolate an MB label position to signal relationship as such:

ssDNA: Distal > Almost proximal ~ Almost distal ~ Proximal

dsDNA: Proximal > Almost proximal ~ Distal > Almost distal

This "Almost distal" middle position proves highly unfavorable for a label as it is electronically (due to encapsulation by negative charges) blocked from approaching the surface. Similarly, rather than affixing the label towards the middle, keeping the label proximal and lifting the whole duplex upwards via a spacer (where the probe effectively has a proximal overhang) produces increasingly lowered signal.[184] *Note: if we were measuring say, some phenoxazine derivative at +0.8 V vs. Ag/AgCl, these observations may no longer apply.*

If the mechanism of conduction through dsDNA stacked nucleobases is assumed this behavior becomes very difficult to explain. To further this point, a distally MB-labeled ssRNA target performed perfectly well in an RNase sensing application in **Appendix I**.

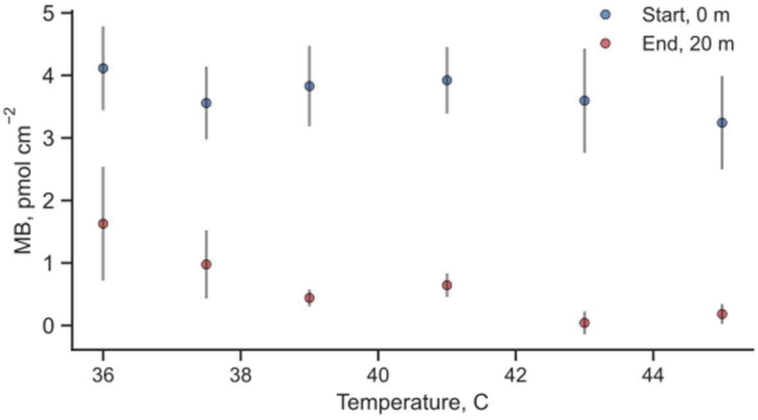


Figure A4 1.3. (from Appendix IV) shows the starting and end MB signal at various temperatures.

Unexpected dsDNA bending has been observed in solution at frequencies of up to a hundred thousand times higher than predicted.[185] One of the proposed mechanisms is the melted-bubble model where DNA spontaneously forms melted sites at ambient conditions.

Figure A4 1.3 shines additional light on the matter of *through-DNA* versus *DNA-mobility* mediated signal transfer. Through-DNA transfer relies on the idea of a fully pi-stacked chain, but we know this is not the case in nature where DNA is constantly partially melting and reannealing. If ds-DNA were the conductor, we would expect a temperature-dependent loss of signal, rendering all melting-based sensors impractical.

An important observation regarding ssDNA came from Uzawa et al.[186] where no impact on charge transfer was noted from probe packing density. This implies that DNA crowding is an unlikely explanation to poor signal transduction.

In our case, the PCR amplicon has distal overhangs which impede the voltammetric signal significantly (see **Appendix IV, Fig. A4 1.2**). To fix the signal transduction, it would have been reasonable to attempt inverting the probe and reporter strands so that the target molecule hangs "downwards" toward the surface, but I was concerned about the impacts this would have on hybridization. With on the order of 3.5×10^{12} probes/cm^2 we suspected our electrodes to be near 10% of the maximum theoretical ssDNA packing[187] and in practical terms at maximal density for dsDNA.[62] The inversion of sandwich geometry therefore raised valid concerns. The DNA probe molecules in the immediate vicinity of the inverted target may repel the oncoming reporter molecules.

A safer approach seemed to collapse the sandwich structure, thus eliminating the signal transduction problems. This was attempted via polyamine containing ZNA–4 probes lowering the net charge of the probe molecules from –21 to –10. This approach was very successful, eliminating the signal transduction problems and granting tolerance for overhanging PCR-produced targets.

> *Note: at the probe charge of –10, a very small amount non-specific reporter adsorption could be observed if the electrode is interrogated immediately after hybridization and without reaching 42 °C. This is acceptable in our system, however, at complete neutrality we would expect unwanted DNA adsorption.*

In contrast to probe-linked polyamines, adding free polyamines into solution would possibly result in uncontrollable polyamine accumulation and possibly lead to non-specific DNA adsorption.

Another successful approach to fixing the charge transfer problems was also attempted. By attaching MB via a flexible polyethylene glycol sidearm rather than directly to DNA, the MB mobility is improved. This approach now works in both DNA– and ZNA–probe sandwiches, with a longer distal (3') sidearm being the most preferable (**Figure A4 4.2**).

In short, while it is believed that charge transduction through dsDNA occurs, I was unable to force electrochemical transformations of DNA-tethered methylene blue in many configurations. It appears that under the experimental conditions used, the charge transfer is occurring via DNA label mobility.

The importance of SNP assays

Distinguishing between two single base-mismatched sequences and their combination can give information about slight differences in proteins between individuals which is highly applicable to diagnostics.

In **Publication 4**, a PCR amplicon is captured onto a solid phase probe, and interrogated with 2 different allele-specific reporters. In addition, an approach similar to gene sequencing allows us to gain extra sequence information during the screening of a specific target (see **Appendix V, Figure A5 5.**).

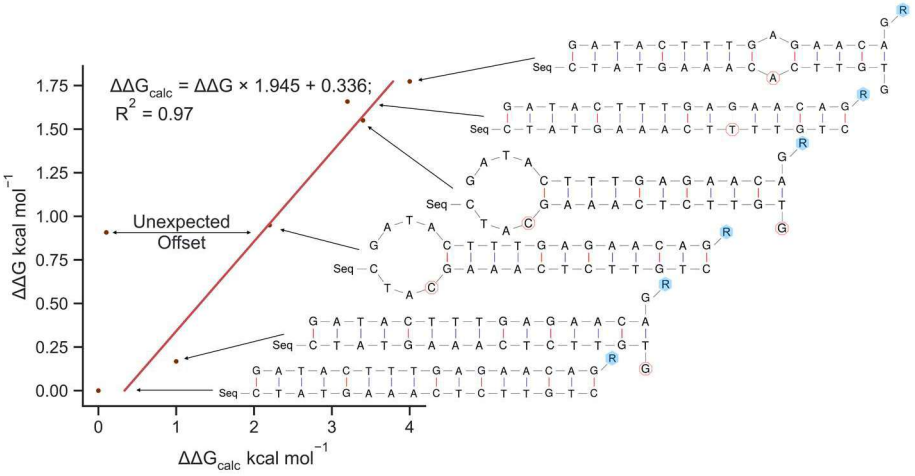


Figure 11. Sequence-dependent changes in hybridization energy. Data from **Publication 4**. Unexpected offset denotes a digitally unaccounted for

nicked site heterocyclic base stacking interaction (and is equal to the stacking affinity) (see **Publication 4**).

Albeit the genosensor was designed for multiplexing, in terms of true scalability, the use of a specific reporter sequence is a major challenge. Objectively speaking, the use of **target-specific reporters** after a certain point is not scalable. Once you are trying to measure up to 200 million sequences it becomes to the best of my knowledge, impossible to manage the fluid handling. While various innovative liquid handling approaches have been proposed such as voltage-mediated dispensing from droplets,[188] or electrowetting on dielectric[189] this is likely an insurmountable obstacle. For instance, Ion Torrent uses on the order of 8-14 solutions in total for any DNA target.[190,191] Therefore, the scope of applications of the proposed assay falls more into the characterization of a handful of genetic targets.

The genosensor was not only able to detect different genotypes in real, non-invasive saliva samples, but also characterize various other mutations by how destabilizing they are. This was also translated into the units of kcal mol^{-1}, allowing for measured vs. calculated energy comparison (**Fig. 11**).

Solution phase Gibbs free energy has been recently used in assay design to predict crosshybridization; with a recommended difference of $\geq -9 + 7.5$ kcal mol^{-1} ΔG which results in around ≥ 1.5 kcal mol^{-1} $\Delta\Delta G$ under given conditions.[192] This is not too dissimilar from the sequences we selected for our study, comprising around 2.2 kcal mol^{-1} (solution phase $\Delta\Delta G$) in the case of homozygotes and half that in the heterozygous allele (see **Publication 4**). The strength of the DNA base stacking interaction was found to be on a similar magnitude. I calculate the A|G base stacking energy to be on the order of **2.0 ± 0.3 kcal mol^{-1}** (literature ~2.1 kcal mol^{-1}).[193]

The obtained equilibrium constants (**Appendix V**, **Figure A5 1**) are quite reasonable as they suggest the binding to be on the order of 10.9–12.2 kcal mol^{-1} depending on the probe density (in agreement with DinaMelt provided sequence-based hybridization ΔG of 12.1 kcal mol^{-1}). Interestingly, when compared to DNA hybridization, antibody-antigen and aptamer-ligand equilibrium dissociation constants are not significantly better.[194,195]

In DNA affinity sensors a fundamental limitation is reached where a sample solution containing a similar quantity of DNA to the amount of the interrogating probe (or size and density of an interrogating surface) will likely give poor signal. At 0.17 pmol/surface (0.0314 cm^2) that is 1.7 nM for a 0.1 ml sample. In practice (see **Appendix IV**, **Figure A5 3**) the signal becomes clear

in the range of 3-20 nM. However, a 1.7 nM solution of the human genome (if amplified and processed) when translated into 30 bp oligos equals a solution with ~350 mM oligos. In practice a DNA oligo solution of 5 mM (on the order of 100 mg/ml), is already highly concentrated and can show marked changes in viscosity. For a more general sequencing application a dramatic reduction in electrode size would be necessary.

> *In short, a novel genotyping platform has been developed, capable of genotyping heterozygous samples at ~ 10 nM of DNA. This suggests that the current sensitivity of the genosensor is perhaps three to four orders of magnitude too low to perform "sequence fishing" in a fragmented whole genome amplicon of a sample, yet, if tergeted amplification is used, it is possible to extract some sequence information.*

A summary of the broader insights

Generally, these genosensors are suitable for the analysis of any nucleic acid sequence, indeed we have observed good signal transduction form an RNA reporter. Besides recognizing a specific oligonucleotide, these assays can be implemented to: glean additional sequence information, quantify relative and absolute abundance, observe nucleolytic reactions and likely others, like ligation, extension, etc.

Significant improvements were introduced to lower the required amount of DNA from the first iteration (~195 pmol) such as *in situ* hybridization signal amplification via a redox reaction (~25 pmol) and *ex situ* hybridization (~0.5 pmol). Attempts of hybridization acceleration, surface miniaturization, attempting to route the redox signal transfer, chemical signal amplification generally provided only marginal improvements in sensitivity. DNA probe density and sample contraction provided only linear improvements, but were impactful in ensuring good sensitivity. MB-labeled DNA appears to perform the redox charge transfer though a chain mobility or other physical proximity mechanism.

Applying this system to real samples research has led to an innovative incorporation of charge-altering ZNA probes enabling the use of targets with larger overhangs. This is yet to be published, but non-charge altering ethylene glycol spacers between the DNA and the MB molecule performed equally well (in combination with both DNA and ZNA probes).

While the DNA concentration inference from the hybridization rate is accurate and also sufficient to detect DNase and RNase with good sensitivities, fundamentally, the dynamic range for nuclease measurement is quite low, as the concentrations needed for rapid hybridization are moderate.

While the chemically (ascorbate) amplified hybridization rate measurement can be performed in real time, the obtained currents were quite small, requiring a considerable amount of time (~ 1 h) to reach saturation. With constant temperature and electrode potential, this approach could provide the benefit of inexpensive and simple electronics.

While the decay curve of DNA melting contains its sequence information, the resolution we currently have is much too small to perform a *de-novo* sequencing of a 16-bp region. Low salt concentration and the addition of formamide allowed us to measure relatively rapid (15-20 min) melting reactions at moderate temperatures (42 °C). This sensor ignores by design any need to carefully control the reporter strand crosshybridization to a mismatched target and exploits this behavior.

CONCLUSIONS

Overall, three nucleotide affinity based biosensor types were produced. The results are as follows:

1. DNA and RNA sequences were detectable voltammetrically (hybridization), amperometrically (hybridization) and voltammetrically (dehybridization) in “synthetic” and real samples.

2. Point mutations were detected in homo- and heterozygous diploid samples, isothermally. 5 human saliva samples were genotyped for CYP2C19 *1 and *17 alleles correctly.

3. Sensor-relevant design features were explored and incorporated.
   - 3.1. SPE use for nuclease detection.
   - 3.2. A prototype analyzer was produced for Nucleases.
   - 3.3. Nanostructured porous gold electrodes were developed allowing to observe spatial and molecular properties via SERS.
   - 3.4. Electrode chemical functionalization assessment via SERS was demonstrated as a proof of concept.
   - 3.5. A direct PCR amplification followed by direct hybridization were used without sample DNA or amplicon purification.
   - 3.6. Isothermal methods significantly lower the device complexity, size and energy use.
   - 3.7. Amperometric DNA quantification was explored as it is important for microelectrodes and would simplify the potentiostat design.
   - 3.8. Analysis of diploid samples achieved on a single surface.
   - 3.9. One-pot melting analysis with solid phase hybridization was achieved, thus removing pumping, heating and waste removal steps.
   - 3.10. *Ex situ* hybridization allows for sample pooling, amplification multiplexing and sample reuse.

Genetinio kodo sekų detekcija yra ypatingai plati sritis turinti didžiulę įvairovę taikinių. Tokie metodai leidžia identifikuoti ir apibrėžti mikro- bei makro-organizmus bei jų savybes. Sveikatos apsaugos sritys remiasi ypatingai svarbiais DNR paremtais diagnostiniais metodais kaip navikų arba sveikų ląstelių žmogaus genomo charakterizavimas. Šie metodai dažnai naudojami parinkti tinkamiausiai gydymo krypčiai. Pavyzdžiui, farmakogenetinis žymuo gali būti nustatytas vieną kartą prieš farmakoterapiją, tuo tarpu vėžinės ligos progreso stebėjimas gali būti naudojamas ir terapijos metu.

Geneojutikliai yra biologiniais procesais paremti prietaisai galintys specifiškai aptikti DNR arba RNR grandis. Genojutikliai pasižymi prieinamumu, tiek savo kaina, tiek savo paprastumu, ir jų naudotojai turi tiek asmeninių duomenų, tiek analitinio instrumento fizinę kontrolę.

Žinoma, žmogaus genomas nėra vienintelis taikinys, mikrobinės taršos nustatymas maisto, vandens ir kitose terpėse taip pat yra svarbi užduotis, tinkama genetinės analizės metodams. Mikrobiologiniai organizmai kaip *Legionella pneumophila*,[9] *Escherichia coli*[10] ir *Enterococcus*[11] gali būti matuojami **vandens mėginiuose**, įvairūs pelėsiai[12] **– oro mėginiuose**, bei *Campylobacter jejuni*[13] ir *Cyclospora cayetanensis*[14] **– maisto mėginiuose**.

Dar viena taikymo kryptis yra infekcijos sukėlėjų identifikacija bei, dažnai tuo pačiu metu atliekami, antibiotikų atsparumo matavimai. Įvairių mikroorganizmų kaip SARS-CoV-2, Ebola, ŽIV, Hepatitas C, *Clostridium difficile*, meticilinui atsparių *Staphylococci*, VanA turičių *Enterococci* bei kitų organizmų aptikimas yra dažnai taikomas.[15,16]

Problematika

Biojutiklių kontekste, nors įvairūs signalo stiprinimo metodai suteikia didelius jautrius, DNR sekos replikacija polimerazėmis atlieka tiek signalo stiprinimą, tiek mėginio apdorojimą vienu metu. Taigi, DNR (arba RNR) amplifikacija yra turbūt dažniausiai naudojama fermentinė reakcija genojutiklių dizaine. Atveijais kai metodas atsiremia į fermentinę (arba kitais baltymais, pvz., antikūnais paremtą) amplifikaciją, tipiškai, metodo veikimas yra apribotas baltymo stabilumo ir tokie metodai gali būti mažiau tinkami komerciniam analizatoriui kurti. Dizaino atžvilgiu, norima signalo pernašą paremti paprastesniais zondais. Žinoma, norint tyrinėti baltymų-DNR sąveiką, tokie metodai yra nepakeičiami.

Metodai nenaudojantys žymėjimo (angl. label-free), yra labai patrauklūs, tačiau, išgaunant signalą tiesiai iš mėginio reikalinga didelė imtis kontrolinių

matavimų, kad įsitikinti ar antriniai mechanizmai negali sukelti nespecifinės detekcijos.

Viena iš didžiausių kliūčių genojutiklių kūrime yra automatizuotas mėginio paruošimas. Paprasti skysčio transporto uždaviniai yra sprendžiami kapiliarinės jėgos arba vakuumo pagalba, tačiau sudėtingesni – reikalauja mikrofluidikos, dielektrinės membranos elektrodrėkinimo technologijų (angl. *electrowetting on dielectric*) arba pipetavimo robotų. Modernūs mėginių apdirbimo instrumentai taip pat dažnai naudoja magnetines nanodaleles, elektroforetinius mėginio apdorojimus bei centrifūgavimą. Kitas svarbus žingsnis yra miniatiūrizacija, t.y. pompų bei kaitinimo sistemų pašalinimas ir elektrodų bei potenciostatų (ir jų maitinimo šaltinių) sumažinimas.

Genotipavimas (DNR atpažinimas organizmo kontekste) yra kitas svarbus iššūkis sprendžiamas daugybiniais elektrodais[120], kintamos temperatūros lydymu[74,141] ir naudojant du aleliams specifiškus zondus kartu ant vieno paviršiaus.[61]

Bendrame kontekste, elektrocheminė detekcija reikalauja skystinio kontakto su analizuojamu mėginiu ir ši mechanika fundamentaliai riboja mėginių nuskaitymo spartą lyginant su pvz. fluorescencija, kur vienas fotodetektorius gali pamatuoti 50-100 mėginių per minutę. Šis trūkumas ženkliai didėja su elektromechaniniais (angl. „QCM“) ir puslaidininkiniais (angl. „gFET“) prietaisais, naudojančiais daug sudėtingesnius paviršius.

Šia disertacija siekiama sukurti biojutiklius tinkamus specifinėms DNR sekoms nustatyti, kurie palengvintų genetinių matavimų atlikimą ir prieinamumą. Šiam tikslui pasiekti buvo apibrėžti 3 uždaviniai:

1. Specifinės DNR sekos aptikimas elektrocheminiais biojutikliais.
2. Taškinės mutacijos aptikimas biojutikliais bei atskyrimas homozigotinių ir heterozigotinių mėginių.
3. Šių uždavinių atlikimo metu, metodo dizainas turi supaprastinti arba palengvinti diagnostinio/analitinio prietaiso kūrimą. Technologiškai priartėjama prie realistiško prietaiso.

Šių uždavinių įgyvendinimą galime plačiai apibrėžti tikslinių nukleino rūgščių specifinio atpažinimo sistemų kūrimu, DNR molekulinių monosluoksnių bei hibridizacijos procesų optimizavimu, elektrocheminių signalų matavimu, bei duomenų analize. Atliekamos papildomos dizaino, charakterizavimo ir gamybinės užduotys.

Gauti rezultatai buvo paskelbti keturiuose straipsniuose. Tolimesni papildantys darbai buvo pridėti kaip disertacijos priedai.

Pirmajame straipsnyje buvo pademonstruotas elektrocheminis metodas bei naujas prietaisas skirtas nukleazių aptikimui. Šis prietaisas gali atlikti kiekybinius deoksiribonukleazės I matavimus ant vienkartinių elektrodų.

Nukleolitiniai fermentai yra svarbūs pramonėje bei diagnostikoje. Šis metodas naudoja dgDNR zondą, kurio skilimas (suvartojimas), sumaišius su kieto paviršiaus tepinėliu arba skystu mėginiu, gali būti pamatuotas pagal hibridizacijos greitį. Kadangi zondo hibridizacija ant komplementarios elektrodo sekos tiesiogiai priklauso nuo zondo koncentracijos, gaunamas hidrolitinės reakcijos našumas ir nukleazės koncentracija gali būti apskaičiuota. DNazės I aptikimo riba – 0,34 mvnt. ml^{-1}; Pirmame disertacijos priede sistema taip pat buvo patikrinta naudojant RNR zondą, kur RNazės A aptikimo riba – 1×10^{-6} Kunitz vnt. ml^{-1}. Šie rezultatai gerai prilygsta komerciškai prieinamiems (chromogeniniams / fluorogeniniams) rinkiniams.

Antrajame straipsnyje aprašomas befermentine redukcija paremtas DNR hibridizacijos signalo (nanoamperų lygio elektros srovės) stiprinimo metodas. Šis metodas paremtas imobilizuotos ant elektrodo paviršiaus, taikiniui komplementarios DNR grandies, ir metileno mėliu žymėtos taikinio DNR grandies hibridizacija matavimo celėje. Atliekant šį taikinio prijungimą su aksorbo rūgštimi tirpale, hibridizacijai ir cheminei metileno mėlio redukcijai palankiomis sąlygomis, išgaunamas amperometrinis signalas realiu laiku. Metodas leido aptikti specifines DNR molekules 5-100 nM koncentracijų intervale. Sistemos veikimas naudojant nežymėtą DNR taikinį papildomai parodytas antrame disertacijos priede.

Trečiame straipsnyje aprašomas vienkartinių bei daugkartinių aukso elektrodų paviršių oksidacinio nanostruktūrizavimo metodas. Šiuo metodu pagaminti elektrodų paviršiai pasižymi reikšmingu paviršiaus sustiprintos Raman sklaidos (SERS) stiprinimo faktoriumi – 1.4×10^{7}. Taigi, šie elektrodai yra tinkami (fiziniai) substratai tiek elektrocheminiams matavimams tiek spektroskopijai. SERS spektrai buvo tinkami identifikuoti tiek prijungtą 4-merkapto benzoinės rūgšties monosluoksnį, tiek nespecifiškai adsorbuotas doksorubicino molekules. Trečiame disertacijos priede yra aptariamas SERS pritaikymas įvertinti kovalentinėms paviršiaus modifikacijoms. Toks struktūrinis monosluoksnio charakterizavimas yra labai svarbus žingsnis kietos fazės DNR sintezei ir jungimo reakcijoms vystyti.

Ketvirtame straipsnyje aprašoma CYP2C19*17 alelio genotipavimo sistema. Citochromo P450 2C19 izoforma yra atsakinga už įvairių mažų

molekulių oksidcinę apykaitą. *17 alelis yra nekoduojančioje genomo dalyje ir įtakoja fermento ekspresiją, kuri yra aktuali vaistų metabolizmui.

Ši sistema sėkmingai identifikavo įprasto (*1), greito (*1/*17) bei itin greito (*17) metabolizmo diplotipus, tiek švariuose sintetinės DNR mėginiuose, tiek seilių mėginių amplikonuose (specifiškumas >2σ). Sistema yra paremta DNR duplekso lydymosi kinetika ir mano žiniomis, tai yra pirmas izotermine disociacijos kinetika paremtas genojutiklis. Taip pat, ši sistema pasižymi reta savybe – diploidinis mėginys gali būti analizuojamas ant vieno elektrodo. Vieno paviršiaus santykinis signalas ženkliai supaprastina elektrodų gamybinio atkartojamumo problematiką.

Metodas buvo sustiprintas zip-nukleino rūgščių (ZNR) pritaikymu DNR atpažinimui ant kietos fazės bei asimetrine skystos fazės PGR – tokiu būdu sistema yra tinkama ilgesniems DNR taikiniams ir taikinių fiksavimas ant elektrodo gali būti įvykdytas iškart po amplifikavimo, be jokių gryninimo, fragmentacijos ar denatūracijos žingsnių.

Metodas taip pat buvo jautrus papildomoms taškinėms mutacijoms ir mano žiniomis, tai yra pirmas elektrocheminis jutiklis pamatavęs nukleobazių stekingo sąveikos stiprį (išraiška vienetais – kcal mol^{-1}).

Apibendrinantys pastebėjimai

Apibendrinant, šie genojutikliai yra platformos, fundamentaliai tinkamos bet kokios (santykinai trumpos) DNR sekos aptikimui ir net RNR yra pritaikoma analitė. Šių matavimų metu taip pat galima išgauti informaciją apie DNR sekos pokyčius, reliatyvų bei absoliutų kiekį, vykstančias nukleolitines reakcijas bei DNR ilgį.

Keičiant genojutiklių dizainą, DNR jautris buvo ženkliai sustiprintas nuo pirmo jutiklio naudojančio *in situ* hibridizaciją elektrocheminėje celėje (~195 pmol), iki *in situ* hibridizacijos redokso stiprinimo (~25 pmol) ir *ex situ* hibridizacijos (~0,5 pmol). Bandyti hibridizacijos greitinimo, elektrodo paviršiaus ploto miniatiūrizacijos, signalo pernašos mechanizmo bei redokso amplifikacijos krūvio pernašos patobulinimai nesuteikė ženklaus (pvz., >3×) DNR jautrio pagerinimo. DNR zondo tankis ant paviršiaus ir mėginio tūrio dydis keičia jautrį tiesiškai, tačiau leidžia reikšmingai ir nesunkiai pagerinti genojutiklio veikimą. Redokso molekule žymėtos, ant kieto paviršiaus esančios DNR krūvio pernašos elgesys sutampa su DNR mobilumo ar kitokiu fizinio suartėjimo mechanizmu. Nors signalo pernašos pagerinimui pritaikėme poliaminais modifikuotą krūvinį ZNR zondą (krūvio kompensacija paremta pernaša), elektrocheminiai žymenys prijungti per lanksčius, nekrūvinius etilenglikolio intarpus taip pat davė puikų signalą (žymens mobilumu paremta pernaša). Abi pernašos pagerinimo strategijos suteikia

galimybę matuoti DNR taikinius besitęsiančius virš atpažinimo zondų, tokiu būdu jutiklis nereikalauja apibrėžto ilgio taikinio.

Nors DNR (bei RNR) koncentracijos apskaičiavimas pagal hibridizacijos greitį yra patikimas ir tinkamas nukleolitinių fermentų reakcijų matavimams, šio metodo dinaminis diapazonas yra palygintinai siauras, kadangi vis mažinant DNR koncentraciją, hibridizacijos laikas ženkliai ilgėja.

Nors MB^+ redukcija askorbo rūgštimi leido matuoti hibridizaciją realiu laiku ir naudojo labai paprastas pastovaus potencialo bei temperatūros sąlygas, išgautos srovės buvo nedidelės, tuo tarpu hibridizacijos reakcija ir srovės prisotinimas gali užtrukti ilgai (kelias valandas).

Nors lydymosi kinetika savyje turi visos DNR sekos informaciją, lydymosi greičio (bei lydymosi energijos) rezoliucija yra ženkliai per maža atliki *de-novo* 16 bazių porų DNR mėginio sekoskaitai. Šis metodas yra labiau tinkamas aptikti vienai ar keletui mutacijų. Formamido pridėjimas kartu su žema [NaCl] leido matuoti greitą (~15-20 min) lydymąsi pakankamai žemose temperatūrose (42 °C). Šis matavimas išsaugo DNR taikinį ant kietos fazės ir automatiškai paruošia elektrodą antro žymens hibridizacijai.

Išvados

1. DNR ir RNR sekų atpažinimas buvo įvykdytas voltamperometriškai (hibridizacija), amperometriškai (hibridizacija), bei voltamperometriškai (dehibridizacija), „sintetiniuose“ ir biologiniuose mėginiuose.

2. Taškinės mutacijos buvo atpažintos homo- ir heterozigotiniuose diploidiniuose mėginiuose izoterminiu metodu. 5 žmogaus seilių mėginių CYP2C19 *1 ir *17 aleliai buvo teisingai genotipuoti.

3. Įgyvendintos automatizavimui ir miniatiūrizacijai svarbios dizaino ypatybės:
   3.1. Vienkartinių elektrodų pritaikymas nukleazių detekcijai.
   3.2. Sukurtas prototipinis nukleazių analizatorius.
   3.3. Sukurti nanostruktūrizuoti vienkartiniai elektrodai tinkami erdviniams ir molekuliniams SERS matavimams.
   3.4. Pademonstruotas paviršiaus cheminio modifikavimo molekulinis kokybės kontrolės pavyzdys, paviršių sintezei.
   3.5. Atlikta tiesioginė mėginių PGR amplifikacija ir tiesioginė amplikono hibridizacija, be gryninimo ar kitų žingsnių (atliktas skiedimas dėl mažo tūrio).

3.6. Izoterminiai metodai ženkliai supaprastina prietaiso energijos sąnaudas, kompleksiškumą ir dydį.
3.7. Panaudota amperometrinė detekcija, kuri supaprastina potenciostato dizainą.
3.8. Pademonstruotas amperometrinis dviejų elektrodų hibridizacijos matavimas vienu metu.
3.9. Įgyvendintas vieno elektrodo (su prihibridizuotu taikiniu) matavimas dvejais zondais diploidiniams mėginiams.
3.10. Įgyvendintas vienos talpos (angl. *„one-pot“*) lydymo matavimas – panaikina pumpavimą, elektrodų plovimą, skystas atliekas ir skystos fazės kaitinimo laiko sąnaudas.
3.11. *Ex situ* hibridizacija leidžia kartoti analizes ir išsaugo mėginį.

Taikomumas

Pirmas straipsnis – DNazės detekcija yra labiausiai susijusi su aplinkos monitoringu, tačiau taip pat gali būti pritaikyta diagnostikoje.

Antras straipsnis – DNR hibridizacijos cheminė signalo amplifikacija ir hibridizacijos matavimas realiu laiku yra artimiausi mokslinių tyrimų sričiai. Tačiau šis metodas yra tinkamas multipotenciostatiniams, pastovios temperatūros ir potencialo matavimams ir gali būti pritaikytas gardelinei DNR kiekybinei analizei.

Trečias straipsnis – Dvigubo taikymo SERS-elektrocheminiai paviršiai šiuo metu yra artimiausi moksliniams tyrimams. Dviejų detekcijų taikymas gali ženkliai sustiprinti duomenų patikimumą. Metodas taip pat ženkliai sustiprintų chemiškai modifikuotų elektrodų gamybą, kokybės kontrolę ir leistų lengvai standartizuoti paviršius.

Ketvirtas straipsnis – specifiška DNR analizė gali būti taikoma labai plačiai, pademonstruotas farmakogenetinis taikinys, kas yra svarbu diagnostikai.

CONFERENCES

2024-10-04; Oral communication
S. Serapinas, D. Stakelytė, K. Tučinskytė, M. Tomkuvienė, D. Ratautas
Detection of single nucleotide polymorphisms in human genomic DNA using electrochemical biosensor based on melting analysis
Eleventh International Workshop on Biosensors, Marrakech, Morroco (2024)

2022-03-01; Poster
S. Serapinas, J. Gineitytė, M. Butkevičius, M. Dagys, R. Danilevičius, D. Ratautas.
Electrochemical biosensor for deoxyribonuclease detection and measurement
International Life Sciences Conference The COINS, Vilnius, Lithuania (2022)

CURRICULUM VITAE

Name	Skomantas Serapinas
Education	**2020-2026** PhD studies in Biochemistry Institute of Biochemistry, Life Sciences Centre, Vilnius University, Saulėtekio al. 7, Vilnius, Lithuania 2012-2016 Master's of Pharmacy (Upper Second-Class Honours) University of Brighton, Moulsecoomb Place, Lewes Road, BN2 4HQ
Employment	**2021-2026** Junior Scientist Institute of Biochemistry, Life Sciences Centre, Vilnius University, Saulėtekio al. 7, Vilnius, Lithuania
Project collaborator	• Development of an electrochemical biosensor for detecting single nucleotide polymorphisms 2023 – 2025; Project funded by Research Council of Lithuania under Researcher Group projects framework, project No. S-MIP-23-127. • Development of a bioelectrochemical L-amino acid-urea analyzer for monitoring of intensive care patients 2023 – 2024; Project funded by Research Council of Lithuania under Technology Development Projects framework, project No. P-TPP-23-047. • Development of the electrochemical device for nuclease detection and determination 2021-2022; The project is funded by the Agency for Science, Innovation and Technology of Lithuania, grant number BIOTECH-02-005
Publications not included in the thesis	1. Ratautas, D.; **Serapinas, S**.; Gineityte, J.; Butkevicius, M.; Danilevicius, R.; Dagys, M. Electrochemical System for the Rapid and Sensitive Detection and Quantification of Nuclease-like Activity Exhibiting Enzymes. EP4209596A1, July 12, 2023. https://patents.google.com/patent/EP4209596A1/en (accessed 2025-05-13). 2. Ratautas, D.; **Serapinas, S.**; Stakelytė, D.; Guobužaitė, S.; Danytė, A.; Dagys, M. Quo Vadis, Electrochemical DNA Biosensor? Lessons from Three Decades of SNP Sensing. ACS Sens. 2026, 11 (7), 5296–5314. https://doi.org/10.1021/acssensors.6c01221.

SOFTWARE USED

The text was compiled in Microsoft Office and Libre Office.

The Figures were generated using PDF XChange editor (10.3.1), Marvin JS (Chemaxon, 22.19.0), Paint.net (4.3.8), Inkscape (1.2), and Python 3 libraries Matplotlib (3.8.4) and Seaborn (0.13.2).

References were managed via Zotero (6.0.36).

REFERENCES

(1) Bard, A. J.; Faulkner, L. R. *Electrochemical Methods: Fundamentals and Applications*, 2nd ed.; Wiley: New York, 2001.

(2) Chowdhury, D. R.; Spiccia, L.; Amritphale, S. S.; Paul, A.; Singh, A. A Robust Iron Oxyhydroxide Water Oxidation Catalyst Operating under near Neutral and Alkaline Conditions. *J. Mater. Chem. A* **2016**, *4* (10), 3655–3660. https://doi.org/10.1039/C6TA00313C.

(3) Amstutz, U.; Henricks, L. M.; Offer, S. M.; Barbarino, J.; Schellens, J. H. M.; Swen, J. J.; Klein, T. E.; McLeod, H. L.; Caudle, K. E.; Diasio, R. B.; Schwab, M. Clinical Pharmacogenetics Implementation Consortium (CPIC) Guideline for Dihydropyrimidine Dehydrogenase Genotype and Fluoropyrimidine Dosing: 2017 Update. *Clinical Pharmacology & Therapeutics* **2018**, *103* (2), 210–216. https://doi.org/10.1002/cpt.911.

(4) Maillard, M.; Schwab, M.; Whirl-Carrillo, M.; Moyer, A. M.; Suarez-Kurtz, G.; Pui, C.-H.; Stein, C. M.; Klein, T. E.; Spahn, C.; Kwon, S.; Hartono, J. L.; de Boer, N. K.; Ahmad, T.; Antillon-Klussmann, F. G.; Caudle, K. E.; Kato, M.; Yeoh, A. E. J.; Schmiegelow, K.; Yang, J. J. Clinical Pharmacogenetics Implementation Consortium (CPIC) Guideline for Thiopurine Dosing Based on TPMT and NUDT15 Genotypes: 2025 Update. *Clinical Pharmacology & Therapeutics* **2026**, *119* (4), 916–927. https://doi.org/10.1002/cpt.70209.

(5) *CYP2C19 genotype testing to guide clopidogrel use after ischaemic stroke or transient ischaemic attack | Guidance | NICE*. https://www.nice.org.uk/guidance/htg724 (accessed 2026-04-12).

(6) Medwid, S.; Kim, R. B. Implementation of Pharmacogenomics: Where Are We Now? *British Journal of Clinical Pharmacology* **2024**, *90* (8), 1763–1781. https://doi.org/10.1111/bcp.15591.

(7) Abou Diwan, E.; Zeitoun, R. I.; Abou Haidar, L.; Cascorbi, I.; Khoueiry Zgheib, N. Implementation and Obstacles of Pharmacogenetics in Clinical Practice: An International Survey. *British Journal of Clinical Pharmacology* **2019**, *85* (9), 2076–2088. https://doi.org/10.1111/bcp.13999.

(8) Ginsburg, G. S. Implications of Pharmacogenomics for Drug Development and Clinical Practice. *Arch Intern Med* **2005**, *165* (20), 2331. https://doi.org/10.1001/archinte.165.20.2331.

(9) Donohue, M. J. Quantification of *Legionella Pneumophila* by qPCR and Culture in Tap Water with Different Concentrations of Residual Disinfectants and Heterotrophic Bacteria. *Science of The Total*

Environment **2021**, *774*, 145142. https://doi.org/10.1016/j.scitotenv.2021.145142.

(10) Sivaganesan, M.; Aw, T. G.; Briggs, S.; Dreelin, E.; Aslan, A.; Dorevitch, S.; Shrestha, A.; Isaacs, N.; Kinzelman, J.; Kleinheinz, G.; Noble, R.; Rediske, R.; Scull, B.; Rosenberg, S.; Weberman, B.; Sivy, T.; Southwell, B.; Siefring, S.; Oshima, K.; Haugland, R. Standardized Data Quality Acceptance Criteria for a Rapid *Escherichia Coli* qPCR Method (Draft Method C) for Water Quality Monitoring at Recreational Beaches. *Water Research* **2019**, *156*, 456–464. https://doi.org/10.1016/j.watres.2019.03.011.

(11) Sivaganesan, M.; Dean, S. A.; Willis, J. R.; Friedman, S. D.; Haugland, R.; Shanks, O. C. A Streamlined qPCR Method for Characterization of *Enterococcus* Spp. Levels in Ambient Surface Water Samples. *Water Research* **2025**, *284*, 123936. https://doi.org/10.1016/j.watres.2025.123936.

(12) Vesper, S. j.; Wymer, L. j.; Meklin, T.; Varma, M.; Stott, R.; Richardson, M.; Haugland, R. a. Comparison of Populations of Mould Species in Homes in the UK and USA Using Mould-Specific Quantitative PCR. *Letters in Applied Microbiology* **2005**, *41* (4), 367–373. https://doi.org/10.1111/j.1472-765X.2005.01764.x.

(13) Nogva, H. K.; Bergh, A.; Holck, A.; Rudi, K. Application of the 5′-Nuclease PCR Assay in Evaluation and Development of Methods for Quantitative Detection of Campylobacter Jejuni. *Appl Environ Microbiol* **2000**, *66* (9), 4029–4036. https://doi.org/10.1128/aem.66.9.4029-4036.2000.

(14) Zhu, H.; Kim, B. J.; Spizz, G.; Rothrock, D.; Yasmin, R.; Arida, J.; Grocholl, J.; Montagna, R.; Schwartz, B.; Trujillo, S.; Almeria, S. Development and Evaluation/Verification of a Fully Automated Test Platform for the Rapid Detection of Cyclospora Cayetanensis in Produce Matrices. *Microorganisms* **2023**, *11* (11), 2805. https://doi.org/10.3390/microorganisms11112805.

(15) *GeneXpert Family of Systems*. https://www.cepheid.com/en-US/systems/genexpert-family-of-systems/genexpert-system.html (accessed 2025-05-30).

(16) *Cepheid-Corporate-Menu-Flyer-US-IVD-0323-English*. https://cepheid.widen.net/content/6rod6rervw/pdf/Cepheid-Corporate-Menu-Flyer-US-IVD-0323-English.pdf?u=bk12mm (accessed 2025-09-04).

(17) Chereau, D.; Kerff, F.; Graceffa, P.; Grabarek, Z.; Langsetmo, K.; Dominguez, R. Actin-Bound Structures of Wiskott–Aldrich Syndrome

Protein (WASP)-Homology Domain 2 and the Implications for Filament Assembly. *Proceedings of the National Academy of Sciences* **2005**, *102* (46), 16644–16649. https://doi.org/10.1073/pnas.0507021102.

(18) Langer, J.; Jimenez de Aberasturi, D.; Aizpurua, J.; Alvarez-Puebla, R. A.; Auguié, B.; Baumberg, J. J.; Bazan, G. C.; Bell, S. E. J.; Boisen, A.; Brolo, A. G.; Choo, J.; Cialla-May, D.; Deckert, V.; Fabris, L.; Faulds, K.; García de Abajo, F. J.; Goodacre, R.; Graham, D.; Haes, A. J.; Haynes, C. L.; Huck, C.; Itoh, T.; Käll, M.; Kneipp, J.; Kotov, N. A.; Kuang, H.; Le Ru, E. C.; Lee, H. K.; Li, J.-F.; Ling, X. Y.; Maier, S. A.; Mayerhöfer, T.; Moskovits, M.; Murakoshi, K.; Nam, J.-M.; Nie, S.; Ozaki, Y.; Pastoriza-Santos, I.; Perez-Juste, J.; Popp, J.; Pucci, A.; Reich, S.; Ren, B.; Schatz, G. C.; Shegai, T.; Schlücker, S.; Tay, L.-L.; Thomas, K. G.; Tian, Z.-Q.; Van Duyne, R. P.; Vo-Dinh, T.; Wang, Y.; Willets, K. A.; Xu, C.; Xu, H.; Xu, Y.; Yamamoto, Y. S.; Zhao, B.; Liz-Marzán, L. M. Present and Future of Surface-Enhanced Raman Scattering. *ACS Nano* **2020**, *14* (1), 28–117. https://doi.org/10.1021/acsnano.9b04224.

(19) Vernick, S.; Trocchia, S. M.; Warren, S. B.; Young, E. F.; Bouilly, D.; Gonzalez, R. L.; Nuckolls, C.; Shepard, K. L. Electrostatic Melting in a Single-Molecule Field-Effect Transistor with Applications in Genomic Identification. *Nat Commun* **2017**, *8* (1), 15450. https://doi.org/10.1038/ncomms15450.

(20) Levy, B.; Baughn, L. B.; Chartrand, S.; LaBarge, B.; Claxton, D.; Lennon, A.; Akkari, Y.; Cujar, C.; Kolhe, R.; Kroeger, K.; Pitel, B.; Sahajpal, N.; Sathanoori, M.; Vlad, G.; Zhang, L.; Fang, M.; Kanagal-Shamanna, R.; Broach, J. A National Multicenter Evaluation of the Clinical Utility of Optical Genome Mapping for Assessment of Genomic Aberrations in Acute Myeloid Leukemia. medRxiv November 10, 2020, p 2020.11.07.20227728. https://doi.org/10.1101/2020.11.07.20227728.

(21) Schmidt, D.; Wilson, M. D.; Spyrou, C.; Brown, G. D.; Hadfield, J.; Odom, D. T. ChIP-Seq: Using High-Throughput Sequencing to Discover Protein-DNA Interactions. *Methods* **2009**, *48* (3), 240–248. https://doi.org/10.1016/j.ymeth.2009.03.001.

(22) Sequenom MassARRAY Technology for the Analysis of DNA Methylation: Clinical Applications. In *Epigenetic Biomarkers and Diagnostics*; Academic Press, 2016; pp 137–153. https://doi.org/10.1016/B978-0-12-801899-6.00007-3.

(23) Verlouw, J. A. M.; Clemens, E.; de Vries, J. H.; Zolk, O.; Verkerk, A. J. M. H.; am Zehnhoff-Dinnesen, A.; Medina-Gomez, C.; Lanvers-Kaminsky, C.; Rivadeneira, F.; Langer, T.; van Meurs, J. B. J.; van den Heuvel-Eibrink, M. M.; Uitterlinden, A. G.; Broer, L. A Comparison of

Genotyping Arrays. *Eur J Hum Genet* **2021**, *29* (11), 1611–1624. https://doi.org/10.1038/s41431-021-00917-7.

(24) *Axiom Genotyping Assay User Manual.pdf*. https://assets.thermofisher.com/TFS-Assets/LSG/brochures/axiom_genotyping_assay_user_manual.pdf (accessed 2025-05-29).

(25) *Illumina Infinium LCG Quad Assay, Manual Protocol.pdf*. https://support.illumina.com/content/dam/illumina-support/documents/documentation/chemistry_documentation/infinium_assays/infinium_lcg_quad_assay/inf_lcg_quad_manual_euc_15025909_reva.pdf (accessed 2025-05-29).

(26) Bergval, I.; Sengstake, S.; Brankova, N.; Levterova, V.; Abadía, E.; Tadumaze, N.; Bablishvili, N.; Akhalaia, M.; Tuin, K.; Schuitema, A.; Panaiotov, S.; Bachiyska, E.; Kantardjiev, T.; Zwaan, R. de; Schürch, A.; Soolingen, D. van; Hoog, A. van 't; Cobelens, F.; Aspindzelashvili, R.; Sola, C.; Klatser, P.; Anthony, R. Combined Species Identification, Genotyping, and Drug Resistance Detection of Mycobacterium Tuberculosis Cultures by MLPA on a Bead-Based Array. *PLOS ONE* **2012**, *7* (8), e43240. https://doi.org/10.1371/journal.pone.0043240.

(27) MRC Holland. *MLPA General Protocol*. https://support.mrcholland.com/file.php/10426MWJTMDBNWJ104254647B954DPD/MLPA-General-Protocol-MDP-v010.pdf (accessed 2025-08-08).

(28) Shackelford, W.; Deng, S.; Murayama, K.; Wang, J. A New Technology for Mutation Detection. *Annals of the New York Academy of Sciences* **2004**, *1022* (1), 257–262. https://doi.org/10.1196/annals.1318.040.

(29) Trimgen. *KRAS Codon 61 Mutation Analysis Reagents User Manual V1.4*. https://www.trimgen.com/sites/default/files/upload/GP06%20KRAS%2061%20Manual%20V1.4.pdf (accessed 2025-08-08).

(30) Claassens, D. M. F.; Vos, G. J. A.; Bergmeijer, T. O.; Hermanides, R. S.; Hof, A. W. J. van 't; Harst, P. van der; Barbato, E.; Morisco, C.; Gin, R. M. T. J.; Asselbergs, F. W.; Mosterd, A.; Herrman, J.-P. R.; Dewilde, W. J. M.; Janssen, P. W. A.; Kelder, J. C.; Postma, M. J.; Boer, A. de; Boersma, C.; Deneer, V. H. M.; Berg, J. M. ten. A Genotype-Guided Strategy for Oral P2Y12 Inhibitors in Primary PCI. *New England Journal of Medicine* **2019**, *381* (17), 1621–1631. https://doi.org/10.1056/NEJMoa1907096.

(31) *QX600 Droplet Digital PCR System – Bio-Rad*. https://www.bio-rad.com/en-lt/product/qx600-droplet-digital-pcr-system?ID=b07d12ac-0585-fc4c-a586-3ddf20d5c4a0 (accessed 2025-05-29).
(32) *Nio®: 7-color digital PCR solution | Stilla*. Stilla Technologies. https://www.stillatechnologies.com/ (accessed 2025-05-29).
(33) LuminUltra. *LuminUltra Acquires Legionella Testing Business from Genomadix and Inks Strategic License to Commercialize Additional Tests for Ultra-portable Molecular Diagnostic Platform*. LuminUltra. https://www.luminultra.com/blog/luminultra-acquires-genomadix-cube/ (accessed 2025-05-30).
(34) *K220026 510(k) Premarket Notification*. https://www.accessdata.fda.gov/scripts/cdrh/cfdocs/cfpmn/pmn.cfm?ID=K220026 (accessed 2026-04-12).
(35) Cawthorn, D.-M.; Steinman, H. A.; Witthuhn, R. C. Comparative Study of Different Methods for the Extraction of DNA from Fish Species Commercially Available in South Africa. *Food Control* **2011**, *22* (2), 231–244. https://doi.org/10.1016/j.foodcont.2010.07.003.
(36) Wehmeier, U. F.; Hilberg, T. Capillary Earlobe Blood May Be Used for RNA Isolation, Gene Expression Assays and microRNA Quantification. *Molecular Medicine Reports* **2014**, *9* (1), 211–216. https://doi.org/10.3892/mmr.2013.1779.
(37) Hlazunova, O. D.; Melnichuk, N. S. Aspects of Gene Expression Analysis in Small–Volume Blood Samples Using the Real–Time PCR. *Biopolym. Cell* **2025**, *41* (1), 3–12. https://doi.org/10.7124/bc.000B11.
(38) Sigma-Aldrich. *GenElute™ Total RNA Purification Kit RNB100 - Product Information*. https://www.sigmaaldrich.com/deepweb/assets/sigmaaldrich/product/documents/365/400/rnb100bul-ms.pdf.
(39) Holmberg, R. C.; Gindlesperger, A.; Stokes, T.; Brady, D.; Thakore, N.; Belgrader, P.; Cooney, C. G.; Chandler, D. P. High-Throughput, Automated Extraction of DNA and RNA from Clinical Samples Using TruTip Technology on Common Liquid Handling Robots. *Journal of Visualized Experiments (JoVE)* **2013**, No. 76, e50356. https://doi.org/10.3791/50356.
(40) *Dynabeads™ DNA DIRECT™ Universal Kit*. https://www.thermofisher.com/order/catalog/product/63006 (accessed 2025-06-23).
(41) Kueppers, C.; Schlappa, S.; Bogdoll, A.; Breitkopf, L.; Seip, N.; Singer, T. The ePrep-System: A New Electrophoretic Approach for DNA

Isolation from Biological Samples. *ELECTROPHORESIS* **2017**, *38* (17), 2200–2209. https://doi.org/10.1002/elps.201600546.

(42) Hung, P.-Y.; Jiang, P.-S.; Lee, E.-F.; Fan, S.-K.; Lu, Y.-W. Genomic DNA Extraction from Whole Blood Using a Digital Microfluidic (DMF) Platform with Magnetic Beads. *Microsyst Technol* **2017**, *23* (2), 313–320. https://doi.org/10.1007/s00542-015-2512-9.

(43) Martorell, S.; Maquieira, Á.; Tortajada-Genaro, L. A. A Genosensor for Detecting Single-Point Mutations in Dendron Chips after Blocked Recombinase Polymerase Amplification. *Analyst* **2022**, *147* (10), 2180–2188. https://doi.org/10.1039/D2AN00160H.

(44) Yenice, C. P.; Chahin, N.; Jauset-Rubio, M.; Hall, M.; Biggs, P.; Dimai, H.-P.; Obermayer-Pietsch, B.; Ortiz, M.; O'Sullivan, C. K. Semiautomated Electrochemical Melting Curve Analysis Device for the Detection of an Osteoporosis Associated Single Nucleotide Polymorphism in Blood. *Anal. Chem.* **2023**, *95* (38), 14192–14202. https://doi.org/10.1021/acs.analchem.3c01668.

(45) Arriola, E.; Lambros, M. B. K.; Jones, C.; Dexter, T.; Mackay, A.; Tan, D. S. P.; Tamber, N.; Fenwick, K.; Ashworth, A.; Dowsett, M.; Reis-Filho, J. S. Evaluation of Phi29-Based Whole-Genome Amplification for Microarray-Based Comparative Genomic Hybridisation. *Laboratory Investigation* **2007**, *87* (1), 75–83. https://doi.org/10.1038/labinvest.3700495.

(46) Chapman, A. R.; He, Z.; Lu, S.; Yong, J.; Tan, L.; Tang, F.; Xie, X. S. Single Cell Transcriptome Amplification with MALBAC. *PLOS ONE* **2015**, *10* (3), e0120889. https://doi.org/10.1371/journal.pone.0120889.

(47) *Nucleic Acid Amplification Technologies: Application to Disease Diagnosis*; Lee, H. H., Morse, S. A., Olsvik, Ø., Eds.; BioTechniques books; Birkhäuser Boston: Cambridge, MA, 1997.

(48) Fahy, E.; Kwoh, D. Y.; Gingeras, T. R. Self-Sustained Sequence Replication (3SR): An Isothermal Transcription-Based Amplification System Alternative to PCR. *Genome Res.* **1991**, *1* (1), 25–33. https://doi.org/10.1101/gr.1.1.25.

(49) Yan, Y.; Ding, S.; Zhao, D.; Yuan, R.; Zhang, Y.; Cheng, W. Direct Ultrasensitive Electrochemical Biosensing of Pathogenic DNA Using Homogeneous Target-Initiated Transcription Amplification. *Sci Rep* **2016**, *6* (1), 18810. https://doi.org/10.1038/srep18810.

(50) Dunn, P.; Albury, C. L.; Maksemous, N.; Benton, M. C.; Sutherland, H. G.; Smith, R. A.; Haupt, L. M.; Griffiths, L. R. Next Generation Sequencing Methods for Diagnosis of Epilepsy Syndromes. *Front. Genet.* **2018**, *9*. https://doi.org/10.3389/fgene.2018.00020.

(51) Aird, D.; Ross, M. G.; Chen, W.-S.; Danielsson, M.; Fennell, T.; Russ, C.; Jaffe, D. B.; Nusbaum, C.; Gnirke, A. Analyzing and Minimizing PCR Amplification Bias in Illumina Sequencing Libraries. *Genome Biology* **2011**, *12* (2), R18. https://doi.org/10.1186/gb-2011-12-2-r18.

(52) Mattes, W. B.; Hartley, J. A.; Kohn, K. W. Mechanism of DNA Strand Breakage by Piperidine at Sites of *N*7-Alkylguanines. *Biochimica et Biophysica Acta (BBA) - Gene Structure and Expression* **1986**, *868* (1), 71–76. https://doi.org/10.1016/0167-4781(86)90088-6.

(53) Gangl, E. T.; Turesky, R. J.; Vouros, P. Detection of in Vivo Formed DNA Adducts at the Part-per-Billion Level by Capillary Liquid Chromatography/Microelectrospray Mass Spectrometry. *Anal. Chem.* **2001**, *73* (11), 2397–2404. https://doi.org/10.1021/ac0100401.

(54) Liao, Q.; Chiu, N. H. L.; Shen, C.; Chen, Y.; Vouros, P. Investigation of Enzymatic Behavior of Benzonase/Alkaline Phosphatase in the Digestion of Oligonucleotides and DNA by ESI-LC/MS. *Anal. Chem.* **2007**, *79* (5), 1907–1917. https://doi.org/10.1021/ac062249q.

(55) Ferguson, B. S.; Buchsbaum, S. F.; Wu, T.-T.; Hsieh, K.; Xiao, Y.; Sun, R.; Soh, H. T. Genetic Analysis of H1N1 Influenza Virus from Throat Swab Samples in a Microfluidic System for Point-of-Care Diagnostics. *J. Am. Chem. Soc.* **2011**, *133* (23), 9129–9135. https://doi.org/10.1021/ja203981w.

(56) Öhrmalm, C.; Jobs, M.; Eriksson, R.; Golbob, S.; Elfaitouri, A.; Benachenhou, F.; Strømme, M.; Blomberg, J. Hybridization Properties of Long Nucleic Acid Probes for Detection of Variable Target Sequences, and Development of a Hybridization Prediction Algorithm. *Nucleic Acids Research* **2010**, *38* (21), e195. https://doi.org/10.1093/nar/gkq777.

(57) Applied Biosystems. A Guide to High Resolution Melting (HRM) Analysis, 2010. https://documents.thermofisher.com/TFS-Assets/LSG/manuals/cms_070283.pdf (accessed 2026-03-29).

(58) Relógio, A.; Schwager, C.; Richter, A.; Ansorge, W.; Valcárcel, J. Optimization of Oligonucleotide-Based DNA Microarrays. *Nucleic Acids Research* **2002**, *30* (11), e51. https://doi.org/10.1093/nar/30.11.e51.

(59) Wang, X.; Zou, M.; Huang, H.; Ren, Y.; Li, L.; Yang, X.; Li, N. Gold Nanoparticle Enhanced Fluorescence Anisotropy for the Assay of Single Nucleotide Polymorphisms (SNPs) Based on Toehold-Mediated Strand-Displacement Reaction. *Biosensors and Bioelectronics* **2013**, *41*, 569–575. https://doi.org/10.1016/j.bios.2012.09.023.

(60) Haley, N. E. C.; Ouldridge, T. E.; Mullor Ruiz, I.; Geraldini, A.; Louis, A. A.; Bath, J.; Turberfield, A. J. Design of Hidden Thermodynamic Driving for Non-Equilibrium Systems via Mismatch Elimination during

DNA Strand Displacement. *Nat Commun* **2020**, *11* (1), 2562. https://doi.org/10.1038/s41467-020-16353-y.

(61) Lu, H.; Ding, B.; Tong, L.; Wu, F.; Yi, X.; Wang, J. Toehold-Mediated Strand Displacement Reaction for Dual-Signal Electrochemical Assay of Apolipoprotein E Genotyping. *ACS Sens.* **2020**, *5* (9), 2959–2965. https://doi.org/10.1021/acssensors.0c01511.

(62) Steel, A. B.; Herne, T. M.; Tarlov, M. J. Electrochemical Quantitation of DNA Immobilized on Gold. *Anal. Chem.* **1998**, *70* (22), 4670–4677. https://doi.org/10.1021/ac980037q.

(63) Simon, L.; Gyurcsányi, R. E. Multiplexed Assessment of the Surface Density of DNA Probes on DNA Microarrays by Surface Plasmon Resonance Imaging. *Analytica Chimica Acta* **2019**, *1047*, 131–138. https://doi.org/10.1016/j.aca.2018.09.048.

(64) Peterson, A. W.; Heaton, R. J.; Georgiadis, R. M. The Effect of Surface Probe Density on DNA Hybridization. *Nucleic Acids Research* **2001**, *29* (24), 5163. https://doi.org/10.1093/nar/29.24.5163.

(65) Aoki, H.; Kitajima ,Akiko; and Tao, H. Label-Free and 'Signal-on' DNA Detection Using a Probe DNA Terminated with Ferrocene and β-Cyclodextrin. *Supramolecular Chemistry* **2010**, *22* (7–8), 455–460. https://doi.org/10.1080/10610278.2010.486034.

(66) Kitamura, Y.; Mishio, K.; Arslan, P.; Ikeda, B.; Imoto, C.; Katsuda, Y.; Ihara, T. Electrochemical Molecular Beacon for Nucleic Acid Sensing in a Homogeneous Solution. *ANAL. SCI.* **2020**, *36* (8), 959–964. https://doi.org/10.2116/analsci.19P456.

(67) Serapinas, S.; Gineitytė, J.; Butkevičius, M.; Danilevičius, R.; Dagys, M.; Ratautas, D. Biosensor Prototype for Rapid Detection and Quantification of DNase Activity. *Biosensors and Bioelectronics* **2022**, *213*, 114475. https://doi.org/10.1016/j.bios.2022.114475.

(68) Persson, B. A Chemically Modified Graphite Electrode for Electrocatalytic Oxidation of Reduced Nicotinamide Adenine Dinucleotide Based on a Phenothiazine Derivative, 3-β-Naphthoyl-Toluidine Blue O. *Journal of Electroanalytical Chemistry and Interfacial Electrochemistry* **1990**, *287* (1), 61–80. https://doi.org/10.1016/0022-0728(90)87160-L.

(69) *Electroanalytical Methods: Guide to Experiments and Applications*, 2nd, rev.extended ed ed.; Scholz, F., Bond, A. M., Eds.; Springer: Heidelberg ; New York, 2010.

(70) Bard, A. J.; Inzelt, G.; Scholz, F. *Electrochemical Dictionary*, 2nd ed.; Springer: Heidelberg, 2012.

(71) Nuzzo, R. G.; Allara, D. L. Adsorption of Bifunctional Organic Disulfides on Gold Surfaces. *J. Am. Chem. Soc.* **1983**, *105* (13), 4481–4483. https://doi.org/10.1021/ja00351a063.

(72) Ulman, A. Formation and Structure of Self-Assembled Monolayers. *Chem. Rev.* **1996**, *96* (4), 1533–1554. https://doi.org/10.1021/cr9502357.

(73) Civit, L.; Fragoso, A.; O'Sullivan, C. K. Thermal Stability of Diazonium Derived and Thiol-Derived Layers on Gold for Application in Genosensors. *Electrochemistry Communications* **2010**, *12* (8), 1045–1048. https://doi.org/10.1016/j.elecom.2010.05.020.

(74) Yang, A. H. J.; Hsieh, K.; Patterson, A. S.; Ferguson, B. S.; Eisenstein, M.; Plaxco, K. W.; Soh, H. T. Accurate Zygote-Specific Discrimination of Single-Nucleotide Polymorphisms Using Microfluidic Electrochemical DNA Melting Curves. *Angewandte Chemie International Edition* **2014**, *53* (12), 3163–3167. https://doi.org/10.1002/anie.201310059.

(75) Olivan, L. A.; Hand, K.; White, R. J. Utilization of Spontaneous Alkyne–Gold Self-Assembly Chemistry as an Alternative Method for Fabricating Electrochemical Aptamer-Based Sensors. *Langmuir* **2024**, *40* (23), 12117–12123. https://doi.org/10.1021/acs.langmuir.4c00972.

(76) Taton, T. A. Preparation of Gold Nanoparticle–DNA Conjugates. *CP Nucleic Acid Chemistry* **2002**, *9* (1). https://doi.org/10.1002/0471142700.nc1202s09.

(77) Westermark, G.; Kariis, H.; Persson, I.; Liedberg, B. An Infrared Study on the Chemisorption of Tertiary Phosphines on Coinage and Platinum Group Metal Surfaces. *Colloids and Surfaces A: Physicochemical and Engineering Aspects* **1999**, *150* (1), 31–43. https://doi.org/10.1016/S0927-7757(98)00536-6.

(78) Jewell, A. D.; Tierney, H. L.; Sykes, E. C. H. Gently Lifting Gold's Herringbone Reconstruction: Trimethylphosphine on Au(111). *Phys. Rev. B* **2010**, *82* (20), 205401. https://doi.org/10.1103/PhysRevB.82.205401.

(79) Brooksby, P. A.; Downard, A. J. Electrochemical and Atomic Force Microscopy Study of Carbon Surface Modification via Diazonium Reduction in Aqueous and Acetonitrile Solutions. *Langmuir* **2004**, *20* (12), 5038–5045. https://doi.org/10.1021/la049616i.

(80) Baranton, S.; Bélanger, D. In Situ Generation of Diazonium Cations in Organic Electrolyte for Electrochemical Modification of Electrode Surface. *Electrochimica Acta* **2008**, *53* (23), 6961–6967. https://doi.org/10.1016/j.electacta.2008.02.105.

(81) Corgier, B. P.; Marquette, C. A.; Blum, L. J. Diazonium–Protein Adducts for Graphite Electrode Microarrays Modification: Direct and Addressed Electrochemical Immobilization. *J. Am. Chem. Soc.* **2005**, *127* (51), 18328–18332. https://doi.org/10.1021/ja056946w.

(82) Harper, J. C.; Polsky, R.; Wheeler, D. R.; Dirk, S. M.; Brozik, S. M. Selective Immobilization of DNA and Antibody Probes on Electrode Arrays: Simultaneous Electrochemical Detection of DNA and Protein on a Single Platform. *Langmuir* **2007**, *23* (16), 8285–8287. https://doi.org/10.1021/la701775g.

(83) Chrétien, J.-M.; Ghanem, M. A.; Bartlett, P. N.; Kilburn, J. D. Covalent Tethering of Organic Functionality to the Surface of Glassy Carbon Electrodes by Using Electrochemical and Solid-Phase Synthesis Methodologies. *Chemistry – A European Journal* **2008**, *14* (8), 2548–2556. https://doi.org/10.1002/chem.200701559.

(84) Liu, J.; Cheng, L.; Liu, B.; Dong, S. Covalent Modification of a Glassy Carbon Surface by 4-Aminobenzoic Acid and Its Application in Fabrication of a Polyoxometalates-Consisting Monolayer and Multilayer Films. *Langmuir* **2000**, *16* (19), 7471–7476. https://doi.org/10.1021/la9913506.

(85) Barbier, B.; Pinson, J.; Desarmot, G.; Sanchez, M. Electrochemical Bonding of Amines to Carbon Fiber Surfaces Toward Improved Carbon-Epoxy Composites. *J. Electrochem. Soc.* **1990**, *137* (6), 1757–1764. https://doi.org/10.1149/1.2086794.

(86) Morales-Martínez, D.; Ramírez-Chan, D. E.; Palacios-Ramírez, J. I.; Galicia, M.; González, F. J. Covalent Modification of Carbon Surfaces by Direct and Redox Catalysed Oxidation of Carboxylates in Acetonitrile – Concepts and Mechanisms. *ChemCatChem* **2023**, *15* (12), e202300470. https://doi.org/10.1002/cctc.202300470.

(87) Harwood, S. J.; Palkowitz, M. D.; Gannett, C. N.; Perez, P.; Yao, Z.; Sun, L.; Abruña, H. D.; Anderson, S. L.; Baran, P. S. Modular Terpene Synthesis Enabled by Mild Electrochemical Couplings. *Science* **2022**, *375* (6582), 745–752. https://doi.org/10.1126/science.abn1395.

(88) Brown, Alex. C.; Walker, J. Elektrolytische Synthese Zweibasischer Säuren. *Justus Liebigs Annalen der Chemie* **1891**, *261* (1), 107–128. https://doi.org/10.1002/jlac.18912610106.

(89) Galán, T.; Prieto-Simón, B.; Alvira, M.; Eritja, R.; Götz, G.; Bäuerle, P.; Samitier, J. Label-Free Electrochemical DNA Sensor Using "Click"-Functionalized PEDOT Electrodes. *Biosensors and Bioelectronics* **2015**, *74*, 751–756. https://doi.org/10.1016/j.bios.2015.07.037.

(90) Authier, L.; Grossiord, C.; Brossier, P.; Limoges, B. Gold Nanoparticle-Based Quantitative Electrochemical Detection of Amplified Human Cytomegalovirus DNA Using Disposable Microband Electrodes. *Anal. Chem.* **2001**, *73* (18), 4450–4456. https://doi.org/10.1021/ac0103221.

(91) Maurer, K.; McShea, A.; Strathmann, M.; Dill, K. The Removal of the T-BOC Group by Electrochemically Generated Acid and Use of an Addressable Electrode Array for Peptide Synthesis. *J. Comb. Chem.* **2005**, *7* (5), 637–640. https://doi.org/10.1021/cc0498175.

(92) Maurer, K.; Cooper, J.; Caraballo, M.; Crye, J.; Suciu, D.; Ghindilis, A.; Leonetti, J. A.; Wang, W.; Rossi, F. M.; Stöver, A. G.; Larson, C.; Gao, H.; Dill, K.; McShea, A. Electrochemically Generated Acid and Its Containment to 100 Micron Reaction Areas for the Production of DNA Microarrays. *PLoS One* **2006**, *1* (1), e34. https://doi.org/10.1371/journal.pone.0000034.

(93) McKenas, C. G.; Fehr, J. M.; Donley, C. L.; Lockett, M. R. Thiol–Ene Modified Amorphous Carbon Substrates: Surface Patterning and Chemically Modified Electrode Preparation. *Langmuir* **2016**, *32* (41), 10529–10536. https://doi.org/10.1021/acs.langmuir.6b02961.

(94) Crudden, C. M.; Horton, J. H.; Ebralidze, I. I.; Zenkina, O. V.; McLean, A. B.; Drevniok, B.; She, Z.; Kraatz, H.-B.; Mosey, N. J.; Seki, T.; Keske, E. C.; Leake, J. D.; Rousina-Webb, A.; Wu, G. Ultra Stable Self-Assembled Monolayers of N-Heterocyclic Carbenes on Gold. *Nature Chem* **2014**, *6* (5), 409–414. https://doi.org/10.1038/nchem.1891.

(95) Maurer, K.; McShea, A.; Strathmann, M.; Dill, K. The Removal of the T-BOC Group by Electrochemically Generated Acid and Use of an Addressable Electrode Array for Peptide Synthesis. *J. Comb. Chem.* **2005**, *7* (5), 637–640. https://doi.org/10.1021/cc0498175.

(96) Mishyn, V.; Hugo, A.; Rodrigues, T.; Aspermair, P.; Happy, H.; Marques, L.; Hurot, C.; Othmen, R.; Bouchiat, V.; Boukherroub, R.; Knoll, W.; Szunerits, S. The Holy Grail of Pyrene-Based Surface Ligands on the Sensitivity of Graphene-Based Field Effect Transistors. *Sensors & Diagnostics* **2022**, *1* (2), 235–244. https://doi.org/10.1039/D1SD00036E.

(97) Faudi, F. Kugelgelenk. CH131172A, January 31, 1929. https://patents.google.com/patent/CH131172A/en (accessed 2025-07-30).

(98) Kunkel, G. R.; Mehrabian, M.; Martinson, H. G. Contact-Site Cross-Linking Agents. *Mol Cell Biochem* **1981**, *34* (1), 3–13. https://doi.org/10.1007/BF02354846.

(99) Grabarek, Z.; Gergely, J. Zero-Length Crosslinking Procedure with the Use of Active Esters. *Analytical Biochemistry* **1990**, *185* (1), 131–135. https://doi.org/10.1016/0003-2697(90)90267-D.

(100) Ziegler, F. E.; Berger, G. D. A Mild Method for the Esterification of Fatty Acids. *Synthetic Communications* **1979**, *9* (6), 539–543. https://doi.org/10.1080/00397917908060958.

(101) Umehara, A.; Shimizu, S.; Sasaki, M. Synthesis of Bulky N-Acyl Heterocycles by DMAPO/Boc2O-Mediated One-Pot Direct N-Acylation of Less Nucleophilic N-Heterocycles with α-Fully Substituted Carboxylic Acids. *Advanced Synthesis & Catalysis* **2023**, *365* (14), 2367–2376. https://doi.org/10.1002/adsc.202300487.

(102) Adler, P.; Gras, M.; Smietana, M. Catalytic and Sustainable Amide Bond Formation Using a DABCO/Dichlorotriazine System. *ChemCatChem* **2023**, *15* (10), e202300264. https://doi.org/10.1002/cctc.202300264.

(103) Liu, J.; Fujita, H.; Kitamura, M.; Shimada, D.; Kunishima, M. Development of a Triazinedione-Based Dehydrative Condensing Reagent Containing 4-(Dimethylamino)Pyridine as an Acyl Transfer Catalyst. *Org. Biomol. Chem.* **2021**, *19* (21), 4712–4719. https://doi.org/10.1039/D1OB00450F.

(104) Lagueux-Tremblay, P.-L.; Fabrikant, A.; Arndtsen, B. A. Palladium-Catalyzed Carbonylation of Aryl Chlorides to Electrophilic Aroyl-DMAP Salts. *ACS Catal.* **2018**, *8* (6), 5350–5354. https://doi.org/10.1021/acscatal.8b00757.

(105) Hutchby, M.; Houlden, C. E.; Haddow, M. F.; Tyler, S. N. G.; Lloyd-Jones, G. C.; Booker-Milburn, K. I. Switching Pathways: Room-Temperature Neutral Solvolysis and Substitution of Amides. *Angewandte Chemie International Edition* **2012**, *51* (2), 548–551. https://doi.org/10.1002/anie.201107117.

(106) El-Faham, A.; Funosas, R. S.; Prohens, R.; Albericio, F. COMU: A Safer and More Effective Replacement for Benzotriazole-Based Uronium Coupling Reagents. *Chemistry – A European Journal* **2009**, *15* (37), 9404–9416. https://doi.org/10.1002/chem.200900615.

(107) Mattson, G.; Conklin, E.; Desai, S.; Nielander, G.; Savage, M. D.; Morgensen, S. A Practical Approach to Crosslinking. *Mol Biol Rep* **1993**, *17* (3), 167–183. https://doi.org/10.1007/BF00986726.

(108) Rostovtsev, V. V.; Green, L. G.; Fokin, V. V.; Sharpless, K. B. A Stepwise Huisgen Cycloaddition Process: Copper(I)-Catalyzed Regioselective "Ligation" of Azides and Terminal Alkynes. *Angewandte Chemie International Edition* **2002**, *41* (14), 2596–2599.

https://doi.org/10.1002/1521-3773(20020715)41:14%3C2596::AID-ANIE2596%3E3.0.CO;2-4.

(109) Lewis, W. G.; Green, L. G.; Grynszpan, F.; Radić, Z.; Carlier, P. R.; Taylor, P.; Finn, M. G.; Sharpless, K. B. Click Chemistry In Situ: Acetylcholinesterase as a Reaction Vessel for the Selective Assembly of a Femtomolar Inhibitor from an Array of Building Blocks. *Angewandte Chemie International Edition* **2002**, *41* (6), 1053–1057. https://doi.org/10.1002/1521-3773(20020315)41:6%3C1053::AID-ANIE1053%3E3.0.CO;2-4.

(110) Akar, E.; Luleburgaz, S.; Gunay, U. S.; Kumbaraci, V.; Tunca, U.; Durmaz, H. Amino-Yne Reaction: An Exquisite Method for Polymer-Polymer Conjugation and Post-Polymerization Modification. *European Polymer Journal* **2023**, *199*, 112470. https://doi.org/10.1016/j.eurpolymj.2023.112470.

(111) Chan, J. W.; Hoyle, C. E.; Lowe, A. B. Sequential Phosphine-Catalyzed, Nucleophilic Thiol–Ene/Radical-Mediated Thiol–Yne Reactions and the Facile Orthogonal Synthesis of Polyfunctional Materials. *J. Am. Chem. Soc.* **2009**, *131* (16), 5751–5753. https://doi.org/10.1021/ja8099135.

(112) Gautier, C.; López, I.; Breton, T. A Post-Functionalization Toolbox for Diazonium (Electro)-Grafted Surfaces: Review of the Coupling Methods. *Mater. Adv.* **2021**, *2* (9), 2773–2810. https://doi.org/10.1039/D1MA00077B.

(113) Sirajuddin, M.; Ali, S.; Badshah, A. Drug–DNA Interactions and Their Study by UV–Visible, Fluorescence Spectroscopies and Cyclic Voltametry. *Journal of Photochemistry and Photobiology B: Biology* **2013**, *124*, 1–19. https://doi.org/10.1016/j.jphotobiol.2013.03.013.

(114) *Nucleic Acids in Chemistry and Biology*, 3. ed.; Blackburn, G. M., Gait, M., Loakes, D., Williams, D., Eds.; Royal Society of Chemistry: Cambridge, 2006.

(115) Nassi, A.; Guillon, F.-X.; Amar, A.; Hainque, B.; Amriche, S.; Maugé, D.; Markova, E.; Tsé, C.; Bigey, P.; Lazerges, M.; Bedioui, F. Electrochemical DNA-Biosensors Based on Long-Range Electron Transfer: Optimization of the Amperometric Detection in the Femtomolar Range Using Two-Electrode Setup and Ultramicroelectrode. *Electrochimica Acta* **2016**, *209*, 269–277. https://doi.org/10.1016/j.electacta.2016.04.144.

(116) Wong, E. L. S.; Erohkin, P.; Gooding, J. J. A Comparison of Cationic and Anionic Intercalators for the Electrochemical Transduction of DNA Hybridization via Long Range Electron Transfer. *Electrochemistry*

Communications **2004**, *6* (7), 648–654. https://doi.org/10.1016/j.elecom.2004.05.002.

(117) Kékedy-Nagy, L.; Kotlyar, A. B.; Ferapontova, E. E. Long-Range Electron Transfer Mediated by G-Quadruplex Wires Attached to Gold Electrodes via Phosphorothioated dA Tags. *Electrochimica Acta* **2024**, *476*, 143761. https://doi.org/10.1016/j.electacta.2024.143761.

(118) Slinker, J. D.; Muren, N. B.; Renfrew, S. E.; Barton, J. K. DNA Charge Transport over 34 Nm. *Nature Chem* **2011**, *3* (3), 228–233. https://doi.org/10.1038/nchem.982.

(119) Sykes, K. S.; White, R. J. Effects of Nucleic Acid Structural Heterogeneity on the Electrochemistry of Tethered Redox Molecules. *Langmuir* **2022**, *38* (23), 7322–7330. https://doi.org/10.1021/acs.langmuir.2c00840.

(120) Ortiz, M.; Jauset-Rubio, M.; Kodr, D.; Simonova, A.; Hocek, M.; O'Sullivan, C. K. Solid-Phase Recombinase Polymerase Amplification Using Ferrocene-Labelled dNTPs for Electrochemical Detection of Single Nucleotide Polymorphisms. *Biosensors and Bioelectronics* **2022**, *198*, 113825. https://doi.org/10.1016/j.bios.2021.113825.

(121) Hajian, R.; Balderston, S.; Tran, T.; deBoer, T.; Etienne, J.; Sandhu, M.; Wauford, N. A.; Chung, J.-Y.; Nokes, J.; Athaiya, M.; Paredes, J.; Peytavi, R.; Goldsmith, B.; Murthy, N.; Conboy, I. M.; Aran, K. Detection of Unamplified Target Genes via CRISPR–Cas9 Immobilized on a Graphene Field-Effect Transistor. *Nat Biomed Eng* **2019**, *3* (6), 427–437. https://doi.org/10.1038/s41551-019-0371-x.

(122) Jiménez-Monroy, K. L.; Renaud, N.; Drijkoningen, J.; Cortens, D.; Schouteden, K.; van Haesendonck, C.; Guedens, W. J.; Manca, J. V.; Siebbeles, L. D. A.; Grozema, F. C.; Wagner, P. H. High Electronic Conductance through Double-Helix DNA Molecules with Fullerene Anchoring Groups. *J. Phys. Chem. A* **2017**, *121* (6), 1182–1188. https://doi.org/10.1021/acs.jpca.7b00348.

(123) Genereux, J. C.; Barton, J. K. Mechanisms for DNA Charge Transport. *Chem. Rev.* **2010**, *110* (3), 1642–1662. https://doi.org/10.1021/cr900228f.

(124) Göeken, K. L.; Schasfoort, R. B. M.; Subramaniam, V.; Gill, R. Spermine Induced Reversible Collapse of Deoxyribonucleic Acid-Bridged Nanoparticle-Based Assemblies. *Nano Res.* **2018**, *11* (1), 383–396. https://doi.org/10.1007/s12274-017-1641-0.

(125) Sykes, K. S.; White, R. J. Nucleic Acid Identity, Structure, and Flexibility Affect the Electrochemical Signal of Tethered Redox

Molecules upon Biopolymer Collapse. *Langmuir* **2021**, *37* (42), 12466–12475. https://doi.org/10.1021/acs.langmuir.1c02161.

(126) Ma, T.; Baker, D. V.; Martinez-Blanco, G.; Bizzotto, D. An EIS Study of the Heterogeneity of Redox Labeled DNA SAMs on Gold before and after Hybridization. *Electrochimica Acta* **2025**, *517*, 145747. https://doi.org/10.1016/j.electacta.2025.145747.

(127) Lin, K.-Y.; Burke, A.; King, N. B.; Kahanda, D.; Mazaheripour, A.; Bartlett, A.; Dibble, D. J.; McWilliams, M. A.; Taylor, D. W.; Jocson, J.-M.; Minary-Jolandan, M.; Gorodetsky, A. A.; Slinker, J. D. Enhancement of the Electrical Properties of DNA Molecular Wires through Incorporation of Perylenediimide DNA Base Surrogates. *ChemPlusChem* **2019**, *84* (4), 416–419. https://doi.org/10.1002/cplu.201800661.

(128) Silva, S. M.; Tavallaie, R.; Gonçales, V. R.; Utama, R. H.; Kashi, M. B.; Hibbert, D. B.; Tilley, R. D.; Gooding, J. J. Dual Signaling DNA Electrochemistry: An Approach To Understand DNA Interfaces. *Langmuir* **2018**, *34* (4), 1249–1255. https://doi.org/10.1021/acs.langmuir.7b02787.

(129) Gu, Q.; Nanney, W.; Cao, H. H.; Wang, H.; Ye, T. Single Molecule Profiling of Molecular Recognition at a Model Electrochemical Biosensor. *J. Am. Chem. Soc.* **2018**, *140* (43), 14134–14143. https://doi.org/10.1021/jacs.8b07325.

(130) Abi, A.; Safavi, A. Determination of the Binding Site Size of Hexaammineruthenium(III) inside Monolayers of DNA on Gold. *Analyst* **2021**, *146* (2), 547–557. https://doi.org/10.1039/D0AN01685C.

(131) Wang, Z.; Zhang, J.; Zhu, C.; Wu, S.; Mandler, D.; Marks, R. S.; Zhang, H. Amplified Detection of Femtomolar DNA Based on a One-to-Few Recognition Reaction between DNA–Au Conjugate and Target DNA. *Nanoscale* **2014**, *6* (6), 3110–3115. https://doi.org/10.1039/C3NR05625B.

(132) Bos, E. S.; van der Doelen ,A. A.; Rooy ,N. van; and Schuurs, A. H. W. M. 3,3′,5,5′-Tetramethylbenzidine as an Ames Test Negative Chromogen for Horse-Radish Peroxidase in Enzyme-Immunoassay. *Journal of Immunoassay* **1981**, *2* (3–4), 187–204. https://doi.org/10.1080/15321818108056977.

(133) Yin, H.; Zhou, Y.; Zhang, H.; Meng, X.; Ai, S. Electrochemical Determination of microRNA-21 Based on Graphene, LNA Integrated Molecular Beacon, AuNPs and Biotin Multifunctional Bio Bar Codes and Enzymatic Assay System. *Biosensors and Bioelectronics* **2012**, *33* (1), 247–253. https://doi.org/10.1016/j.bios.2012.01.014.

(134) Golgi, C. *Untersuchungen über den feineren Bau des centralen und peripherischen Nervensystems*; Jena : G. Fischer, 1894.

(135) Hwang, S.; Kim, E.; Kwak, J. Electrochemical Detection of DNA Hybridization Using Biometallization. *Anal. Chem.* **2005**, *77* (2), 579–584. https://doi.org/10.1021/ac048778g.

(136) Si, Y.; Sun, Z.; Zhang, N.; Qi, W.; Li, S.; Chen, L.; Wang, H. Ultrasensitive Electroanalysis of Low-Level Free MicroRNAs in Blood by Maximum Signal Amplification of Catalytic Silver Deposition Using Alkaline Phosphatase-Incorporated Gold Nanoclusters. *Anal. Chem.* **2014**, *86* (20), 10406–10414. https://doi.org/10.1021/ac5028885.

(137) Alfonta, L.; Singh, A. K.; Willner, I. Liposomes Labeled with Biotin and Horseradish Peroxidase: A Probe for the Enhanced Amplification of Antigen−Antibody or Oligonucleotide−DNA Sensing Processes by the Precipitation of an Insoluble Product on Electrodes. *Anal. Chem.* **2001**, *73* (1), 91–102. https://doi.org/10.1021/ac000819v.

(138) Chandra, S.; Gäbler, C.; Schliebe, C.; Lang, H.; Bahadur, D. Fabrication of a Label-Free Electrochemical Immunosensor Using a Redox Active Ferrocenyl Dendrimer. *New J. Chem.* **2016**, *40* (11), 9046–9053. https://doi.org/10.1039/C6NJ00830E.

(139) Yao, B.; Liu, Y.; Tabata, M.; Zhu, H.; Miyahara, Y. Sensitive Detection of microRNA by Chronocoulometry and Rolling Circle Amplification on a Gold Electrode. *Chem. Commun.* **2014**, *50* (68), 9704–9706. https://doi.org/10.1039/C4CC03330B.

(140) Hsieh, K.; Patterson, A. S.; Ferguson, B. S.; Plaxco, K. W.; Soh, H. T. Rapid, Sensitive, and Quantitative Detection of Pathogenic DNA at the Point of Care through Microfluidic Electrochemical Quantitative Loop-Mediated Isothermal Amplification. *Angewandte Chemie International Edition* **2012**, *51* (20), 4896–4900. https://doi.org/10.1002/anie.201109115.

(141) Chahin, N.; Escobar-Nassar, S.; Osma, J.; Bashammakh, A. S.; AlYoubi, A. O.; Ortiz, M.; O'Sullivan, C. K. Low-Cost Platform for Multiplexed Electrochemical Melting Curve Analysis. *ACS Meas. Sci. Au* **2022**, *2* (2), 147–156. https://doi.org/10.1021/acsmeasuresciau.1c00044.

(142) Fukunaga, K.; Hishinuma, E.; Hiratsuka, M.; Kato, K.; Okusaka, T.; Saito, T.; Ikeda, M.; Yoshida, T.; Zembutsu, H.; Iwata, N.; Mushiroda, T. Determination of Novel CYP2D6 Haplotype Using the Targeted Sequencing Followed by the Long-Read Sequencing and the Functional Characterization in the Japanese Population. *J Hum Genet* **2021**, *66* (2), 139–149. https://doi.org/10.1038/s10038-020-0815-x.

(143) Smith, L. M.; Sanders, J. Z.; Kaiser, R. J.; Hughes, P.; Dodd, C.; Connell, C. R.; Heiner, C.; Kent, S. B. H.; Hood, L. E. Fluorescence Detection in Automated DNA Sequence Analysis. *Nature* **1986**, *321* (6071), 674–679. https://doi.org/10.1038/321674a0.

(144) Huang, X. C.; Quesada, M. A.; Mathies, R. A. DNA Sequencing Using Capillary Array Electrophoresis. *Anal. Chem.* **1992**, *64* (18), 2149–2154. https://doi.org/10.1021/ac00042a021.

(145) Woolley, A. T.; Mathies, R. A. Ultra-High-Speed DNA Fragment Separations Using Microfabricated Capillary Array Electrophoresis Chips. *Proceedings of the National Academy of Sciences* **1994**, *91* (24), 11348–11352. https://doi.org/10.1073/pnas.91.24.11348.

(146) *US6143152A - Microfabricated capillary array electrophoresis device and method - Google Patents*. https://patents.google.com/patent/US6143152A (accessed 2026-02-26).

(147) Alaverdian, L.; Alaverdian, S.; Bilenko, O.; Bogdanov, I.; Filippova, E.; Gavrilov, D.; Gorbovitski, B.; Gouzman, M.; Gudkov, G.; Domratchev, S.; Kosobokova, O.; Lifshitz, N.; Luryi, S.; Ruskovoloshin, V.; Stepoukhovitch, A.; Tcherevishnick, M.; Tyshko, G.; Gorfinkel, V. A Family of Novel DNA Sequencing Instruments Based on Single-Photon Detection. *ELECTROPHORESIS* **2002**, *23* (16), 2804–2817. https://doi.org/10.1002/1522-2683(200208)23:16%3C2804::AID-ELPS2804%3E3.0.CO;2-9.

(148) Emrich, C. A.; Tian, H.; Medintz, I. L.; Mathies, R. A. Microfabricated 384-Lane Capillary Array Electrophoresis Bioanalyzer for Ultrahigh-Throughput Genetic Analysis. *Anal. Chem.* **2002**, *74* (19), 5076–5083. https://doi.org/10.1021/ac020236g.

(149) Shibata, K.; Itoh, M.; Aizawa, K.; Nagaoka, S.; Sasaki, N.; Carninci, P.; Konno, H.; Akiyama, J.; Nishi, K.; Kitsunai, T.; Tashiro, H.; Itoh, M.; Sumi, N.; Ishii, Y.; Nakamura, S.; Hazama, M.; Nishine, T.; Harada, A.; Yamamoto, R.; Matsumoto, H.; Sakaguchi, S.; Ikegami, T.; Kashiwagi, K.; Fujiwake, S.; Inoue, K.; Togawa, Y.; Izawa, M.; Ohara, E.; Watahiki, M.; Yoneda, Y.; Ishikawa, T.; Ozawa, K.; Tanaka, T.; Matsuura, S.; Kawai, J.; Okazaki, Y.; Muramatsu, M.; Inoue, Y.; Kira, A.; Hayashizaki, Y. RIKEN Integrated Sequence Analysis (RISA) System—384-Format Sequencing Pipeline with 384 Multicapillary Sequencer. *Genome Res.* **2000**, *10* (11), 1757–1771. https://doi.org/10.1101/gr.152600.

(150) Margulies, M.; Egholm, M.; Altman, W. E.; Attiya, S.; Bader, J. S.; Bemben, L. A.; Berka, J.; Braverman, M. S.; Chen, Y.-J.; Chen, Z.; Dewell, S. B.; Du, L.; Fierro, J. M.; Gomes, X. V.; Godwin, B. C.; He, W.; Helgesen, S.; Ho, C. H.; Irzyk, G. P.; Jando, S. C.; Alenquer, M. L.

I.; Jarvie, T. P.; Jirage, K. B.; Kim, J.-B.; Knight, J. R.; Lanza, J. R.; Leamon, J. H.; Lefkowitz, S. M.; Lei, M.; Li, J.; Lohman, K. L.; Lu, H.; Makhijani, V. B.; McDade, K. E.; McKenna, M. P.; Myers, E. W.; Nickerson, E.; Nobile, J. R.; Plant, R.; Puc, B. P.; Ronan, M. T.; Roth, G. T.; Sarkis, G. J.; Simons, J. F.; Simpson, J. W.; Srinivasan, M.; Tartaro, K. R.; Tomasz, A.; Vogt, K. A.; Volkmer, G. A.; Wang, S. H.; Wang, Y.; Weiner, M. P.; Yu, P.; Begley, R. F.; Rothberg, J. M. Genome Sequencing in Microfabricated High-Density Picolitre Reactors. *Nature* **2005**, *437* (7057), 376–380. https://doi.org/10.1038/nature03959.

(151) Rothberg, J. M.; Hinz, W.; Rearick, T. M.; Schultz, J.; Mileski, W.; Davey, M.; Leamon, J. H.; Johnson, K.; Milgrew, M. J.; Edwards, M.; Hoon, J.; Simons, J. F.; Marran, D.; Myers, J. W.; Davidson, J. F.; Branting, A.; Nobile, J. R.; Puc, B. P.; Light, D.; Clark, T. A.; Huber, M.; Branciforte, J. T.; Stoner, I. B.; Cawley, S. E.; Lyons, M.; Fu, Y.; Homer, N.; Sedova, M.; Miao, X.; Reed, B.; Sabina, J.; Feierstein, E.; Schorn, M.; Alanjary, M.; Dimalanta, E.; Dressman, D.; Kasinskas, R.; Sokolsky, T.; Fidanza, J. A.; Namsaraev, E.; McKernan, K. J.; Williams, A.; Roth, G. T.; Bustillo, J. An Integrated Semiconductor Device Enabling Non-Optical Genome Sequencing. *Nature* **2011**, *475* (7356), 348–352. https://doi.org/10.1038/nature10242.

(152) Jain, M.; Fiddes, I. T.; Miga, K. H.; Olsen, H. E.; Paten, B.; Akeson, M. Improved Data Analysis for the MinION Nanopore Sequencer. *Nat Methods* **2015**, *12* (4), 351–356. https://doi.org/10.1038/nmeth.3290.

(153) Loman, N. J.; Quick, J.; Simpson, J. T. A Complete Bacterial Genome Assembled de Novo Using Only Nanopore Sequencing Data. *Nat Methods* **2015**, *12* (8), 733–735. https://doi.org/10.1038/nmeth.3444.

(154) Wang, Y.; Yang, Q.; Wang, Z. The Evolution of Nanopore Sequencing. *Front. Genet.* **2015**, *5*. https://doi.org/10.3389/fgene.2014.00449.

(155) *Genapsys sequencer*. Prayoga Lifesciences Inc. https://www.prayogalifesciences.com/genapsys-sequencer-new/ (accessed 2026-03-26).

(156) Killpack, J.; Galova, K.; Christova, R.; Palmer, E.; Barratt, G.; Greenwood, C.; Fraccari, R.; Acquah, J.; Reed, S.; Wisniewski, M. *Innovative Technology to Automate and Improve the Detection Sensitivity of Ultra-Low Frequency Mutations Directly from Blood Liquid Biopsies*; DNAe, 2025. https://www.dnae.com/wp-content/uploads/2025/11/DNAe_AMP_Oncology_Poster_print.pdf (accessed 2026-03-26).

(157) Kokoris, M.; McRuer, R.; Nabavi, M.; Jacobs, A.; Prindle, M.; Cech, C.; Berg, K.; Lehmann, T.; Machacek, C.; Tabone, J.; Chandrasekar, J.; McGee, L.; Lopez, M.; Reid, T.; Williams, C.; Barrett, S.; Lehmann, A.; Kovarik, M.; Busam, R.; Miller, S.; Banasik, B.; Kesic, B.; Arryman, A.; Rogers-Peckham, M.; Kimura, A.; LeProwse, M.; Wolfin, M.; Kritzer, S.; Leadbetter, J.; Babazadeh, M.; Chase, J.; Thiessen, G.; Lint, W.; Goodman, D.; O'Connell, D.; Lumanpauw, N.; Hoffman, J.; Vellucci, S.; Collins, K.; Vellucci, J.; Taylor, A.; Murphy, M.; Lee, M.; Corning, M. Sequencing by Expansion (SBX) – a Novel, High-Throughput Single-Molecule Sequencing Technology. bioRxiv March 15, 2025, p 2025.02.19.639056. https://doi.org/10.1101/2025.02.19.639056.

(158) Nabsys. The OhmX™ Platform: Electronic Genome Mapping. https://cdn.prod.website-files.com/67608f2c14ae5d4abe8a107c/68edd0b6b99c19707839d5b6_OhmX%20White%20Paper.pdf (accessed 2026-03-26).

(159) Henry, E.; Charalambous, E.; Betsou, F.; Mathieson, W. Implementing Routine Monitoring for Nuclease Contamination of Equipment and Consumables into the Quality Management System of a Laboratory. *Heliyon* **2024**, *10* (2), e24603. https://doi.org/10.1016/j.heliyon.2024.e24603.

(160) Cholet, F.; Ijaz, U. Z.; Smith, C. J. Differential Ratio Amplicons (Ramp) for the Evaluation of RNA Integrity Extracted from Complex Environmental Samples. *Environmental Microbiology* **2019**, *21* (2), 827–844. https://doi.org/10.1111/1462-2920.14516.

(161) Ratautas, D.; Serapinas, S.; Gineityte, J.; Butkevicius, M.; Danilevicius, R.; Dagys, M. Electrochemical System for the Rapid and Sensitive Detection and Quantification of Nuclease-like Activity Exhibiting Enzymes. EP4209596A1, July 12, 2023. https://patents.google.com/patent/EP4209596A1/en (accessed 2025-09-05).

(162) Wang, Y.-Y.; Hung, A. C.; Lo, S.; Hsieh, Y.-C.; Yuan, S.-S. F. MRE11 as a Molecular Signature and Therapeutic Target for Cancer Treatment with Radiotherapy. *Cancer Letters* **2021**, *514*, 1–11. https://doi.org/10.1016/j.canlet.2021.05.013.

(163) Zhou, C.; Feng, M.; Chen, X.; Gao, Y.; Chen, L.; Li, L.; Li, D.; Cao, Y. Exonuclease 1 (EXO1) Is a Potential Prognostic Biomarker and Correlates with Immune Infiltrates in Lung Adenocarcinoma. *Onco Targets Ther* **2021**, *14*, 1033–1048. https://doi.org/10.2147/OTT.S286274.

(164) Dave, N.; Liu, J. Fast Molecular Beacon Hybridization in Organic Solvents with Improved Target Specificity. *J. Phys. Chem. B* **2010**, *114* (47), 15694–15699. https://doi.org/10.1021/jp106754k.

(165) Vanderhoeven, J.; Pappaert, K.; Dutta, B.; Vanhummelen, P.; Baron, G. V.; Desmet, G. Exploiting the Benefits of Miniaturization for the Enhancement of DNA Microarrays. *ELECTROPHORESIS* **2004**, *25* (21–22), 3677–3686. https://doi.org/10.1002/elps.200406116.

(166) Dandy, D. S.; Wu, P.; Grainger, D. W. Array Feature Size Influences Nucleic Acid Surface Capture in DNA Microarrays. *Proceedings of the National Academy of Sciences* **2007**, *104* (20), 8223–8228. https://doi.org/10.1073/pnas.0606054104.

(167) Shchepinov, M. S.; Case-Green, S. C.; Southern, E. M. Steric Factors Influencing Hybridisation Of Nucleic Acids To Oligonucleotide Arrays. *Nucleic Acids Research* **1997**, *25* (6), 1155–1161. https://doi.org/10.1093/nar/25.6.1155.

(168) Ammar, R.; Smith, A. M.; Heisler, L. E.; Giaever, G.; Nislow, C. A Comparative Analysis of DNA Barcode Microarray Feature Size. *BMC Genomics* **2009**, *10* (1), 471. https://doi.org/10.1186/1471-2164-10-471.

(169) Gineitytė, J.; Serapinas, S.; Ratautas, D. Electrochemical DNA Hybridization Signal Amplification System Using Methylene Blue and Ascorbic Acid. *Electrochimica Acta* **2024**, *507*, 145146. https://doi.org/10.1016/j.electacta.2024.145146.

(170) Boal, A. K.; Barton, J. K. Electrochemical Detection of Lesions in DNA. *Bioconjugate Chem.* **2005**, *16* (2), 312–321. https://doi.org/10.1021/bc0497362.

(171) Kasprzak, A.; Zuchowska, A.; Poplawska, M. Functionalization of Graphene: Does the Organic Chemistry Matter? *Beilstein J. Org. Chem.* **2018**, *14*, 2018–2026. https://doi.org/10.3762/bjoc.14.177.

(172) Lim, C. Y.; Owens, N. A.; Wampler, R. D.; Ying, Y.; Granger, J. H.; Porter, M. D.; Takahashi, M.; Shimazu, K. Succinimidyl Ester Surface Chemistry: Implications of the Competition between Aminolysis and Hydrolysis on Covalent Protein Immobilization. *Langmuir* **2014**, *30* (43), 12868–12878. https://doi.org/10.1021/la503439g.

(173) Lozano-Chamizo, L.; Márquez, C.; Marciello, M.; Galdon, J. C.; de la Fuente-Zapico, E.; Martinez-Mazón, P.; Gonzalez-Rumayor, V.; Filice, M.; Gamiz, F. High Enhancement of Sensitivity and Reproducibility in Label-Free SARS-CoV-2 Detection with Graphene Field-Effect Transistor Sensors through Precise Surface Biofunctionalization Control. *Biosensors and Bioelectronics* **2024**, *250*, 116040. https://doi.org/10.1016/j.bios.2024.116040.

(174) Brustoloni, C. J.-M.; Soltan Khamsi, P.; Kammarchedu, V.; Ebrahimi, A. Systematic Study of Various Functionalization Steps for Ultrasensitive Detection of SARS-CoV-2 with Direct Laser-Functionalized Au-LIG Electrochemical Sensors. *ACS Appl. Mater. Interfaces* **2024**, *16* (37), 49041–49052. https://doi.org/10.1021/acsami.4c09571.

(175) Fujimoto, N.; Bade, S.; Röckendorf, N.; Ramaker, K.; Frey, A. Polyethylene Glycol-Conjugated Alkylamines - A Novel Class of Surfactants for the Saturation of Immunoassay Solid Phase Surfaces. *Talanta* **2020**, *211*, 120741. https://doi.org/10.1016/j.talanta.2020.120741.

(176) Ricci, A. M.; Méndez De Leo, L. P.; Williams, F. J.; Calvo, E. J. Some Evidence for the Formation of an Azo Bond during the Electroreduction of Diazonium Salts on Au Substrates. *ChemPhysChem* **2012**, *13* (8), 2119–2127. https://doi.org/10.1002/cphc.201100882.

(177) Kenkel, S.; Mittal, S.; Bhargava, R. Closed-Loop Atomic Force Microscopy-Infrared Spectroscopic Imaging for Nanoscale Molecular Characterization. *Nat Commun* **2020**, *11* (1), 3225. https://doi.org/10.1038/s41467-020-17043-5.

(178) Muzyka, K.; Rico, F.; Xu, G.; Casuso, I. DNA at Conductive Interfaces: What Can Atomic Force Microscopy Offer? *Journal of Electroanalytical Chemistry* **2023**, *938*, 117448. https://doi.org/10.1016/j.jelechem.2023.117448.

(179) Muller, D. A. Structure and Bonding at the Atomic Scale by Scanning Transmission Electron Microscopy. *Nature Mater* **2009**, *8* (4), 263–270. https://doi.org/10.1038/nmat2380.

(180) Gong, P.; Lee, C.-Y.; Gamble, L. J.; Castner, D. G.; Grainger, D. W. Hybridization Behavior of Mixed DNA/Alkylthiol Monolayers on Gold: Characterization by Surface Plasmon Resonance and 32P Radiometric Assay. *Anal. Chem.* **2006**, *78* (10), 3326–3334. https://doi.org/10.1021/ac052138b.

(181) Špringer, T.; Šípová, H.; Vaisocherová, H.; Štěpánek, J.; Homola, J. Shielding Effect of Monovalent and Divalent Cations on Solid-Phase DNA Hybridization: Surface Plasmon Resonance Biosensor Study. *Nucleic Acids Research* **2010**, *38* (20), 7343–7351. https://doi.org/10.1093/nar/gkq577.

(182) Colthup, N. B.; Daly, L. H.; Wiberley, S. E. *Introduction to Infrared and Raman Spectroscopy*, 3rd ed.; Academic Press: Boston, 1990.

(183) Silva, S. M.; Hoque, S.; Gonçales, V. R.; Gooding, J. J. The Impact of the Position of the Redox Label on Charge Transfer and Hybridization

Efficiency at DNA Interfaces. *Electroanalysis* **2018**, *30* (7), 1529–1535. https://doi.org/10.1002/elan.201800197.

(184) Khuda, N.; Somasundaram, S.; Urgunde, A. B.; Easley, C. J. Ionic Strength and Hybridization Position near Gold Electrodes Can Significantly Improve Kinetics in DNA-Based Electrochemical Sensors. *ACS Appl. Mater. Interfaces* **2023**, *15* (4), 5019–5027. https://doi.org/10.1021/acsami.2c22741.

(185) Cloutier, T. E.; Widom, J. DNA Twisting Flexibility and the Formation of Sharply Looped Protein–DNA Complexes. *Proceedings of the National Academy of Sciences* **2005**, *102* (10), 3645–3650. https://doi.org/10.1073/pnas.0409059102.

(186) Uzawa, T.; Cheng, R. R.; White, R. J.; Makarov, D. E.; Plaxco, K. W. A Mechanistic Study of Electron Transfer from the Distal Termini of Electrode-Bound, Single-Stranded DNAs. *J. Am. Chem. Soc.* **2010**, *132* (45), 16120–16126. https://doi.org/10.1021/ja106345d.

(187) Steel, A. B.; Levicky, R. L.; Herne, T. M.; Tarlov, M. J. Immobilization of Nucleic Acids at Solid Surfaces: Effect of Oligonucleotide Length on Layer Assembly. *Biophys J* **2000**, *79* (2), 975–981.

(188) Jia, Y.; Sobolev, Y. I.; Cybulski, O.; Klucznik, T.; Quintana, C.; Ahumada, J. C.; Grzybowski, B. A. Aerodynamically Levitated Droplets as Small-Scale Chemical Reactors and Liquid Microprinters. *Angewandte Chemie International Edition* **2024**, *63* (39), e202318038. https://doi.org/10.1002/anie.202318038.

(189) Barman, S. R.; Khan, I.; Chatterjee, S.; Saha, S.; Choi, D.; Lee, S.; Lin, Z.-H. Electrowetting-on-Dielectric (EWOD): Current Perspectives and Applications in Ensuring Food Safety. *J Food Drug Anal 28* (4), 595–621. https://doi.org/10.38212/2224-6614.1239.

(190) *Ion 550™ Kit—Chef 8 reactions | Contact Us | Ion Torrent™ | thermofisher.com.* https://www.thermofisher.com/order/catalog/product/A34541 (accessed 2025-07-30).

(191) Rothberg, J. M.; Hinz, W.; Rearick, T. M.; Schultz, J.; Mileski, W.; Davey, M.; Leamon, J. H.; Johnson, K.; Milgrew, M. J.; Edwards, M.; Hoon, J.; Simons, J. F.; Marran, D.; Myers, J. W.; Davidson, J. F.; Branting, A.; Nobile, J. R.; Puc, B. P.; Light, D.; Clark, T. A.; Huber, M.; Branciforte, J. T.; Stoner, I. B.; Cawley, S. E.; Lyons, M.; Fu, Y.; Homer, N.; Sedova, M.; Miao, X.; Reed, B.; Sabina, J.; Feierstein, E.; Schorn, M.; Alanjary, M.; Dimalanta, E.; Dressman, D.; Kasinskas, R.; Sokolsky, T.; Fidanza, J. A.; Namsaraev, E.; McKernan, K. J.; Williams, A.; Roth, G.

T.; Bustillo, J. An Integrated Semiconductor Device Enabling Non-Optical Genome Sequencing. *Nature* **2011**, *475* (7356), 348–352. https://doi.org/10.1038/nature10242.

(192) Kim, S.; Im, J.; Wang, S. X.; Lee, J.-R. Design and Validation of Specific Oligonucleotide Probes on Planar Magnetic Biosensors. *Anal. Chem.* **2024**, *96* (49), 19447–19455. https://doi.org/10.1021/acs.analchem.4c03973.

(193) Abraham Punnoose, J.; Thomas, K. J.; Chandrasekaran, A. R.; Vilcapoma, J.; Hayden, A.; Kilpatrick, K.; Vangaveti, S.; Chen, A.; Banco, T.; Halvorsen, K. High-Throughput Single-Molecule Quantification of Individual Base Stacking Energies in Nucleic Acids. *Nat Commun* **2023**, *14* (1), 631. https://doi.org/10.1038/s41467-023-36373-8.

(194) Hock, B.; Seifert, M.; Kramer, K. Engineering Receptors and Antibodies for Biosensors. *Biosensors and Bioelectronics* **2002**, *17* (3), 239–249. https://doi.org/10.1016/S0956-5663(01)00267-6.

(195) Strehlitz, B.; Nikolaus, N.; Stoltenburg, R. Protein Detection with Aptamer Biosensors. *Sensors* **2008**, *8* (7), 4296–4307. https://doi.org/10.3390/s8074296.

(196) *RNaseAlert™ Lab Test Kit 25 reactions | Contact Us | Invitrogen™ | thermofisher.com.* https://www.thermofisher.com/order/catalog/product/AM1964 (accessed 2025-01-21).

(197) Stein, J. A. C.; Ianeselli, A.; Braun, D. Kinetic Microscale Thermophoresis for Simultaneous Measurement of Binding Affinity and Kinetics. *Angewandte Chemie International Edition* **2021**, *60* (25), 13988–13995. https://doi.org/10.1002/anie.202101261.

(198) Immoos, C. E.; Lee, S. J.; Grinstaff, M. W. DNA-PEG-DNA Triblock Macromolecules for Reagentless DNA Detection. *J. Am. Chem. Soc.* **2004**, *126* (35), 10814–10815. https://doi.org/10.1021/ja046634d.

(199) Alagic, A.; Koprianiuk, A.; Kluger, R. Hemoglobin–Superoxide DismutaseChemical Linkages That Create a Dual-Function Protein. *J. Am. Chem. Soc.* **2005**, *127* (22), 8036–8043. https://doi.org/10.1021/ja050339r.

(200) Žalnėravičius, R.; Talaikis, M.; Klimas, V.; Serapinas, S.; Butkevičius, M.; Vaičiūnienė, J.; Morkvėnas, A.; Karabanovas, V.; Niaura, G.; Jagminas, A.; Dagys, M. Fabrication of Porous Black Gold Films by One-Step Anodic Treatment: Towards the Development of SERS-Active Nanosensors. *Materials Today Chemistry* **2025**, *47*, 102849. https://doi.org/10.1016/j.mtchem.2025.102849.

(201) *About dbSNP (Updated March 11, 2025).* https://www.ncbi.nlm.nih.gov/snp/docs/about/ (accessed 2025-07-17).
(202) *rs12248560 RefSNP Report - dbSNP - NCBI.* https://www.ncbi.nlm.nih.gov/snp/rs12248560 (accessed 2025-07-16).

APPENDICES

Appendix I: Further application – The application of the DNase biosensor for RNase detection.

Appendix II: The mechanistic implications for live DNA hybridization monitoring: Exploration of the signal transduction mechanism of the methylene blue – ascorbic acid couple.

Appendix III: The application of the prepared SERS-active electrodes for quality control of chemical surface modifications.

Appendix IV: The mechanistic implications for melting-based DNA mismatch detection: Exploration of the signal transduction mechanism from the methylene blue-labeled DNA reporter strand and the hybridization impacts of solid-phase DNA probe density.

Appendix V: Application – the detection of double SNPs, miniaturization and sequencing.

1. Appendix I

The application of the DNase biosensor for RNase detection

Materials and Methods

Detection of RNases is typically performed at lower concentration than DNases, as RNases are more stable, difficult to inhibit and are generally more problematic due to low RNA stability.

Name	Composition (Sequence 5'-3')
Ribonuclease working buffer solution	20mM PBS, 20mM NaCl, pH 6
RNase stock solution	1000 Kunitz unit ml^{-1} RNAse A, 50mM Tris, 50% glycerol, pH 7
RNase sensor target stock solution	40 µM Oligonucleotide target, 20mM Tris, pH 7.00
RNase sensor probe sequence	Thiol-C6- AAT TAT CAA ACA CAA ACA GAC TTA A
RNase sensor target sequence	Atto MB2-g gca ggg cag ggc agu cgu uaa guc ugu uug ugu uug aua auu

Lyophilized Ribonuclease A was from bovine pancreas and glycerol were purchased from Sigma-Aldrich. DNase Alert kit was purchased from Sigma. All solutions were prepared in nuclease-free water. The working PBS buffer solution was heated to boiling in a household microwave and aliquoted into sterile test tubes and stored at ~4 °C.

RNA nucleic acid sequence (oligonucleotide target) was purchased from Metabion and used as received without additional purification procedures. Samples were prepared to measure the nuclease-like activity in laboratory water (nuclease-free) 0 KU ml^{-1}, 1×10^{-7} KU ml^{-1}, 1×10^{-6} KU ml^{-1}, 5×10^{-6} KU ml^{-1}, 1×10^{-5} KU ml^{-1}.

The oligonucleotide target was introduced into the samples and kept for 30 min at 37 ºC. The digested solution hybridization was monitored for 30 min.

Results

The DNase sensor when measured in parallel was comparable to a commercial kit (DNase Alert) (Fig. A1 1).

In samples with higher activity of RNase A (e.g., 1×10^{-5} KU ml^{-1}), the hybridization rate was negligible, since the enzyme cleaved the overwhelming

majority target present in the solution. It was impossible to quantify the RNase from 1×10^{-5} KU ml^{-1} onward. The LOD can be comfortably set at 1×10^{-6} KU ml^{-1} as these datapoints are over 3×SD away from control. (**Fig. A1 2**) At the activity given by the manufacturer of RNase Alert of 82 KU mg^{-1}, we can estimate a lower limit of detection of 12.2 pg ml^{-1} of sample. Using a commercial assay RNase Alert we would expect a detection limit of 2.5-5 pg/ml, (manufacturer also states this value as 3.5×10^{-7} units per 0.1 ml of sample[196]), meaning a very similar sensitivity is achieved.

One shortcoming of this iteration of assay design is the use of 3.5 ml of sample, because the hybridization is ultimately measured in a relatively large volume. The hybridization cell can be reasonably miniaturized to ~1 ml requiring an estimated 0.5 ml of sample for such assay. However, in the future the methods of external hybridization may be applied to avoid such problems. External hybridization can be easily performed in a 0.1 ml volume.

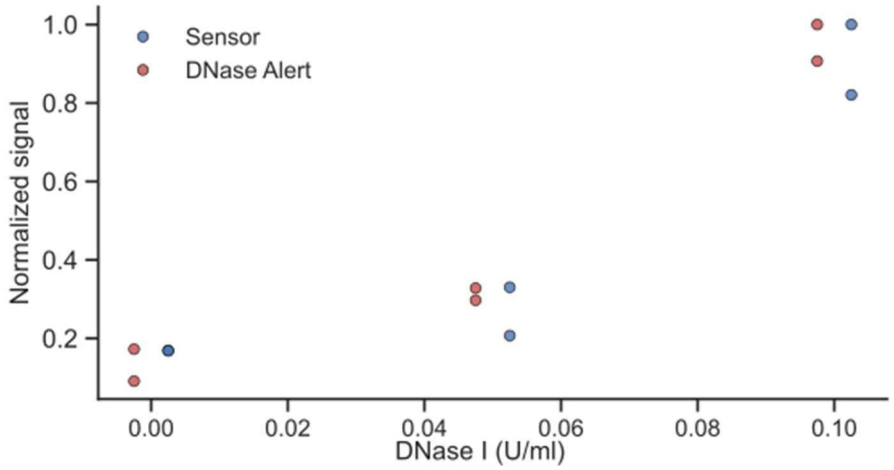


Figure A1 1. A comparison of the DNase sensor versus a commercial kit (signal normalized to 1 at the maximal value for simplicity, unitless).

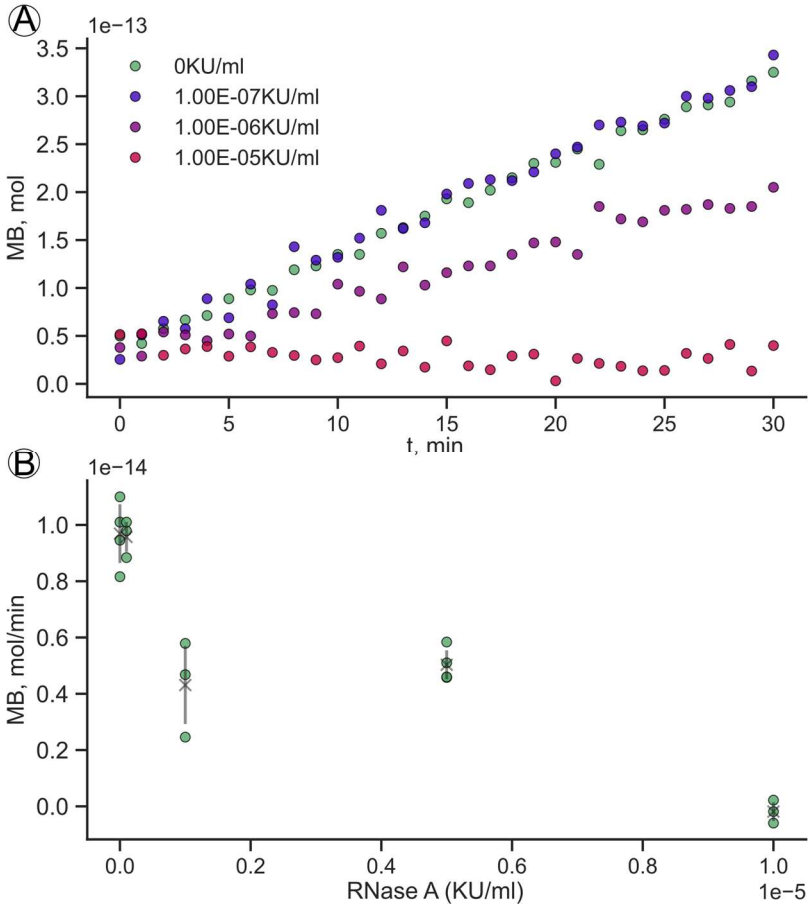


Figure A1 2. A: An example of hybridization kinetics using RNase A pretreated target; B: RNase concentration measurements (Mean ± SD).

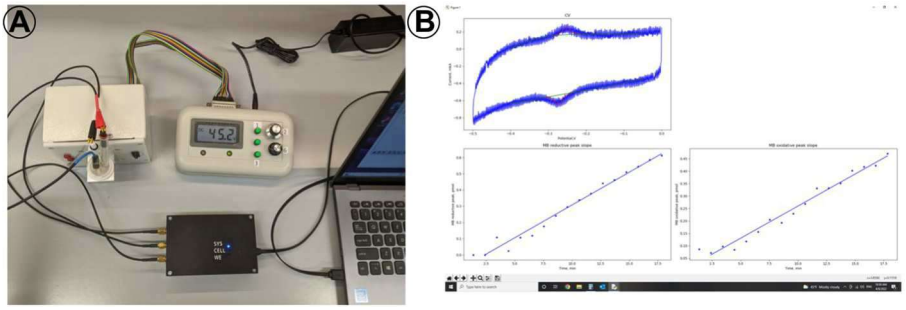


Figure A1 3. A representation of A) a prototype device and B) prototype software (from **Publication 1 SI**).

2. Appendix II

The mechanistic implications for live DNA hybridization monitoring: Exploration of the signal transduction mechanism of the methylene blue – ascorbic acid couple

Name	Sequence 5'-3'
DNA Probe (DNAP)	Thiol-C6-CGC ATT ATC TCT TAC ATC AGA
ZNA Probe (ZNAP)	Thiol-C6-CGC ATT ATC TCT TAC ATC AGA-(ZNA-4)
Reporter *1 HEG5	Atto MB2-(HEG-spacer)×2-GAT GCT TTG AGA ACA
Reporter *1 HEG3	GAT GCT TTG AGA ACA-(HEG-spacer)×4-Atto MB2
Reporter *1 5	Atto MB2-GAT GCT TTG AGA ACA
Reporter *1 3	GAT GCT TTG AGA ACA-Atto MB2
Target *1s	C TGT TCT CAA AGC ATC TCT GAT GTA AGA GAT AAT GCG

Methods

The experiments were carried out according to Gineitytė et. al.,[169] using 3 M NaCl, 30 mM Ascorbate, pH 7, 25 °C, 1500 rpm stirring with -100 mV vs. Ag/AgCl (3 M KCl) at 0.5 Hz. The reporter sequences were introduced at 150 s (no visible signal was observed) and the target sequence **Target *1s** was introduced at 400 s. The DNA and the ZNA electrodes were measured simultaneously with PalmSens4 bipotentiostat.

$$I_t = A(1 - e^{-Bt}) + C \qquad \text{Equation (A1)}$$

$$I_t = k\ n\ F\ [AA]\ ptMB_{max}(1 - e^{-k_{on}[Targ]t}) \qquad \text{Equation (A2)}$$

The current was zeroed and the baseline was fitted according to Eq. A1 and the hybridization was fitted according to Eq. A2, where:

- n = 2 (electrons participating in a process),
- F = 96485 C mol^{-1} (Faraday's constant),
- [AA] = 0.03 M (ascorbic acid concentration),
- [Targ] = 20 × 10^{-9} M (+ 4× excess of the reporters was used),
- $ptMB_{max}$ = 0.0205 × 10^{-12} M – this value was not fitted as per publication but rather is a reasonable estimate from previous CV experiments [Appendix IV],
- The parameters k and k_{on} were fitted

Results

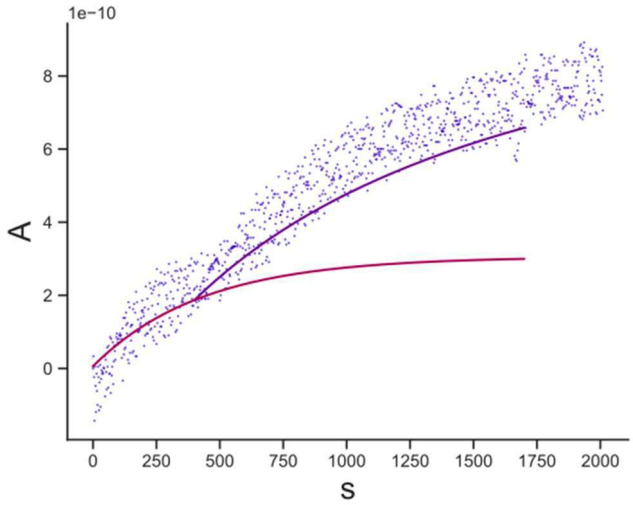


Figure A2 1. Typical experimental data with baseline and hybridization fits shown.

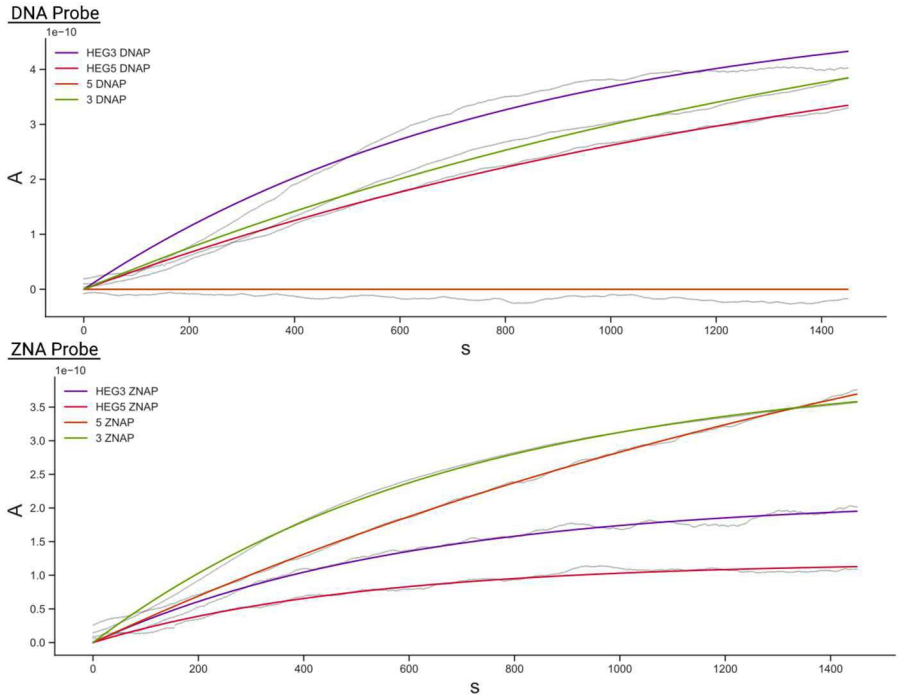


Figure A2 2. Hybridization currents after zeroing, smoothing and baselining (the dots represent processed data, average of 2 electrodes and the lines represent the fitted curves).

While these results successfully demonstrate the hybridization kinetics in sandwich format, the previously obtained (8 M^{-1} s^{-1})[169] bimolecular constant was not improved and the signal is generally poor (~0.3 nA/20 nM Target).

These experiments were predominantly exploratory in nature as an improvement in electron transfer rate constant of ~100× is reported in literature via MB position change.[130] The observed changes in the signal are not noteworthy and further optimization was not pursued. Modifying the solid phase for probes containing a distal ZNA-4 modification similarly shows no large improvement.

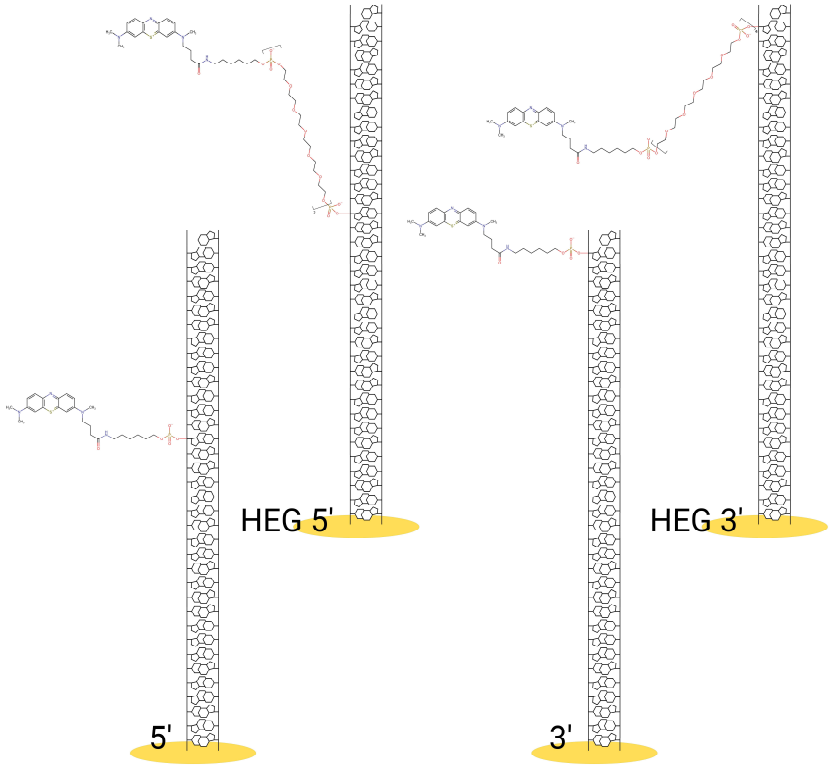


Figure A2 3. Label position on distal and proximal sides of the reporter and via an ethylene glycol bridge.

The k_{on} constant is reported in literature in the range of 500 [63]–1 500 000 [197] M^{-1} s^{-1} and is [NaCl] and probe coverage dependent. In these experiments the k_{on} was much higher than in our publication.

Name	k (M^{-1} s^{-1})	k_{on} (M^{-1} s^{-1})	Name	k (M^{-1} s^{-1})	k_{on} (M^{-1} s^{-1})
HEG3 DNAP	4.35	62150	HEG3 ZNAP	1.80	83869
HEG5 DNAP	4.63	32239	HEG5 ZNAP	1.00	99203
5 DNAP	0.00	0	5 ZNAP	5.81	26286
3 DNAP	5.49	30570	3 ZNAP	3.42	72877

Table A2 1. The measured constants of various duplex-ascorbic acid reaction.

Interestingly the 5 DNAP sandwich – a sandwich with expected low MB mobility due to DNA duplex repulsion – (to move the label, the entire DNA chain with a large negative charge must bend sharply) shows an abysmal response. HEG extension has lowered the reaction rate constant (k) in all cases as it likely increases the label travel distance. This is indicative of a mobility-driven charge transfer. Internal PEG bridges have been previously used to lower the rate of label-surface collisions.[198]

Another interesting observation is that the hybridization rates were overall improved using the ZNA probes, suggesting a potential application for more rapid measurements.

3. Appendix III

The application of the prepared SERS-active electrodes for quality control of chemical surface modifications

Materials and Methods

Electrode manufacturing

Methrohm C220AT SPE gold electrodes were prepared in 300 mM aqueous oxalic acid at 5 °C, +3 V vs. $Hg/HgSO_4$.

Synthetic methods (adapted from[199]) (Fig. A3 1)

4,4'-Dithiobisphenylacetic acid (**I**)

I_2 (88 mg; 0.35 mmol) was dissolved in ~3ml of anhydrous ethanol and triethylamine (300 µl) was added, then 4-mercaptophenylacetic acid (106mg; 0.63mmol) in a minimal amount of EtOH was added and the solution instantly discolored. The reaction was left overnight in a capped vial. 300 µl of 10% aq. Na_2SSO_3 was added for quenching followed by ~30 ml of 50 mM aq. HCl, the precipitate was collected by filtration and washed with water, dried; yield: 62 mg (59 %).

4,4'-Dithiobisphenylacetyl chloride (**II**)

(62 mg; 0.185 mmol) of **I** was dissolved in 3 ml dichloromethane and 1 ml $SOCl_2$ in a flask and agitated with ultrasound for ~5 min. The solution was left to stir overnight at room temperature, volatiles removed by vacuum distillation leaving ~ 60 mg of a yellow residue which was flushed with argon to remove any trace of $SOCl_2$ and processed as-is immediately.

4,4'-Dithiobis-N-(4-**C**ya**n**ophenyl)-**P**henyl**A**cetamide (SSCNPA)

Into the flask containing (~60 mg; ~0.161 mmol) of **II**, 2 ml of DMAc was added, followed by catalytic dimethylaminopyridine (~2 mg) and 4-aminobenzonitrile (42 mg; 0.356 mmol). The solution was left to stir overnight. Water and 50 mM HCl were added until no more precipitate was formed. The suspension was centrifuged under 1800 g, mixed with another 30 ml of 50 mM HCl which was decanted after centrifugation and then with water which was processed likewise. The resulting light yellow powder was recrystallized from $CHCl_3$ and checked with TLC-UV with EtOAc-hexanes 1:1 (a single spot separate from the starting materials). Yield: 26 mg (30 %) of lightweight white-parchment color powder which is highly insoluble.

Thin-layer chromatography (TLC) was performed on Macherey-Nagel silica gel 60 aluminium plates containing UV indicator.

Spectroscopic methods

The Raman spectra were recorded employing inVia (Renishaw, UK) spectrometer equipped with a thermoelectrically cooled CCD camera (−70 °C) with a confocal LEICA microscope. A 785 nm laser beam was used as an excitation source. 1200 lines/mm gratings were used to record the Raman spectra. The laser power at the sample surface was restricted to 8 mW (10%). The 50x/NA 0.75 objective was used during all the measurements. The laser was focused to ~ 1,3 μm diameter spot on the sample. The total integration time for each spectrum was 100 s. The measurements were performed on Metrohm C220AT screen printed gold electrodes with electrochemical structurization[200] and chemical modification.

4-mercaptophenylacetic acid was grafted from a 3 mM methanolic solution at room temperature overnight. Adsorbed 4-aminobenzonitrile was dropcast as a 10 μl volume of 12 μM methanolic solution (practically, a small amount, but on the order of 1000× excess relative to monolayer). SSCNPA was grafted from a 200 μM acetone solution overnight. All electrodes were washed with a large amount of methanol.

The spectra were flattened via asymmetric least squares, the regions 937-1859 and 1860-2627 cm^{-1} were trimmed, additively offset to align and joined, the intensity was normalized to the common 1076 cm^{-1} peak and then the complete spectra were offset from each other in Python.

NMR experiments were performed on a Bruker Avance Neo NMR console equipped with Bruker Ascend 14.1 T superconducting magnet and 5 mm high-resolution probe. 1H NMR spectra were collected at 25 ppm width with 64 k point density after excitation with a 10 μs rectangular pulse.

ATR-FTIR was performed on a Bruker LUMOS II FTIR microscope running OPUS 8.5 software. A MIR source, ZnSe beamsplitter, room temperature TE-MCT detector and a germanium crystal at medium contact pressure were used. Spectra were recorded on household aluminium foil in the range 4000-600 cm^{-1}, at 4 cm^{-1} resolution, averaged from 64 spectra.

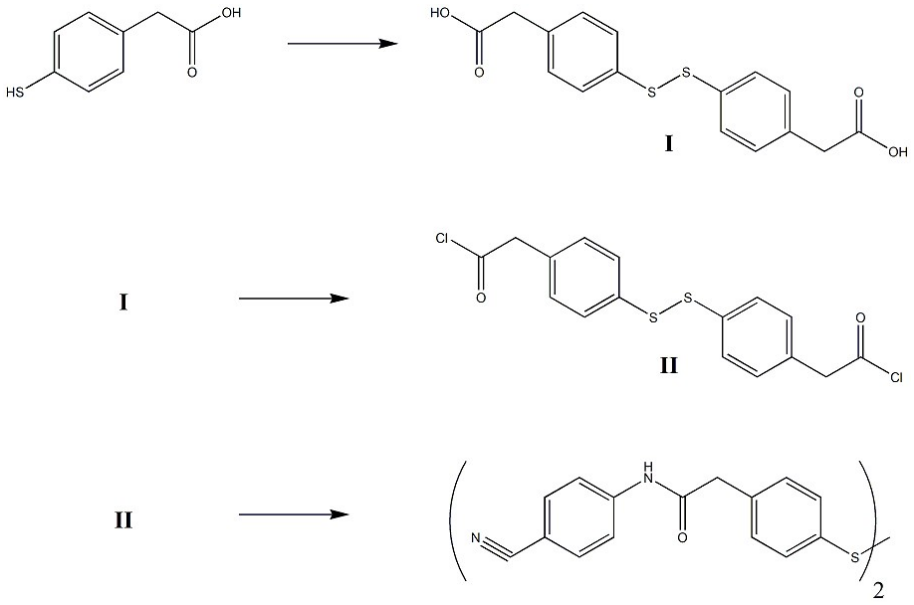


Figure A3 1. SSCNPA synthesis: **I**: EtOH/I_2, rt; **II**: $SOCl_2$/$MeCl_2$, rt; **SSCNPA**: DMAc/4-aminobenzonitrile, rt.

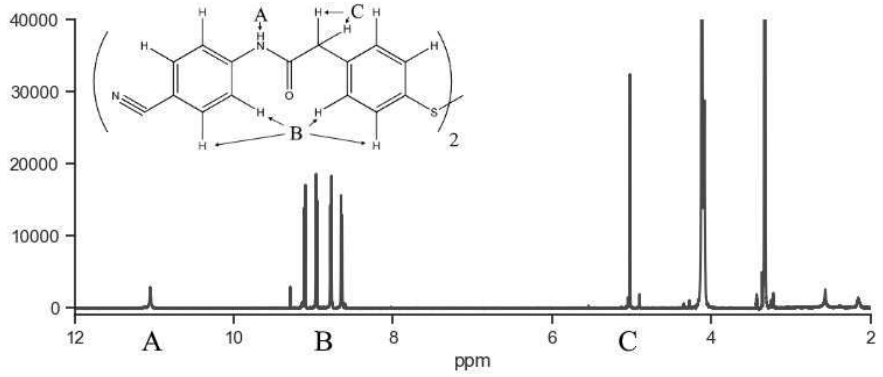


Figure A3 2. SSCNPA ^{1}H NMR (600 MHz) in Acetone-d6.

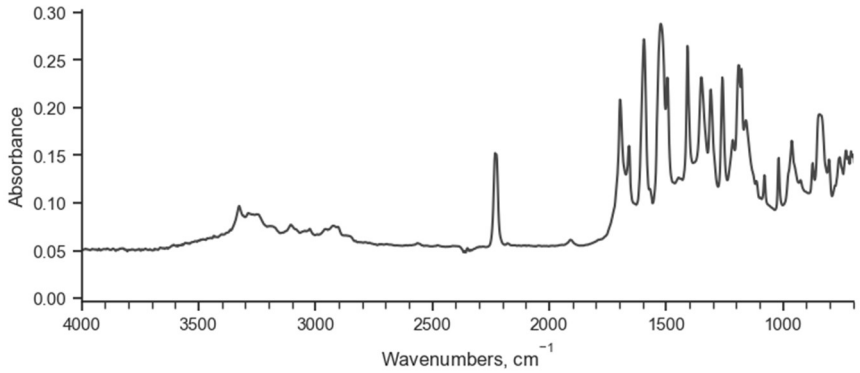


Figure A3 3. An ATR-FTIR spectrum of SSCNPA as a thin film (~1-10 μg) cast from acetone onto aluminium foil. The triple bond frequency is very clear at ~2230 cm^{-1}, with N-H stretching at 3325 cm^{-1} and the carbonyl at 1700 cm^{-1}.

Results

Raman spectroscopy is one of the very few (perhaps the only) methods for rapid and approachable structural characterization of solid phase molecular monolayers.

First, a diisocyanate surface activation (somewhat analogous to the ubiquitous glutaral) was investigated as it is exceptionally rarely employed in biosensors. The coupling of hexyl diisocyanate (often referred to as HMDI) was attempted onto mixed terminal -OH of mercaptohexanol/mercaptoethanol layers in THF, MeCN and in DMF under various concentrations, temperatures and organic base catalysts. Unfortunately, perhaps due to layer thickness or the crosslinker reactivity to air or to itself, the SCN vibration was never observed in a SERS spectrum. These measurements already inform us that the attempted Au-S-Hex-O-C(=O)-N-Hex-N=C=O reactive layer formation was likely unsuccessful, possibly explaining the sparse literature reporting.

SERS application for verifying amide (specifically, anilide) formation on a surface adsorbed monolayer was investigated.

SSCNPA spectra were recorded (**Figure A3 4**) as a:

- preassembled unit bound as a monolayer (simulated “perfect” solid phase coupling; **SSCNPA**)
- a surface with a free carboxyl monolayer and the nitrile dropcast (10 nM solution in MeOH) on top (simulated unsuccessful solid phase coupling + adsorption; **SPA + CN**)

- and the acid alone (simulated unsuccessful solid phase coupling, clean surface; **SPA**).

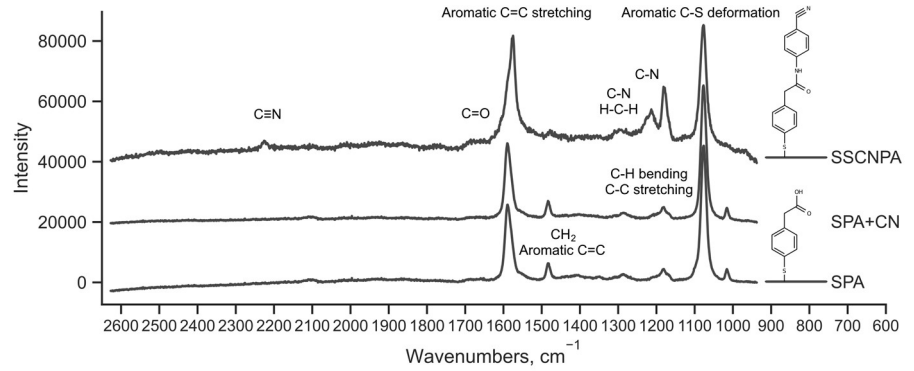


Figure A3 4. SERS spectra of SSCNPA (coupled), SPA + CN (adsorbed) and SPA (clean) with tentative peak assignments.[182]

Interestingly, the cyanide group enhancement (~2230 cm^{-1}) was very mild (unlike in FTIR, where a very sharp and distinct peak was observed, albeit from a significantly larger (~microgram) quantity of material), and the ~1200 cm^{-1} C-N vibrations (common in nitrile and amine) were a much better indicator of coupling. Other features that were clear indicators of coupling include the 1590 cm^{-1} region aromatic bands.

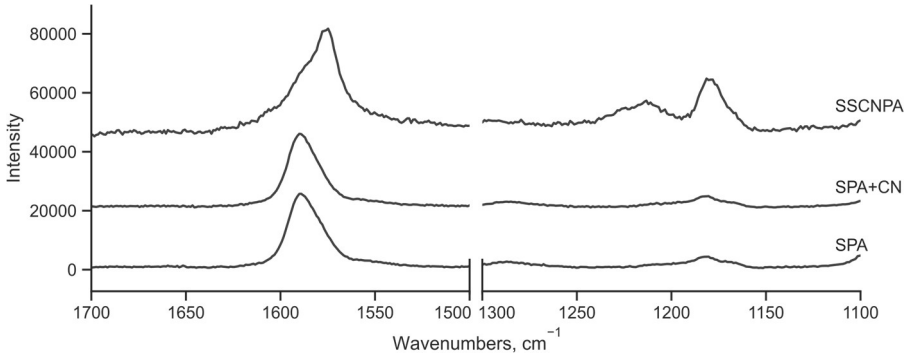


Figure A3 5. SERS spectra of SSCNPA (coupled), SPA + CN (adsorbed) and SPA (clean) 1590 cm^{-1} and 1200 cm^{-1} regions.

Interestingly the dropcast aminobenzonitrile contamination was not observable, despite a relatively large amount (~0.12 nmol) applied. The results, however are encouraging as ultimately we can observe a tremendous difference between coupling test and control groups and clearly identify non-coupled electrodes and gain insight whether any crossreaction was adsorptive or covalent. Thus, solid phase synthesis/coupling optimization and success for novel reactions could be monitored via SERS moving forward.

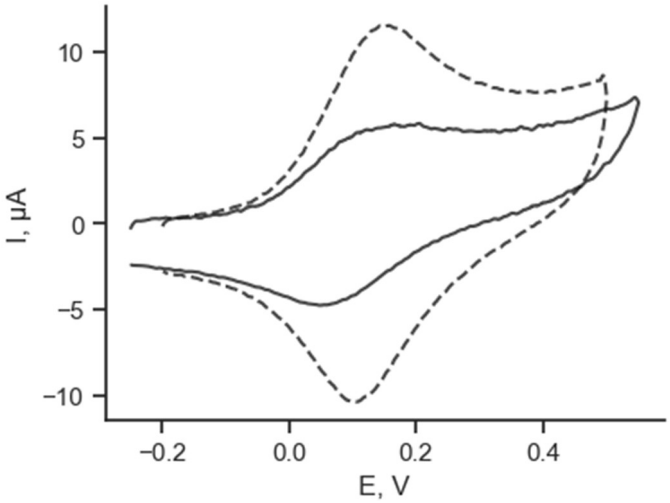


Figure A3 6. A directed ligation chemistry currently in development. **Dashed line:** directed ligation, **solid line:** simultaneous non-directed coupling side-reaction onto a nearby electrode.

4. Appendix IV

The mechanistic implications for melting-based DNA mismatch detection: Exploration of the signal transduction mechanism from the methylene blue-labeled DNA reporter strand and the hybridization impacts of solid-phase DNA probe density

Materials and Methods

DNA Probe density was measured according to Steel.[62]

Name	Sequence 5'-3'
DNA Probe	Thiol-C6-CGC ATT ATC TCT TAC ATC AGA
Probe 3MB	Thiol-C6-CGC ATT ATC TCT TAC ATC AGA-Atto MB2
ZNA Probe	Thiol-C6-CGC ATT ATC TCT TAC ATC AGA-(ZNA-4)
R*1 HEG5	Atto MB2-(HEG-spacer)×2-GAT GCT TTG AGA ACA
R*1 HEG3	GAT GCT TTG AGA ACA-(HEG-spacer)×4-Atto MB2
R*1 5MB	Atto MB2-GAT GCT TTG AGA ACA
R*17 5MB	Atto MB2-GAT ACT TTG AGA ACA G
R*1	GAT GCT TTG AGA ACA-Atto MB2
R*17	GAT ACT TTG AGA ACA G-Atto MB2
T*1	**CAA ATT TGT GTC TT** CTG TTC TCA AAG CAT C TCT GAT GTA AGA GAT AAT GCG **CCA C**
T*1m	**CAA ATT TGT GTC TT** CTG TTC TCA AAG CAT C TCT GAT GTA AGA GAT AAT GCG
T*1s	CTG TTC TCA AAG CAT C TCT GAT GTA AGA GAT AAT GCG
T*17	**CAA ATT TGT GTC TT** CTG TTC TCA AAG TAT C TCT GAT GTA AGA GAT AAT GCG **CCA C**

Results

When using a target with 5'-overhangs we encountered a very large loss of signal and peak overpotential (**Fig. A4 1.2**). It is suspected that as the label is now (due to the overhangs at the top) located towards the middle of the duplex it is fairly well insulated from approaching the electrode surface. The MB label is in other words, surrounded by negative charges from both sides.

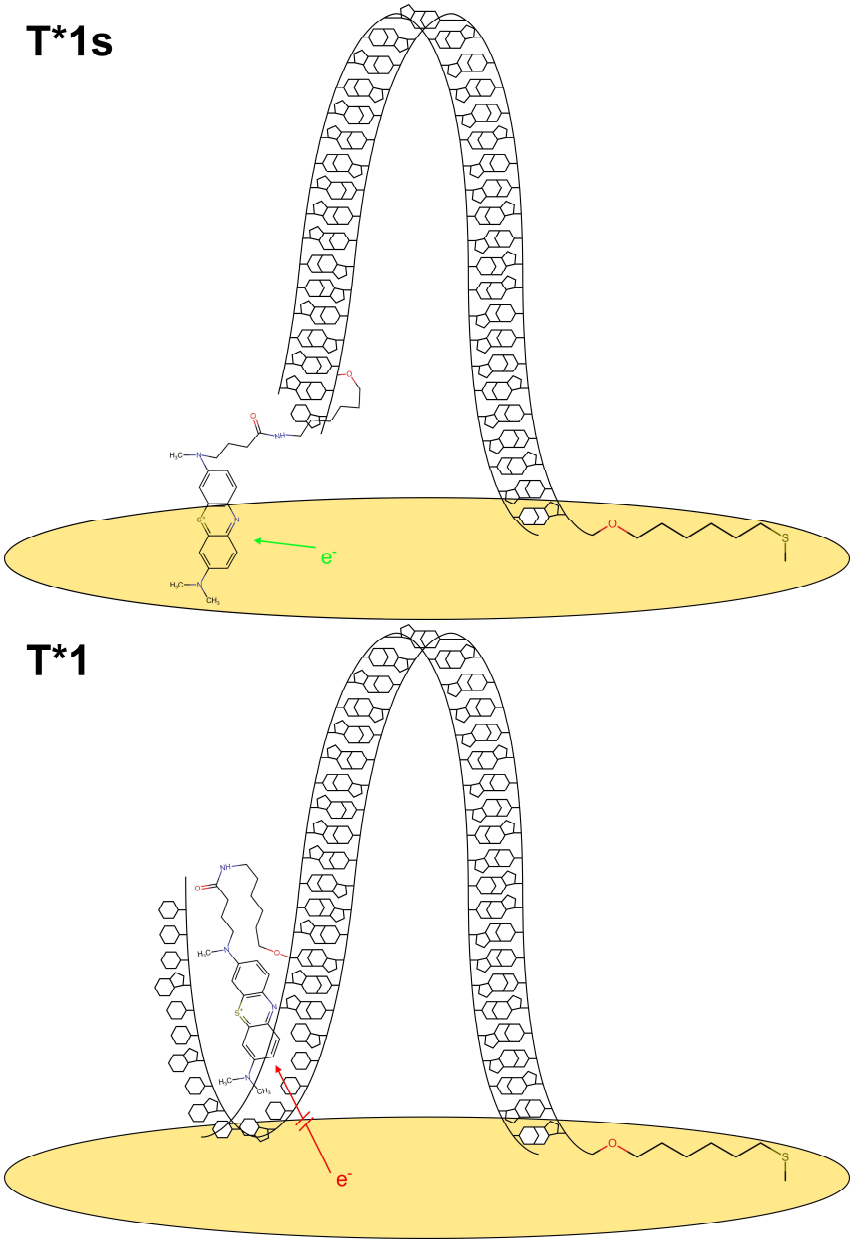


Figure A4 1.1 Sandwich representation containing the **DNA probe** and **R*1**. With a 1-bp overhang (**T*1s**), the signal is clear. With a 15-bp overhang (**T*1**), the signal becomes becomes very poor. Only the upper overhang is shown. The sandwich is likely in a more "upright" conformation than shown. This is an attempt to represent a macromolecular structure. The average conformation is not known. Elements are not to scale.

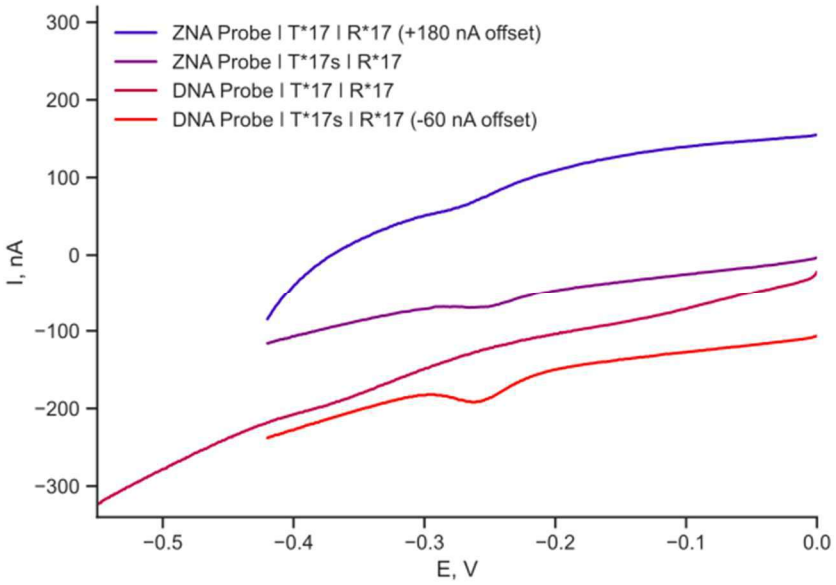


Figure A4 1.2. Linear sweep voltammograms of various sandwich duplexes. Average of 2 electrodes each. We can see that the DNA probe works well with T*17s ("short") but very poorly with T*17 (overhanging). The introduced ZNA-4-modified probe works well with both targets. *The DNA and ZNA probe densities are not physically standardized relative to each other.*

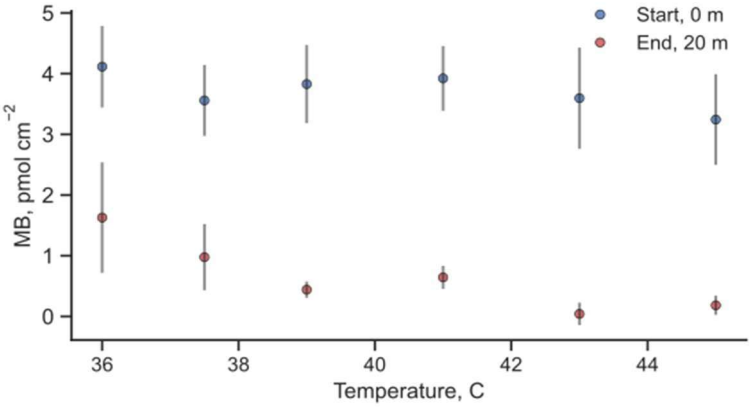


Figure A4 1.3. T*1s construct on DNA Probe at various temperatures. We can see that the starting signal is mostly stable over the 9 °C range, and the full melting is achieved at around 41 °C (at 20 minutes).

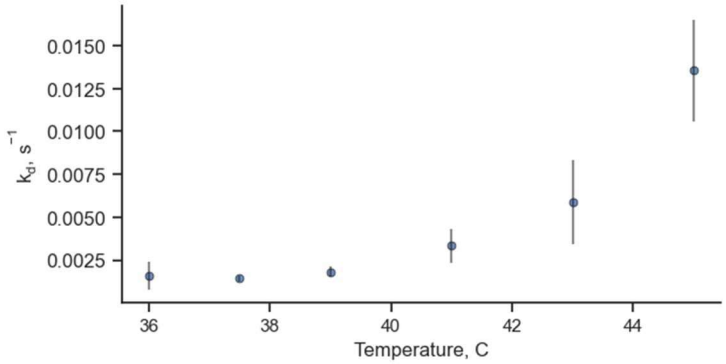


Figure A4 1.4. T*1s construct on DNA Probe at various temperatures. The relationship between the dissociation rate constant and the temperature appears exponential.

An attempt was made to "plug in" the label via a labeled probe, so that the path MB(target)→MB(probe)→Probe chain→electrode is made very direct if the signal transduction were occurring via the DNA duplex (**Figure A4 2.2**). Since from the MB(probe) molecule everything is covalently linked to the electrode and the target | probe duplex should display π–π stacking – better signal transduction was expected. However, no powerful signals were ever observed.

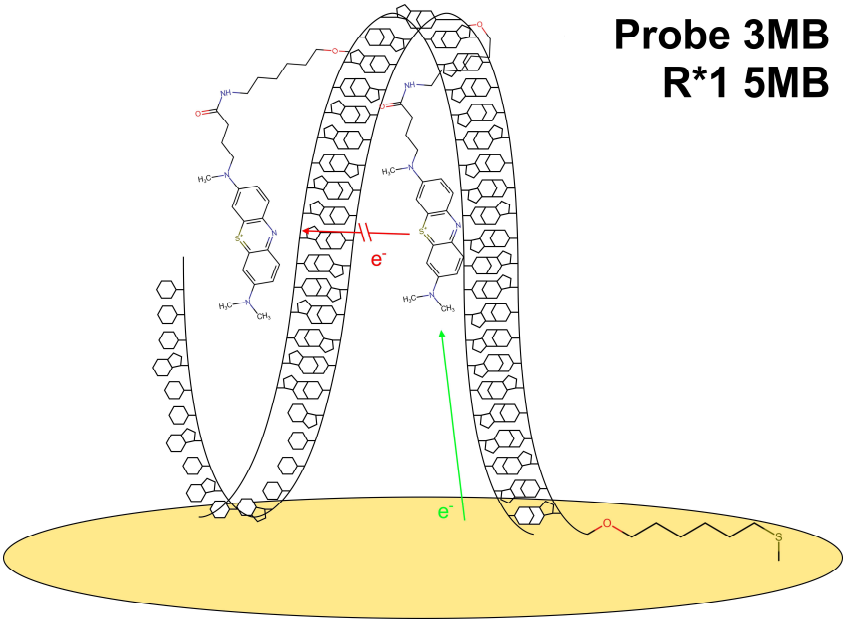


Figure A4 2.1. Sandwich representation containing the labeled DNA probe **Probe 3MB** and the inverted reporter **R*1 5MB**. Only the upper overhang is

shown. The sandwich is likely in a more "upright" conformation than shown. This is an attempt to represent a macromolecular structure. The average conformation is not known. Elements are not to scale.

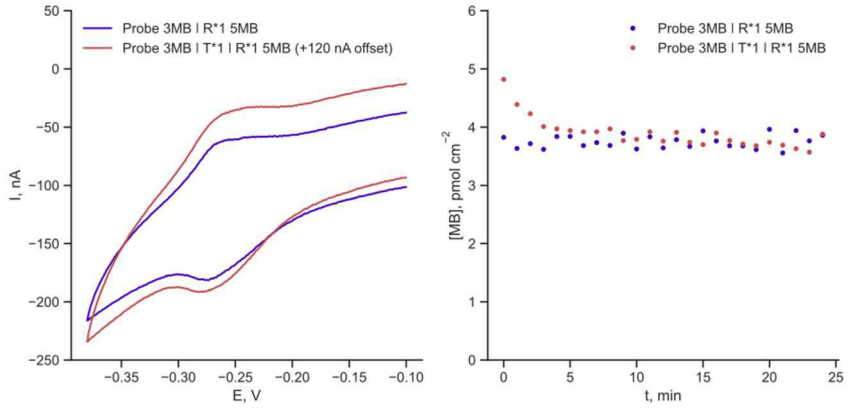


Figure A4 2.2. Inverted reporter | labeled probe sandwich (Probe 3MB | R*1 5MB). The results displayed are of 1 replicate, but were performed subsequently on the same electrode, therefore are directly comparable. We can see that the signal increase from the reporter is very small, generally a hybridization efficiency of 80% and therefore a signal of 180% would not be unreasonable. It is unclear as to why the melting appears to be so rapid, simultaneous gain of MB and mobility-loss-mediated quenching may offer some explanation.

Plugging in the reporter label was unsuccessful and gave weak and inconsistent results every time. The probe density appears to be reasonable from the MB density. The existing MB label could change intensity due to other reasons such as probe mobility or screening and presented a risk of false results. This system was not pursued further.

A ZNA probe was introduced to screen the DNA duplexes and allow greater mobility (DNA collapse) and higher stability. The ZNA-4 chain ideally should change the probe charge from -21 to -10, approximately halving it. Introducing free polycations in solution may, for instance, cause uneven screening and a minuscule change in the concentration (e.g., 100 nM) of a dissolved polycation could result in a change from partial (-10) to complete (-0) screening. Complete screening would likely allow other DNA oligomers to adsorb negating any specificity of the sensor. The measurement of the **ZNA** probe surface density with RuHex was unsuccessful ($\sim 2\times10^{12} \pm 2\times10^{12}$ molecules cm^{-2}) and the optimal density is unknown, but as

the charge was halved, the concentration of the probe was thus also halved producing practically functional electrodes. The **DNA** probe density achieved was $4.6\times10^{12} \pm 3\times10^{11}$ molecules cm^{-2}, which is generally considered to be excellent. The ZNA probes were later optimized further via easy-to-manufacture physical blocking [**Appendix V**] producing improvements in hybridization of almost an order of magnitude with excellent repeatability.

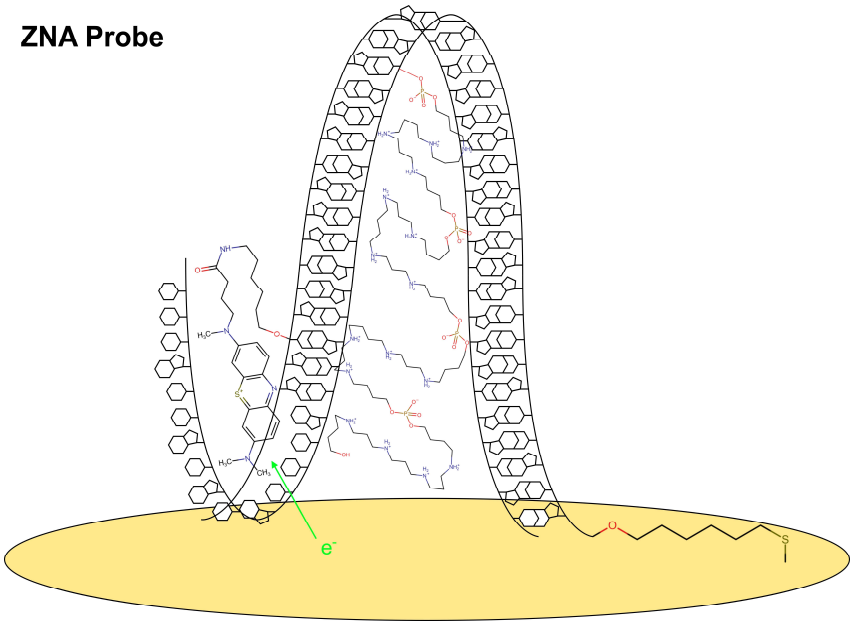


Figure A4 3. A sandwich representation containing the **ZNA probe** and **R*1**. Only the upper overhang is shown. The sandwich is likely collapsed, releasing the MB bringing it closer to the surface. This is an attempt to represent a macromolecular structure. The average conformation is not known. Elements are not to scale.

To further interrogate the signal transduction, "freely moving" labels were tested. A PEG chain from the sandwich middle and from the top – minus the overhang was extended to approximately reach the electrode surface – these were the HEG inserted reporters.

The HEG reporters both showed excellent signal transduction with both DNA and ZNA probes and any target overhangs. This reinforces the idea that the label mobility is greatly important in the signal transduction. Perhaps the MB is still able to intercalate somewhere near the electrode and transduce some of its signal via π–π stacking or perhaps it overwhelmingly occurs via

relocation to the surface. This finding does not completely rule out small dsDNA conductivity, but it does convincingly show that removing the MB from entrapment inside negative charges is very important, either via mobility (PEG) or via charge screening (ZNA). The fourth publication was carried out with ZNA probes and regular DNA reporters as this combination showed good results, however the HEG reporters show promise for future applications. *Note: the HEG reporter melting may occur in a completely different manner. I would like to also add an anecdotal report of a HEG reporter showing large reductive (but not oxidative – asymmetric) peak broadening under different voltammetric conditions and electrolytes than discussed here.*

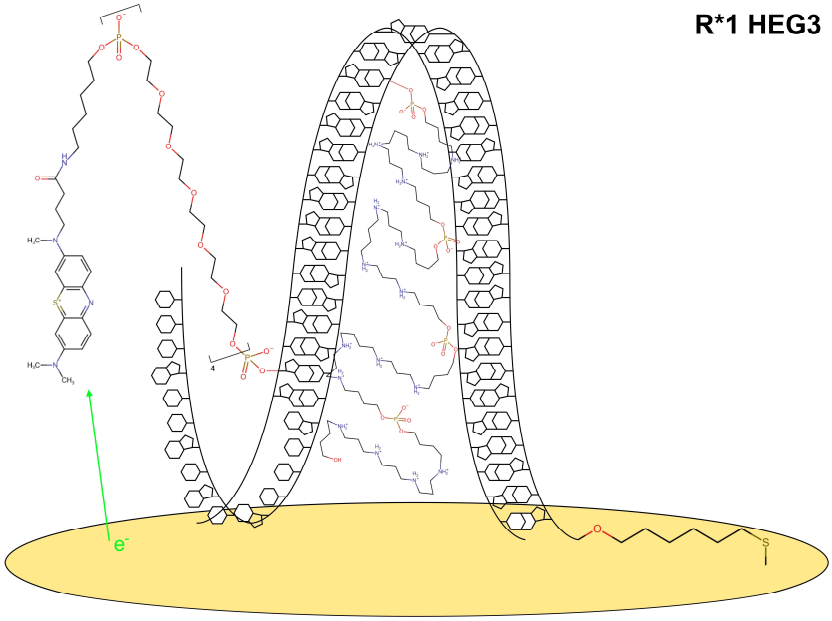


Figure A4 4.1. A sandwich representation containing the **ZNA probe** and **R*1 HEG3**. Only the upper overhang is shown. The sandwich is likely collapsed, and the "long" distal (6×4 ethylene moieties) PEG chain allows for extensive mobility of the MB. The PEG-MB chain was chosen to be long enough to reach the electrode in an "upright" configuration from the very top. This is an attempt to represent a macromolecular structure. The average conformation is not known. The elements are not to scale.

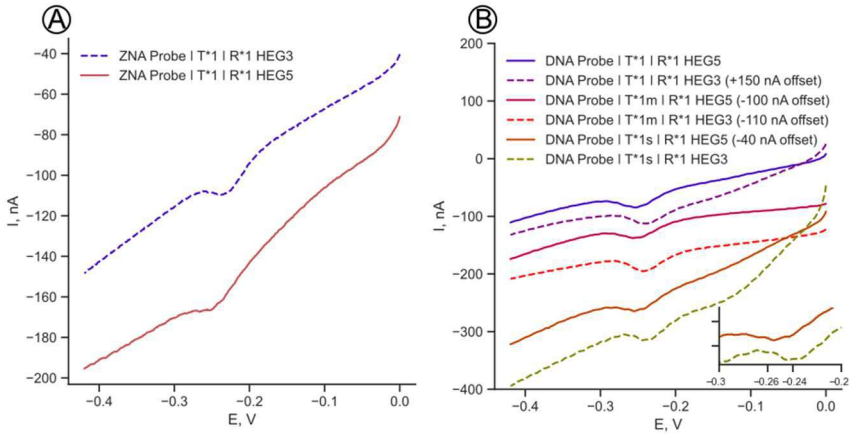


Figure A4 4.2. Linear sweep voltammograms of the HEG reporters. A) **ZNA probes** (2 electrode averages); B) **DNA probes** (1 electrode each). T*1m and T*1s are overhang-removed target sequences. Broadly in all cases R*1 HEG3 (the "long" distal PEG chain) reporter has a lower overpotential (inset) at ~-240mV vs. ~-250mV with DNA and even lower with ZNA.

5. Appendix V

Application – the detection of double SNPs, miniaturization and sequencing

Name	Sequence 5'-3'
DNA Probe	Thiol-C6-CGC ATT ATC TCT TAC ATC AGA
ZNA Probe	Thiol-C6-CGC ATT ATC TCT TAC ATC AGA-(ZNA-4)
R*1	GAT GCT TTG AGA ACA-Atto MB2
R*17	GAT ACT TTG AGA ACA G-Atto MB2
T*1	**CAA ATT TGT GTC TT** CTG TTC TCA AAG CAT C TCT GAT GTA AGA GAT AAT GCG **CCA C**
T*1s	CTG TTC TCA AAG CAT C TCT GAT GTA AGA GAT AAT GCG
T*17	**CAA ATT TGT GTC TT** CTG TTC TCA AAG TAT C TCT GAT GTA AGA GAT AAT GCG **CCA C**

Methods

Electrode preparation:

The 0.5 mm electrodes were manufactured in house from 0.5 mm 99.99 % gold wire (Sigma Aldrich). A 0.6 mm hole was drilled into a 2 mm copper cylinder serving as an electrical and mechanical contact, wherein ~10 mm length of gold wire was inserted and a short section crimped. Two gold-tip copper rods were inserted side-by-side into an upright brass tube with a PTFE spacer disc to keep the wires from drifting and cast in polypropylene at 140-200 °C in a commercial oven under air. While these electrodes are excellent mechanically and chemically, I must note that polypropylene has notable thermal expansion and is not an ideal material choice for encasing metals.

The electrodes were prepared and measured as per **Publication 4**. The dsZNA condition entails physical blocking – preparing a ZNA Probe|T*1 duplex prior to gold modification (i.e., using sacrificial DNA target as a "spacer" during solid phase modification), thus physically blocking excess probe adsorption. The electrodes prepared with dsZNA probe were washed in pure water at 37 °C overnight to ensure target removal prior to measurement.

30% EtOH hybridization buffer: 10 mM HEPES, 300 mM NaCl, 30% EtOH, salmon testes DNA 50 µg/ml, pH 7.6

20X SSC hybridization buffer: 300 mM monosodium citrate, 3 M NaCl, pH 7 (diluted to 5X and SDS added to 0.1%)

Melting buffer: 20 mM PBS, 280 mM NaCl, 10% Formamide, 0.05% Tween-20, pH 7. *Note: melting is not appreciably occurring at room temperature; only non-specific adsorption is being removed.*

In **Figure A5 2:** 3 cyclic voltammograms (0.1 V → –0.38 V, 50 mVs^{-1}) with intermittent stirring at 37° C were recorded and averaged to obtain 1 datapoint. The DNA probe and the short target (T*1s) are used with at least 4× excess of R*1. Hybridization is carried out in one-pot at 37° C. A melting buffer with 200 mM NaCl is used.

In **Figure A5 3:** 4 linear sweep voltammograms (0 V → –0.42 V, 50 mVs^{-1}) with constant stirring at 25° C were recorded and averaged to obtain 1 datapoint. The ZNA probe and the full target (T*1) are used with at least 2× excess of R*1 or at least 80 nM R*1. Both strands are hybridized in one-pot at 37° C for 20 min.

The following equation was used to fit the Langmuir constant with the MB $cm^{-2}{}_{max}$ taken as 1.5 pmol for ssZNA and 2.3 pmol for dsZNA, Olig being the target concentration and K_L being the Langmuir constant (nM^{-1}).

$$MB\ cm^{-2} = \frac{MB\ cm^{-2}{}_{max} \times K_L \times Olig}{1 + K_L \times Olig}$$

Total hybridization ΔG was calculated from:

$$\Delta G = -RTlnK_L$$

Results

Controlling the SAM density experimentally via a sacrificial DNA target was very simple and produced reasonably good sensitivity of a few nM compared to tens of nM from previous design. Changing the hybridization buffer did not meaningfully improve the signal (**Figure A5 2**). Changing the electrode size did not meaningfully improve the sensitivity (**Figure A5 3A**). If the Langmuir adsorption model is fitted, the following reciprocal Langmuir constants (i.e., equilibrium constants) are obtained:

Ø	K_D
0.5 mm (ds-SAM)	3.5 nM
1.6 mm (ds-SAM)	3.7 nM
2.0 mm (ds-SAM)	3.8 nM
2.0 mm (ss-SAM)	28.5 nM



Figure A5 1. The hybridization sensitivities of different electrode disc sizes.

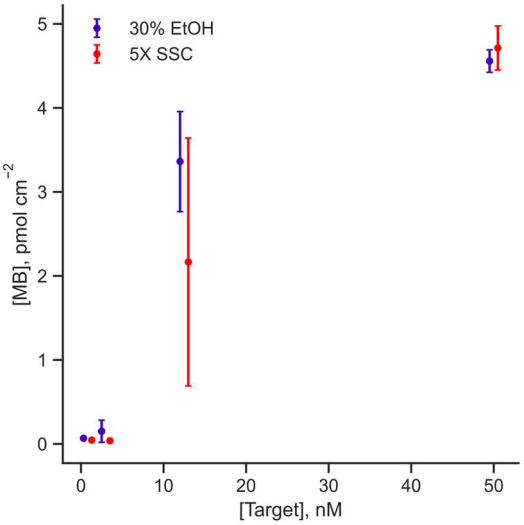


Figure A5 2. The comparison of hybridization buffers. DNA probe: T*1s | R*1 sandwich with varying T*1s concentration. Mean and SD. [Target], nM staggered, n = 3.

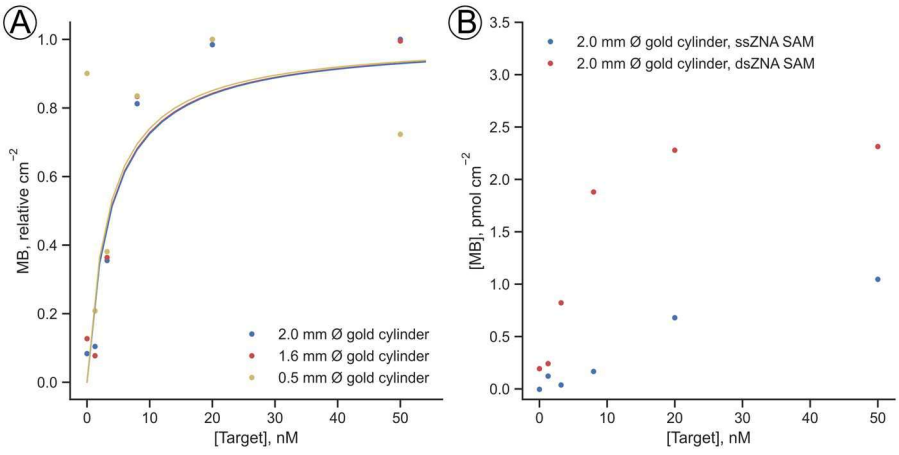


Figure A5 3. The measurement of low DNA target concentrations.

A – A comparison of electrode sizes. (ds)ZNA probe | T*1 | R*1 sandwich with varying T*1 concentration. Fit represents the Langmuir adsorption model. *Mean normalized to surface area and to 1. Ø 2.0 mm and 1.6 mm n = 2 as the replicates were almost overlapping; Ø 0.5 mm n = 5 as there was noise due to low currents. The dsZNA-SAM was a necessary experimental consideration to ensure the electrodes had very similar surfaces and were comparable.*

B – A comparison of probe density. ZNA probe | T*1 | R*1 sandwich with varying T*1 concentration, n=2.

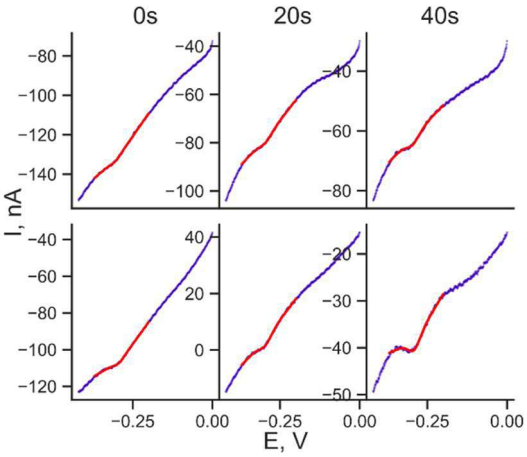


Figure A5 3.1. LSV peaks with fitting under non-melting conditions (these LSVs are averaged to produce the 20 nM datapoints in Figure A5 3A). Top: 0.5 mm, bottom: 1.6 mm electrode.

Sequencing calculations

A library of sequences was generated by checking every base in every position in the T*17s reporter complementary fragment C TGT TCT CAA AGT ATC; and if a base is not found in the position a new sequence is generated with a new substituted base:

C TGT TCT CAA AGT ATC → **C**==A? → False → **A** TGT TCT CAA AGT ATC

For each new base the process was repeated to generate every possible secondary mismatch:

A **T**GT TCT CAA AGT ATC → **T**==A? → False → **A** **A**GT TCT CAA AGT ATC

Note: tertiary mismatches were not generated as there is a very large number of them and our system likely will not be able to measure them – most triple mismatches will melt too fast.

Thus a library of 1129 sequences was rapidly generated and (together with the experimentally used R*17 sequence) was fed to the DINAMelt Two state hybridization model. The DINAMelt parameters were DNA at 42°C, 0.01 mM, 0.28 M Na^+, 0 M Mg^{++}, oligo mode. The model provided the ΔG values in a matter of a few seconds and the $\Delta\Delta G$ values were calculated by subtracting the perfect match. The energies range from 0 to 8.2 kcal mol^{-1} and at 1 decimal point precision and a library with only *79 energy levels* is obtained. This means that the range 0-8.2 kcal mol^{-1} at intervals of 0.1 is much too narrow to map 1129 sequences. The provided Gibbs free energy resolution is however, sensible as measuring at 0.01 kcal mol^{-1} intervals may be

practically unachievable. The obtained propagated standard deviations were on the order of 0.2 kcal mol^{-1}.

The goal is to measure the $\Delta\Delta G$ value of an unknown sequence and to reference it to our library of values, thus predicting the unknown DNA sequence. Unfortunately, in practice this leaves us with on the order of 20-70 hits per experimental result.

To demonstrate the workflow, I will remove the wild-type target **"S2"** from the dataset and treat it as an unknown sample.

First, a relationship between the calculated energies and the experimental values is established (**Figure A5 5, 1**). From the linear regression, the **S2** (excluded from **Figure A5 5, 1**) measurement is converted into the corresponding calculated value, which can then be used to look up sequences from the library. In our case a value of 2.194 kcal mol^{-1} was obtained and this value at ±0.15 kcal mol^{-1} or closer (arbitrary author's choice – a large, but fair window) was considered a match. The true $\Delta\Delta G_{calc}$ should be 2.2 kcal mol^{-1}, however we presume this is an unknown sequence for the sake of demonstration. If searching for a single nucleobase difference (**Figure A5 2, 2**), we can see 3 matching sequences:

G1	CTGTTC**G**CAAAGTATC
G2	CTGTTCTC**G**AAGTATC
G3	CTGTTCTCAAAG**C**ATC

With G3 being the correct match.

When searching through the entire library (Fig. 2, 3A-3D), a total of **39 matches** was found.

In our study another limitation is present: the PCR amplification forces most of the positions in the sequence, leaving only the positions 9-16. This still outputs **13/276 hits**: 10 various relaxed permutations of **S2** and 3 unrelated sequences.

CTGTTCTC**G**AAGTATC	Complete miss
CTGTTCTC**G**AAGTAT**A**	
CTGTTCTC**G**AAGTAT**G**	
CTGTTCTCAAAG**C**ATC	Hit/patrial hit
CTGTTCTCAAAG**C**C**T**C	
CTGTTCTCAAAG**C**G**T**C	
CTGTTCTCAAAG**C**T**T**C	
CTGTTCTCAAAG**C**A**A**C	
CTGTTCTCAAAG**C**A**C**C	
CTGTTCTCAAAG**C**A**G**C	
CTGTTCTCAAAG**C**AT**A**	
CTGTTCTCAAAG**C**AT**G**	
CTGTTCTCAAAG**C**AT**T**	

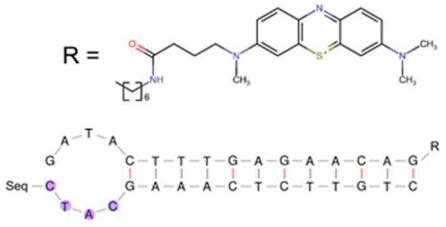


Figure A5 4. Exemplary search results of a known (blinded) sequence S2.

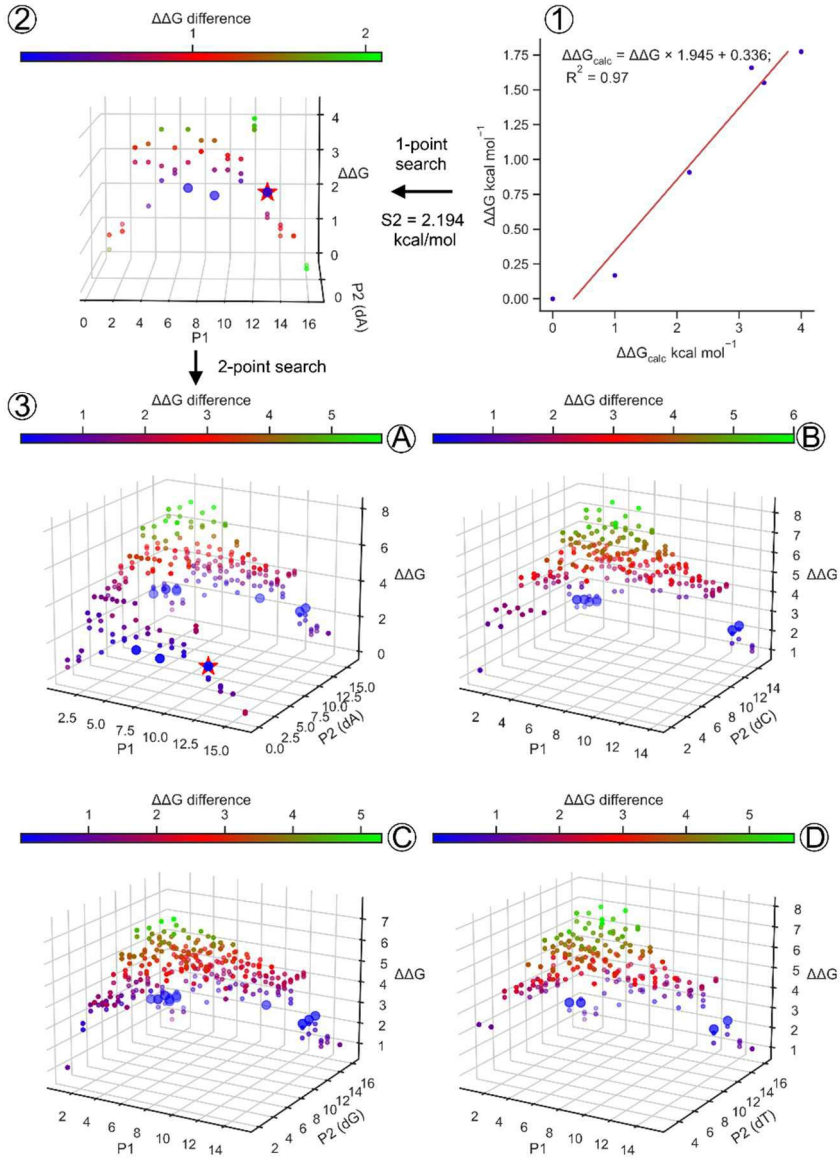


Figure A5 5. The isothermal dissociation library

1: The measured sequence energies compared to their calculated values. S2 is deliberately removed and used as an unknown sample.

2: Screening in the 1 mismatch library. *ΔΔG* represents kcal mol^{-1}. The bottom axes represent the positions in the target sequence. While the term "*ΔΔG* difference" sounds redundant the color scale represents the distance of the library entry from the searched datapoint.

3: Each P1 location has 3 nucleobase datapoints (e.g., dA, dG, dT) plus the original sequence (P1 = 0; P2 = 0; *not shown*). The mutations do not go backwards, e.g., **P1 : 1A, P2 : 2A** but no **P1 : 2A, P2 : 1A** as this just duplicates the sequence. Each P2 location represents only 1 nucleobase to reduce graph complexity (e.g., only dA). The large spheres ● represent the hits and the star ★ represents the true sequence.

We can see that:

a) The **electrochemical sequencing by isothermal dissociation** approach actually guesses both the *position* and the variant *nucleobase* well, e.g., 13T→C and variants were correctly guessed, while 13T→G was correctly **not** guessed, even though the middle positions are clearly "highly" destabilizing and the terminal ones are "mildly" destabilizing.

b) Both our measurement and the library need a significant increase in the precision of the $\Delta\Delta G$ values to narrow down the number of hits to a usable number (e.g., from 39 hits to 1). This may be practically unachievable.

c) While this approach seems unsuitable for an exhaustive profiling of a segment (any position, any base ± any other base), for any practical application the human genome is far more conservative than:
$9 \times (3\,080\,000\,000 + 3\,079\,999\,999 + ...) + (3 \times 3\,080\,000\,000) = 4.27 \times 10^{19}$ variants. Only around 5×10^{9} are listed in dbSNP.[201]
In our region of interest, of the given 1129 sequences only ~9 are listed in dbSNP.[202]

Calculations used for the conclusions section (data from **Publication 4**)

ΔΔG, kcal mol^{-1}	(Dinamelt) Solution phase *ΔΔG* calc., kcal mol^{-1}	Slope	Intercept	S6 *ΔΔG* measured, kcal mol^{-1}	Extrapolated total S6 *ΔΔG* solution phase kcal mol^{-1}	S6 solution phase mismatch *ΔΔG* calc., kcal mol^{-1}	Solution phase G|A stack, kcal mol^{-1}
0.00	0.00	1.948	0.317	0.907	2.085	0.1	1.985
0.17	1.00						
0.96	2.20						
1.66	3.20						
1.55	3.40						
1.77	4.00						

Allele 2 (heterozygous sample)	Expected solid phase *ΔΔG*, kcal mol^{-1}	Allele 1 (homozygous sample)	Expected solid phase *ΔΔG*, kcal mol^{-1}	Difference, kcal mol^{-1}	2×SD, kcal mol^{-1}
1 + 0	955	0 + 1	0	955	320
1 + 1	478	0 + 2	0	478	320
1 + 2	318	0 + 3	0	318	320
1 + 3	239	0 + 4	0	239	320

For instance, 1+3 heterozygosity (a tetraploid sample with 1 fraction of wild type allele and 3 fractions of the different one) would produce <2×SD change in signal and be sometimes mistaken as having (0+4) no Allele 2.

ACKNOWLEDGEMENTS

I would like to express my thanks to a number of people who have helped me complete these tasks. First and foremost, Dr. Marius Dagys for the supervision and for the push to develop these sensors while giving me the freedom to create my own designs.

I am very grateful to Dr. Dalius Ratautas for overseeing many of my experiments, for the innumerable consultations and the support in writing and publishing. My gratitude also goes out to the current and former members of the Department of Bioanalysis for a broad scope of expertise and assistance.

I would like to personally thank:

Dr. Jonas Šarlauskas for the countless brilliant discussions.

Dr. Miglė Tomkuvienė and Kornelija Tučinskytė for their expertise, support and positivity and the DNA amplification reactions at the Department of Biological DNA Modification.

Dr. Laurynas Dagys for the NMR spectroscopy at The Institute of Chemical Physics and the fruitful conversations.

Dr. Ilja Ignatjev for the much needed help with Raman measurements at The Center for Physical Sciences and Technology.

Dr. Mantas Jonušis, from The Laboratory of Bioorganic Compounds Chemistry for the GCMS measurements.

Dr. Tadas Ragaliauskas for the atomic gold deposition at the Institute of Biochemistry.

Dr. Rasa Petraitytė-Burneikienė and The Department of Eukaryote Gene Engineering for the help with gel imaging.

Zdislav Staševskij for the ^{32}P DNA postlabelling and autoradiographic imaging.

Dr. Marija Jankunec for the help with atomic force microscopy at the Department of Bioelectrochemistry and Biospectroscopy.

Jonas Špečkauskas from Protogama, for the CNC-machined parts.

I am also grateful to my family and relatives for personal support.

Vilniaus universiteto leidykla
Saulėtekio al. 9, III rūmai, LT-10222 Vilnius
El. p. info@leidykla.vu.lt, www.leidykla.vu.lt
bookshop.vu.lt, journals.vu.lt
Tiražas 15 egz.